MASSACHUSETTS INSTITUTE OF TECHNOLOGY
DEPARTMENT OF OCEAN ENGINEERING
CAMBRIDGE, MASS. 02139

(9) Technical Report, No. 1,

on

(6) INTEGRATION OF M.I.T. STUDIES ON PREDICTION AND CONTROL OF DISTORTION IN WELDED ALUMINUM STRUCTURES

(15) Prepared Under
Contract No. N00014-75-C-0469 NR 031-773
(M.I.T. OSP #82558)

DEVELOPMENT OF ANALYTICAL AND EMPIRICAL SYSTEMS FOR PARAMETRIC STUDIES OF DESIGN AND FABRICATION OF WELDED STRUCTURES

to

Office of Naval Research

September 20, 1976

by
(10) Vassilios Papazoglou
Koichi Masubuchi

(12) 170 p.

(11) 20 Sep 76

406 856

ACKNOWLEDGMENT

This is the first technical report of the Contract No. N00014-75-C-0469, NR 031-773.

The authors greatly appreciate the g dance and encouragement given by many people in the U.S. Navy, especially Dr. B. A. MacDonald and Dr. F. S. Gardner of the Office of Naval Research.

The authors would also like to thank Mr. F. R. Miller of the U.S. Air Force, Materials Laboratory for donating laser welded specimens for determining residual stresses.

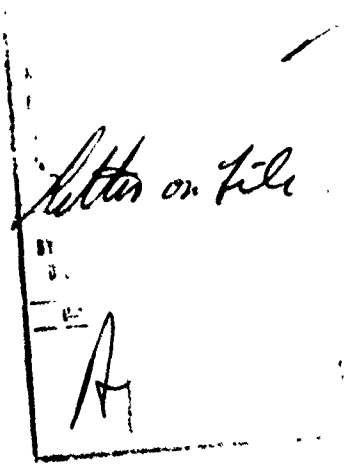

ABSTRACT

This report covers the development of analytical means for predicting and controlling weld distortion of welded aluminum structures. The report presents basic background information and covers the present state-of-the-art by integrating results obtained recently at M.I.T.

Distortion in welded stuructures is caused by three fundamental dimensional changes, namely transverse shrinkage, longitudinal shrinkage and angular change. During the fabrication of actual structures, such as ships, airplanes and buildings which have various types of joints, these dimensional changes are combined. Therefore, shrinkage distortion that occurs in structures can be extremely complex.

After a brief introduction, Section 2 discusses thermal stresses during welding, residual stresses and distortion in a general manner. The subsequent Sections up to Section 6 discuss the analytical and experimental investigations carried out at M.I.T. on the prediction of various fundamental types of distortion. Section 7 deals with methods of distortion reduction, as they were tested by various investigators at M.I.T. Section 8 covers results on residual-stress measurements of laser-welded joints.

TABLE OF CONTENTS

SUMMARY

Welding is used extensively in the fabrication of many structures, including ships, airplanes, buildings, pressure vessels, etc., providing many advantages over other techniques such as riveting, casting, and forging. However, welding is by no means a trouble-free procedure. One of the most troublesome problems encountered is that of distortion. And the more complex a structure is, the more significant and great these dimensional changes are.

The present report covers the state-of-the-art on prediction and control of distortion in welded aluminum structures by integrating results obtained recently at M.I.T. The report covers all the information in seven main sections, as summarized below. At the same time an effort will be done towards giving hints on practical applications of the above results.

After a brief introduction, Section 2 discusses thermal stresses during welding, residual stresses and distortion in weldments in aluminum alloys. Computer programs have been developed to calculate the following:

1. Temperature distribution during welding by both the analytical and the finite-element method.
2. Thermal stresses and metal movement during welding for both the plane-stress and plane-strain conditions, using elasto-plastic finite-element analysis.

The various types of weld distortion can be found in Figure 2.2.

Section 3 deals with the transverse shrinkage of aluminum

butt welds. After an explanation of the mechanism of transverse shrinkage, the effects of various parameters are discussed. The investigations done at M.I.T. aiming towards testing methods for transverse shrinkage reduction are then outlined. All the efforts were driven by the proposed methods shown in Figure 3.6. Figures 3.10 - 3.15 show some results of this investigations. As one can see, chilling the plates with dry-ice causes promotion of heat transfer but does not affect the temperature distribution. On the other hand, an approximate 30% reduction in transverse shrinkage occurs in restraint joints.

Section 4 discusses longitudinal distortion of welded aluminum beams. Previous investigations on that area are first cited and the concept of apparent shrinkage force is introduced. The experiments conducted at M.I.T. are then discussed. Figure 4.6 snows one of the major observations. During the welding process the beams were bent in a convex shape, while concave deflection resulted during the cooling stage. This result led to the establishment of the method of differential heating as a technique for reducing longitudinal distortion of built-up beams. We will discuss this technique in a later paragraph. Eq. (4.6) is also noted as a reasonable approximation of longitudinal deflection at the mid-point of a T-section beam. A computer program was developed for the calculation of the residual deflection at mid-length. Figure 4.9 shows an example of a parametric study done using this program. It can be seen that when welding speed is increased, while current and voltage are kept constant, the amount of distortion decreases rather dractically. On the other hand, when welding speed is increased, while heat input is kept

unchanged, residual distortion increases. There is also an indication that a welding speed exists where distortion becomes maximum.

Out-of-plane distortion in aluminum fillet welds is extensively covered in Section 5. This type of distortion is of significant interest, since it occurs in the very common panel structures (see Fig. 5.1). A one-dimensional semi-analytical method is first discussed. Equation (5.3) and Figures 5.5 and 5.7 summarize the results of this analysis. To be more precise, Eq. (5.3) gives the angular change, ϕ, in a restrained joint (Fig. 5.2b) as a function of structure geometry, of the "coefficient of rigidity for angular changes" C (given in Fig. 5.7) and of the angular change in a free joint, ϕ_o (given in Fig. 5.5 as a function of plate thickness and weight of electrode consumed per weld length). It is noticeable the fact that the angular change is maximum when plate thickness is around 0.3 in.

A two-dimensional analysis using the finite element method is then outlined. This analysis is an extension of the one-dimensional one. However, absolute agreement of analytical and experimental results was not accomplished. The Section ends with a discussion on out-of-plane distortion in actual panel structures and on allowable out-of-plane distortion. It seems that the old Navy specifications for unfairness are difficult to meet although they guarantee the structural integrity of the ship. On the contrary, the new specifications are easy to meet but may not provide this guarantee (see Figs. 5.14 and 5.15).

Section 6 deals with the subject of buckling distortion of thin aluminum plates. An analytical model is first outlined which can give answers to almost all practically realizable boundary conditions (see Table 6.1). Then, results from the experimental investigation are presented, showing good agreement between theory and experiments in most cases. Finally, a systematic approach is proposed which can be used for an overall solution of the problem (Fig. 6.4).

The methods of distortion reduction in aluminum weldments are overviewed in Section 7. After a brief discussion of the commonly used methods, elastic prestraining, as shown in Figure 7.1, is outlined. The basic idea of this technique is to induce a curvature to the plate under consideration, by means of a round bar, in such a way, so that the resulting out-of-plane distortion due to welding is counteracted. Figure 7.6, showing the radius necessary for this counteraction, is a typical result of the experimental investigation.

Next, the well known clamping method is discussed and, finally, the method of differential heating is extensively covered. In the latter method, a web or a flange is heated to a certain temperature before welding to compensate for the welding distortion. Distortion can be reduced significantly by selecting a proper temperature differential. Figure 7.25 summarizes this fact with results obtained by a computer program developed for this analysis.

1. INTRODUCTION

The objective of this research contract is to develop analytical and empirical systems to assist designers, metallurgists and welding engineers in selecting optimum parameters in the design and fabrication of welded structures.

The program includes the following two tasks:

Task 1: Development of a monograph for predicting stresses, strains, and other effects produced by welding.

Task 2: Prediction and control of distortion in welded aluminum structures.

The program started on December 1, 1975, and it is expected to be completed in three years. The program has been conducted under the direction of Professor K. Masubuchi.

1.1 Progress of Task 1

The objective of Task 1 is to develop a monograph. The monograph which is now entitled "Analysis of Welded Structures - Design and Fabrication Considerations," consists of the following sections:

Section I: For practical users

Section II: Text

Section III: Additional tables and figures

Section IV: Computer programs

Section V: Material properties

Section IV: Annotated bibliography

2

Table 1.1 Original Schedule of the Preparation of the Monograph

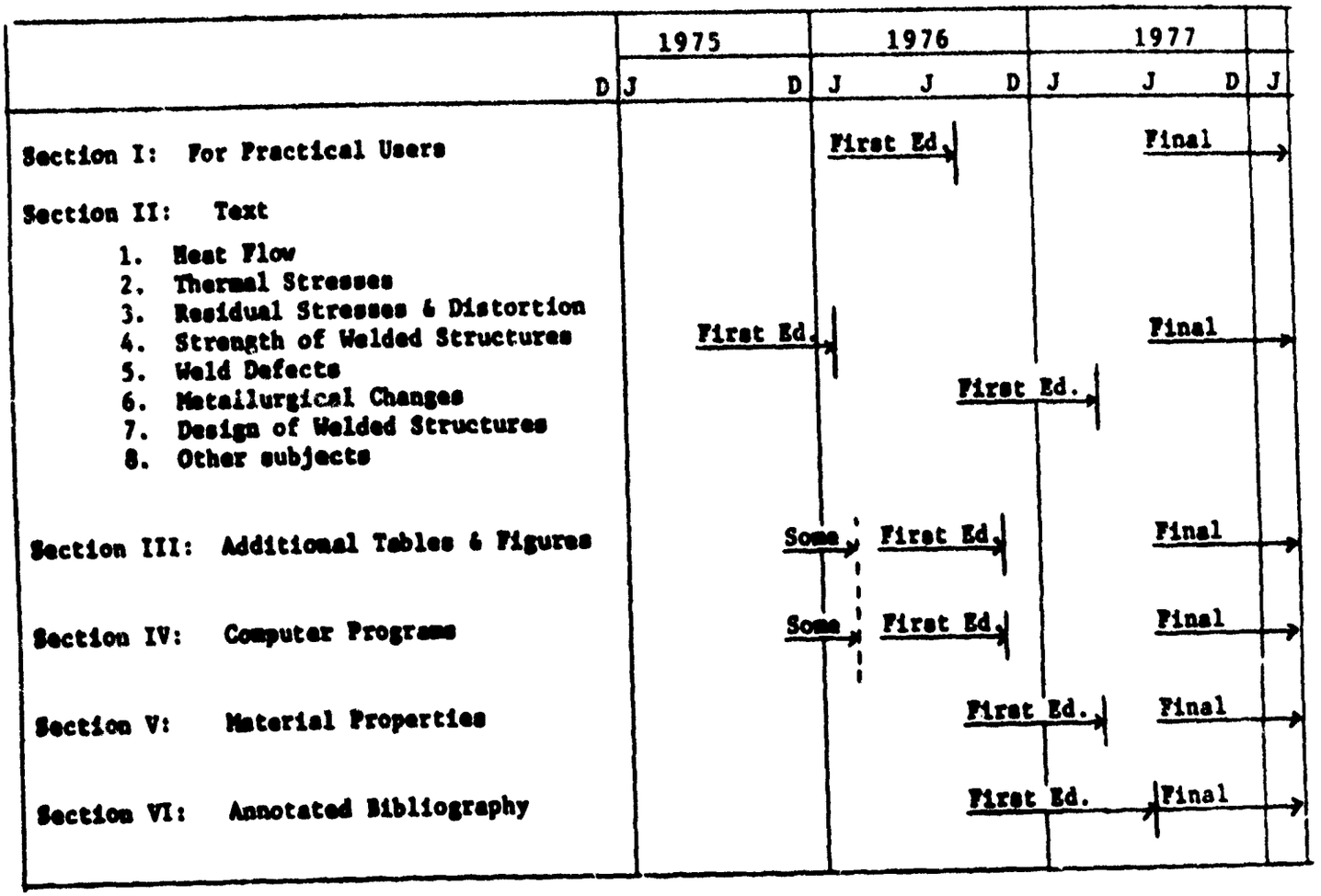

Table 1.2 Contents as of June 1, 1976 of Section II Text of the Monograph*

on

"Analysis of Welded Structures - Design and Fabrication Considerations"

* The contracts are subject to change

Table 1-1 shows the original schedule of the preparation of the monograph.

The emphasis of the efforts so far has been placed on Sections II and IV. Table 1-2 shows the contents as of June 1, 1976 of Section II. The first drafts of Chapter 1, 2, 3, 4, 8, 9, and 10 have been completed and circulated for review. As seen by comparing Tables 1-1 and 1-2, the contents of the monograph have been considerably expanded, while at the same time we are experiencing some delays in preparation. However, we are still confident that the monograph will be completed during the three-year period.

1.2 Progress of Task 2

The objectives of Task 2 are as follows:

(1) Identify potential areas where distortion can cause problems during welding fabrication of aluminum structures, especially surface effect ships. And analyze, as much as possible, the extent of the problems.

(2) Conduct parametric studies of some of the problems and suggest possible remedies which include changes of design and welding procedures.

(3) Conduct research on methods for reducing and controlling distortion of several structural members of surface effect ships.

The program has progress as originally proposed. The progress report[1] dated June 7, 1976 describes the progress made before May 31, 1976. The progress made thus far is described briefly in the following pages.

Fairness Tolerance

First, an analysis was made of out-of-plane distortion of welded panel structures. Computer programs have been developed by Kitamura and Taniguchi to do the following:

(1) Determine allowable unfairness as a function of service conditions (compressive stresses and water pressure) and structural parameters (plate thickness, floor spacing, etc.)

(2) Then determine the maximum weld size to produce the allowable unfairness.

Calculations were made of steel and aluminum structures. Analytical results were compared with unfairness values allowed by Navy specifications. Results of the analysis are described in the Special Report dated July 3, 1975.[2]

The results obtained by the analysis indicate that serious distortion problems can occur during welding fabrication of aluminum structures using plates thinner than 1/2" or 3/8". However, little data have been published on the two-dimensional distribution of distortion in panel structures of aluminum, i. e. a structure in which longitudinal and transverse stiffeners are fillet welded to a plate. Brito conducted a study with the following objectives:

(1) To determine experimentally the out-of-plane distortion in welded panel structures, and compare the data with the Navy specification.

(2) To develop an analytical procedure for predicting out-of-plane distortion caused by angular changes along the fillet welds.

(3) To study experimentally how distortion can be reduced by altering the thermal pattern during the welding of a panel structure.

Beauchamp also studied ways of reducing out-of-plane distortion in panel structures. He studied the effects of both buckling distortion due to butt welds and angular distortion due to fillet welds. He also studied how distortion can be reduced by clamping.

Buckling Distortion

Buckling distortion may become a serious problem in welding fabrication of structures in thin plates, say, 1/4" or less. When the plate is thin, it may buckle due to residual stresses only. A particular nature of buckling distortion is that the amount of distortion is much greater than that caused by angular distortion. Consequently, buckling distortion can be avoided by (1) avoiding the use of plates that are too thin and (2) reducing the spacing between the stiffeners.

As the first step, Pattee studied buckling distortion of butt welds in aluminum. The objectives of his study included the following:

(1) To experimentally determine the buckling behavior (during and after welding) of aluminum plates of various dimensions using a number of different boundary conditions. The experiments were made using 18 butt welds 1/16" to 3/16" thick, 1 to 4 feet wide, and 6 feet long.

(2) To analyze these transient temperature and strain changes by utilizing one-dimensional and two-dimensional computer programs developed at M.I.T. comparing the analytical results with the experimental data.

(3) To determine the critical panel size under which buckling distortion would not occur.

As a result of this study, a computer-aided system has been developed for the prediction and control of buckling distortion. Since the study by Pattee was well under way when this research contract started, only a small portion of his work was supported by the funds from ONR.

The best way to control buckling distortion is to prevent its happening by properly selecting design parameters and welding procedures.** Currently there are no Navy specifications that deal with buckling.

Although Pattee's study provides basic data on butt welds, it is very important to extend the study to cover stiffened panel structures, because in most practical applications the thin plate

** The following is a typical example of buckling distortion that occurred in a manufacturing plant. Workers experienced a sudden increase of distortion after some changes of welding procedures of stiffened panel structures. Stiffeners were spot welded to a thin plate. Spacings between spot welds were decreased to increase the fatigue strength of the structure, and the sudden increase of distortion followed.

Answer: Buckling distortion occurred because the amount of welding exceeded the critical value. Therefore, the problem can be solved by (1) increasing plate thickness, (2) reducing stiffener spacing, or (3) reducing the amount of welding, or using some combination of the above three methods.

structures have stiffeners. Beauchamp has developed data on thermal strains and residual stresses in welded thin panel structures. It is expected that the research on buckling distortion will be continued during the third year.

Longitudinal Distortion of Built-Up Beams

During the last few years, a series of research programs were carried out at M.I.T. on the longitudinal distortion produced during the welding fabrication of T-beams.

Nishida carried out a study program having the following objectives:

(1) To develop a computer program for the analysis of thermal structures and metal movement during the welding fabrication of a built-up beam.

(2) To analyze the effects of the use of clamping and the effects of the thermal pattern on weld distortion.

As a part of the thesis study, Nishida has developed a computer program for analyzing the deflection that occurs during welding fabrication of a T-shaped beam by fillet welding a flange plate to a web plate. The program is capable of studying the effects of clamping and differential heating.*

Nishida analyzed experimental data obtained by Serotta on differential heating. The computer programs developed by Nishida

* In this technique a web or a flange is heated to a certain temperature before welding to compensate for the welding distortion. Distortion can be reduced significantly by selecting a proper temperature differential.

can be used to determine optimum welding and preheating conditions for joining T-beams of various sizes.

Residual Stresses in Laser-Welded Joints

Laser welding, although not fully developed, seems to offer attractive possibilities. We have been fortunate to receive two laser welded specimens (in carbon steel and titanium) through the courtesies of the Air Force Materials Laboratory, Sciaky Brothers, Inc., and Avco Everett Research Laboratories, Inc.

A study was made by Papazoglou to determine the residual stresses in these plates. The results are given in the Appendix A of the progress report dated June 7, 1976.[1] It has been found that residual stresses in the titanium welds are as we expected: high tensile residual stresses exist in the longitudinal direction in areas near the weld, but the width of the tension zone is very narrow. However, the results obtained on the carbon-steel welds are inconclusive. We are hoping to obtain, if possible, another carbon steel specimen to verify the experimental data.

1.3 Scope of This Technical Report

This technical report has been prepared as a part of Task 2. This report provides the present state-of-the-art on prediction and control of distortion in welded aluminum structures by integrating results obtained recently at M.I.T. To avoid excessively lengthy discussion, it is assumed that potential readers of this report have already read or have access to the following two Welding Research Council Bulletins:

(1) WRC No. 149, "Control of Distortion and Shrinkage in Welding," by K. Masubuchi, April 1970.

(2) WRC No. 174, "Residual Stresses and Distortion in Welded Aluminum Structures and Their Effects on Service Performance," by K. Masubuchi.

During the last few years, a number of experimental and analytical studies have been done at M.I.T. on various subjects related to thermal stresses, metal movement, residual stresses and distortion of weldments. These studies were supported by various organizations, including the National Science Foundation, Welding Research Council, Office of Naval Research and a group of companies.* The following is a list of theses on weld distortion since May, 1974:

(1) Yoshinari Iwamura, "Effects of Cooling Rate on Transverse Shrinkage of Butt Joints," M.S. Thesis in May, 1974.

(2) Robert W. Henry, "Reduction of Out-of-Plane Distortion in Fillet Welded High-Strength Aluminum," M.S. thesis in May, 1974.

(3) Frank M. Pattee, "Buckling Distortion of Thin Aluminum Plates During Welding," M.S. Thesis in August, 1975.

(5) Michael D. Serotta, "Reduction of Distortion in Weldments," M.S. Thesis in August, 1975.

---

* Hitachi Shipbuilding and Engineering Co., Ishikawajima-Harima Heavy Industries, Kawasaki Heavy Industries, Kobe Steel Works, Mitsubishi Heavy Industries, Mitsui Engineering and Shipbuilding Co., Nippon Kokan K.K., Nippon Steel Corp., Sasebo Heavy Industries, and Sumitomo Heavy Machineries Co.

(6) Jye-Suan Hwang, "Residual Stresses in Weldments in High-Strength Steels," M.S. Thesis in January, 1976.

(7) Michio Nishida, "Analytical Prediction of Distortion in Welded Structures," M.S. Thesis in March, 1976.

(8) Victor M. B. Brito, "Reduction of Distortion in Welded Aluminum Frame Structures," M.S. Thesis in May, 1976.

(9) David G. Beauchamp, "Distortion in Simple, Welded Aluminum Structures," M.S. Thesis in May, 1976.

Most of the above theses dealt with aluminum structures.

Studies also were conducted by several post doctoral researchers including Dr. T. Muraki, Dr. K. Kitamura, and Professor C. Taniguchi.

This report integrates important results obtained in these studies. We recognize fully that a number of research programs have been carried out recently in various laboratories in the world on weld distortion in welded aluminum structures. We intend to integrate results obtained in other laboratories in the final report which will be published around the end of 1977.

We feel that there is a definite advantage of publishing a technical report now, because of the following reasons:

(1) People in the Navy and other organizations who are interested in this research program will have the opportunity to obtain the results generated in this research and other related studies at M.I.T. now instead of waiting until the completion of this program.

(2) We hope that some of the readers of this report will provide us some comments and ciriticisms, which will be incorporated in the final report.

2. THERMAL STRESSES DURING WELDING, RESIDUAL STRESSES AND DISTORTION

This chapter serves as an introduction to the following ones. After a brief outline of the state of the art of temperature distribution prediction during welding, an effort is made towards an understanding of the mechanism of residual stress formation. This is followed by a brief introduction to the various kinds of distortion, as established by Masubuchi.[3, 4]

2.1 Temperature Distribution During Welding

Deformations during welding are caused by a plastic flow, due to the non-uniform heating of the material. Accurate determination of the magnitude of the deformation presupposes the exact knowledge of the temperature distribution during welding.

A lot of effort has been done during the last years at M.I.T. and elsewhere towards this aim.

The first analytical attack to the problem was done by Rosenthal[5, 6, 7] thirty years ago. He solved the governing equation of heat transfer:

$$\frac{\partial}{\partial x}(k\frac{\partial T}{\partial x}) + \frac{\partial}{\partial y}(k\frac{\partial T}{\partial y}) + \frac{\partial}{\partial z}(k\frac{\partial T}{\partial z}) + W_i = \rho c\frac{\partial T}{\partial t} \qquad (2.1)$$

where

(x, y, z) = Cartesian coordinates

T = temperature

k = thermal conductivity

ρ = material density

c = specific heat

W_i = heat source

using a moving heat source, under the following basic assumptions:

(1) The physical characteristics of the metal are independent of temperature and uniform in space.

(2) The speed v of the moving source and the rate of heat input are constant.

The solution to the above equation for the 2D case is:

$$T = T_o + \frac{q}{2\pi k} e^{-\frac{\upsilon}{2\lambda}\xi} K_o\left(\frac{\upsilon}{2\lambda} r\right) \qquad (2.2)$$

where

$q = \frac{1}{h} \eta_a (0.24\ VI)$

$\xi = x - \upsilon t$

$r = \sqrt{\xi^2 + y^2}$

K_o = modified Bessel function of second kind and zero order

T_o = initial temperature

V = voltage

I = current (amps)

η_a = arc efficiency

q = intensity of heat source

h = plate thickness (in)

y = welding coordinate perpendicular to weld path (x)

λ = thermal diffusivity (= $\frac{k}{\rho c}$)

Nishida[8] contained in his thesis some refinements to the above solution taking into account effects of heat loss from the surface, finite breadth of plates and variable properties (adopting

an iterative procedure). He also enclosed a computer program performing these calculations.

It is worth noting at this place that the above analytical method is very useful, giving reasonably accurate results, for the cases of workpieces having regular shape and small thickness or for sufficiently long rectangular bars.

The analytical method is also useful for predicting the temperature distribution if electron-beam welding or laser welding is used even for the case of thick plates. In usual practice, however, some kind of welding groove is made and multipass techniques are used, which make the heat flow and heat dissipation near the weld extremely complex and difficult to predict from the point of view of welding distortion. To overcome these computational difficulties one has to rely on numerical methods using the high-speed computers which are available today.

The numerical methods mentioned comprise the finite difference methods and the finite element method. Both methods are examined in Nishida's thesis, where the pros and cons of each one are investigated. At the present time there is, at M.I.T., a computer program developed by Muraki,[9] which can calculate the 3D temperature distribution during welding using the finite element method. The program as well as instructions for its use can be found in reference.[9] However, it should be pointed out that due to its inefficiency (high cost) the program has not yet been tested exhaustively.

2.2 Thermal Stresses During Welding-Residual Stresses

Due to local heating by the welding arc, complex thermal stresses are produced in regions near the welding arc. Figure 2.1 shows schematically changes of temperature and stresses during welding. A butt joint is being welded along the x-axis. The welding arc, which is moving at speed V is presently located at the origin 0, as shown in Figure 2.1a.

Figure 2.1b shows the temperature distribution along several cross sections. Along section A-A, which is ahead of the welding arc, the temperature change due to welding, ΔT, is almost zero (see Fig. 2.1b-1). Along section B-B, which crosses the welding arc, the temperature distribution is very steep (Fig. 2.1b-2). Along section C-C, which is some distance behind the welding arc, the temperature change due to welding again diminishes (Fig. 2.1b-4).

Figure 2.1c shows the distribution of stresses in the x-direction, σ_x, across the sections. Stresses in the y-direction, σ_y, and shearing stresses, τ_{xy}, also exist in a 2D field.

Along section A-A thermal stresses due to welding are almost zero (Fig. 2.1c-1). The stress distribution along section B-B is shown in Fig. 2.1c-2. Stresses in regions somewhat away from the arc are compressive. The expansion of these areas is restrained by the surrounding metal which is at a lower temperature. Since the temperature of these areas is quite high and the yield strength of the material is low, stresses in these regions are as high as the yield strength of the material at the corresponding temperatures. The magnitude of the compressive stress passes through a maximum

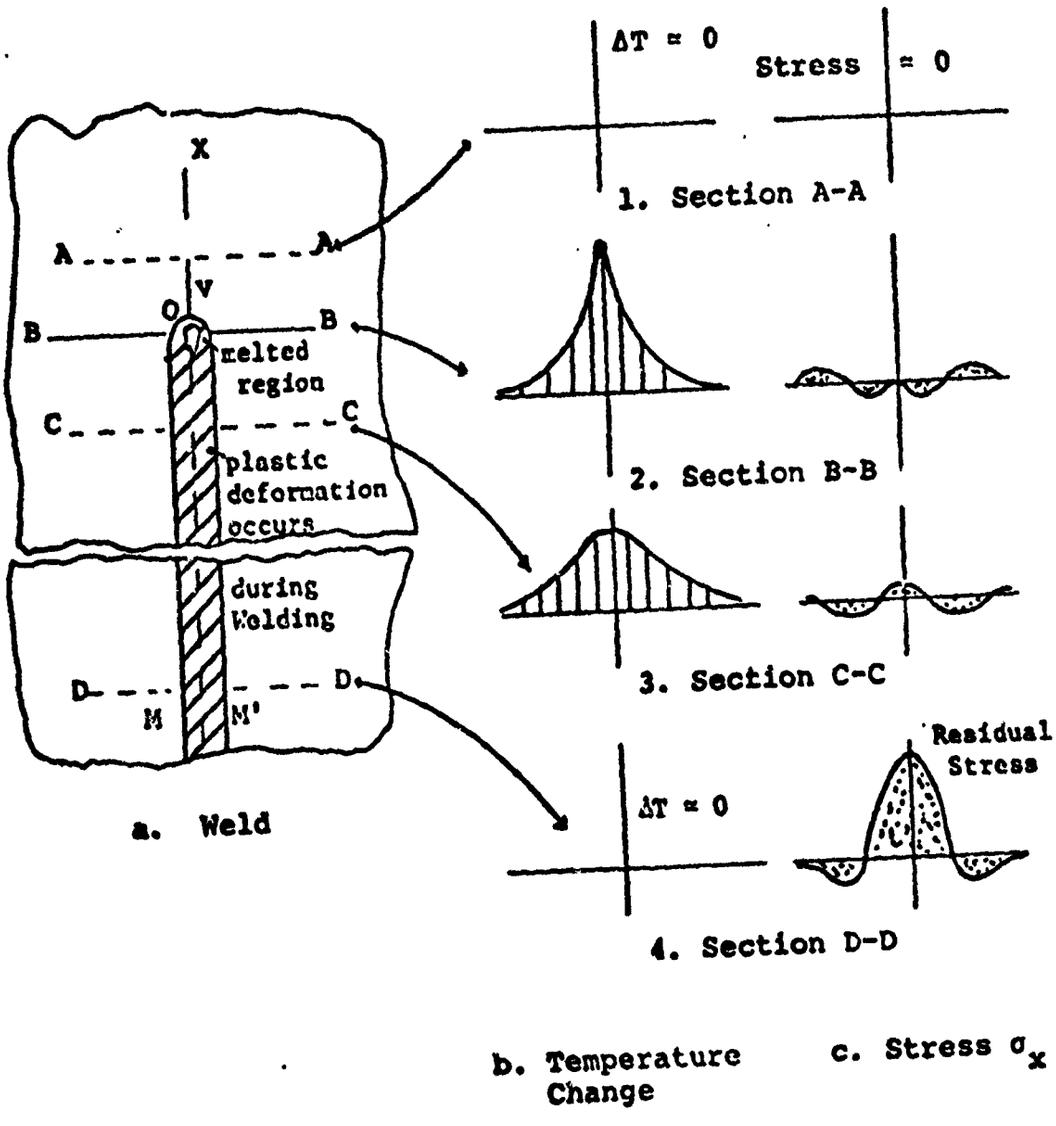

Figure 2.1 Schematic Representation of Changes in Temperature and Stress during Welding

as the distance from the weld increases. However, stresses in areas well away from the weld are tensile and balance with compressive stresses in areas near the weld. In other words

$$\int \sigma_x dy = 0 \qquad (2.3)$$

across section B-B. Thus, the stress distribution is as shown in Figure 2.1c-2.

Stresses are distributed along section C-C as shown in Figure 2.1c-3. Since the weld metal and base metal regions near the weld have cooled, they try to shrink causing tensile stresses in regions close to the weld. As the distance from the weld increases, the stresses first change to compressive and then to tensile.

Figure 2.1c-4 shows the stress distribution along section D-D. High tensile stresses are produced in regions near the weld, while compressive stresses are produced in regions away from the weld. The distribution of residual stresses that remain after welding is completed is as shown in the figure.

The cross-hatched area M-M in Figure 2.1a shows the region where plastic deformation occurs during the welding thermal cycle. The ellipse near the origin indicates the region where the metal is molten. The region outside the cross-hatched area remains elastic during the entire thermal cycle.

As shown in Figure 2.1, thermal stresses during welding are produced by a complex mechanism which involves plastic deformations over a wide range of temperatures from room temperature up to the melting temperature. Because of the difficulty in analyzing

plastic deformation, especially at elevated temperatures, mathematical analyses were limited for very simple cases, such as spot welding.*

At M.I.T. systematic research has been conducted since 1968 on transient thermal stresses and residual stresses, especially in connection with distortion. Computer programs were developed both for the one-dimensional and the two-dimensional cases.

The 1-D computer program is an improvement over the one developed at Battelle.** Details for this can be found in reference.(10)

The current M.I.T. 2-D computer programs, as developed by Muraki,(11) are based upon elasto-plastic finite-element analyses of thermal stresses and metal movement during welding. The programs are capable of computing stresses under the plane-stress and plane-strain conditions. A finite-element formulation has been derived in the general form which includes temperature dependency of material properties and the yield condition. Reference (11) descrives this program.

2.3 Weld Distortion

As it was mentioned before, during welding, complex strains in the weld metal and in the adjacent base metal region are caused by the non-uniform heating and cooling cycle. Their respective

---

* The WRC Bulletin 149 written by K. Masubuchi describes examples of past calculations.

** The 1-D program is based upon the assumption that stress changes in the welding direction are much less than those in the transverse direction, i.e. $\frac{\partial \sigma}{\partial x} \ll \frac{\partial \sigma}{\partial y}$, in Fig. 2.1. Then, from the equilibrium conditions of stresses, one can assume that: $\sigma_x = t(y)$, $\sigma_y = \tau_{xy} = 0$

stresses combine and react to produce internal forces that can cause bending, rotation and buckling. Collectively they are known as welding shrinkage distortion. The induced stresses are usually accompanied by plastic upsetting and even material yield in some instances.

The distortion found in fabricated structures is caused by three fundamental dimensional changes that occur during the welding process:[3]

(1) Transverse shrinkage, occurring perpendicular to the weld line.

(2) Longitudinal shrinkage, occurring parallel to the weld line.

(3) Angular distortion, consisting of rotation around the weld line.

These distortion are shown in Figure 2.2 and are classified by their appearance as follows:

(a) Transverse shrinkage. Shrinkage perpendicular to the weld line.

(b) Angular change (or transverse distortion). Due to non-uniform thermal distribution in the direction of thickness, distortion (angular change) is caused close to the weld line.

(c) Rotational distortion. Angular distortion in the plane of the plate due to thermal expansion.

(d) Longitudinal Shrinkage. Shrinkage in the direction of the weld line.

(e) Longitudinal distortion. Distortion in a plane through the weld line and perpendicular to the plate.

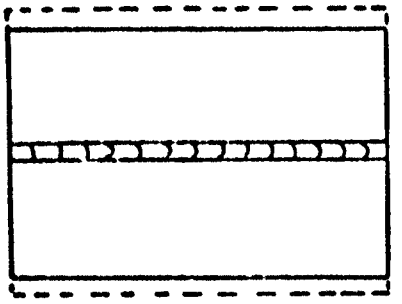

(a) Transverse Shrinkage

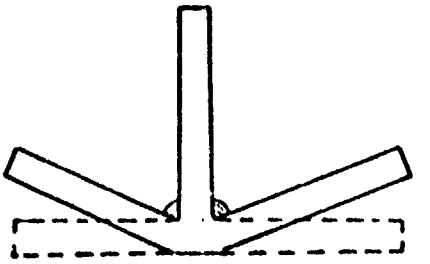

(b) Angular Change

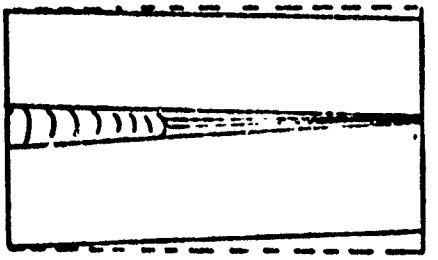

(c) Rotational Distortion

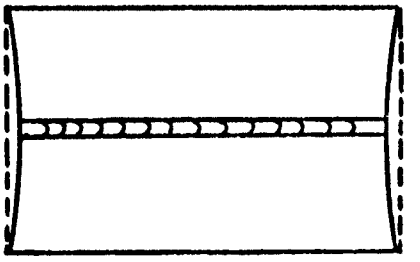

(d) Longitudinal Shrinkage

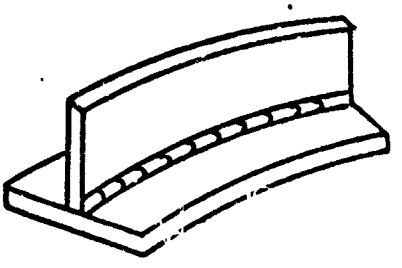

(e) Longitudinal Distortion

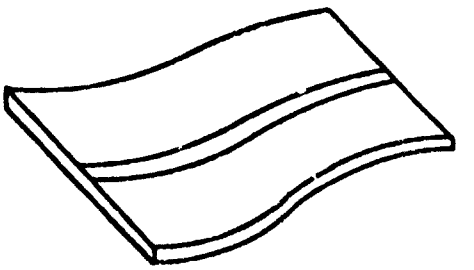

(f) Buckling Distortion

FIG. 2.2 VARIOUS TYPES OF WELD DISTORTION

(f) Buckling distortion. It is due to the instability generated in thin plates by thermal compressive stresses.

The distortion of a structure has been found to cause many problems, the main one being a reduction in the strength of the welded structure due to the locked-in residual stresses. But other than this the finished geometry of a welded structure with distortion is very obvious. The part of structure you end up with is not necessarily the one you require. This leads to costly repair work or total refabrication.

In the following chapters an effort will be done to summarize the state of the art of distortion evaluation as it was established at M.I.T. during recent research studies. The last chapter will cover the various methods of distortion reduction that were tried at the same period.

3. TRANSVERSE SHRINKAGE OF ALUMINUM BUTT WELDS

As it was pointed out in section 2.3, by transverse shrinkage we mean the one occurring perpendicular to the weld line. Excessive shrinkage causes mismatch of joints or loss of the functions of a structure. Current techniques do not allow the removel of existing transverse shrinkage. Common practice, however, is to prepare structural parts to be welded in enlarged dimensions, taking into account an estimated amount of shrinkage.

Many investigators, including Capel,[12] Gilde,[13] Cline,[14] Campus,[15] Weck,[16] Gyuot,[17] Sparangen and Ettinger,[18] Malisius,[19] Watanabe and Satoh,[20] and Naka,[21] have proposed formulas for the estimation of transverse shrinkage of butt welds, which by and large are based on empirical information. Some of these formulas are contained in Welding Research Council (WRC) Bulletins 149 and 174, written by Masubuchi.

The mechanism of transverse shrinkage of butt welds was analyzed by Naka[21] and Matsui[22] in Japan. A summary of their analysis will be included in the following. Experimental results on aluminum butt welds obtained by Iwamura[23] during his stay at M.I.T. will be also included.

3.1 Mechanism of Transverse Shrinkage of Butt Welds

Figure 3.1 shows schematic changes of transverse shrinkage of a single-pass butt weld in a free joint after welding.

Shortly after welding, the heat of the weld metal is transmitted into the base metal. This causes the base metal to expand,

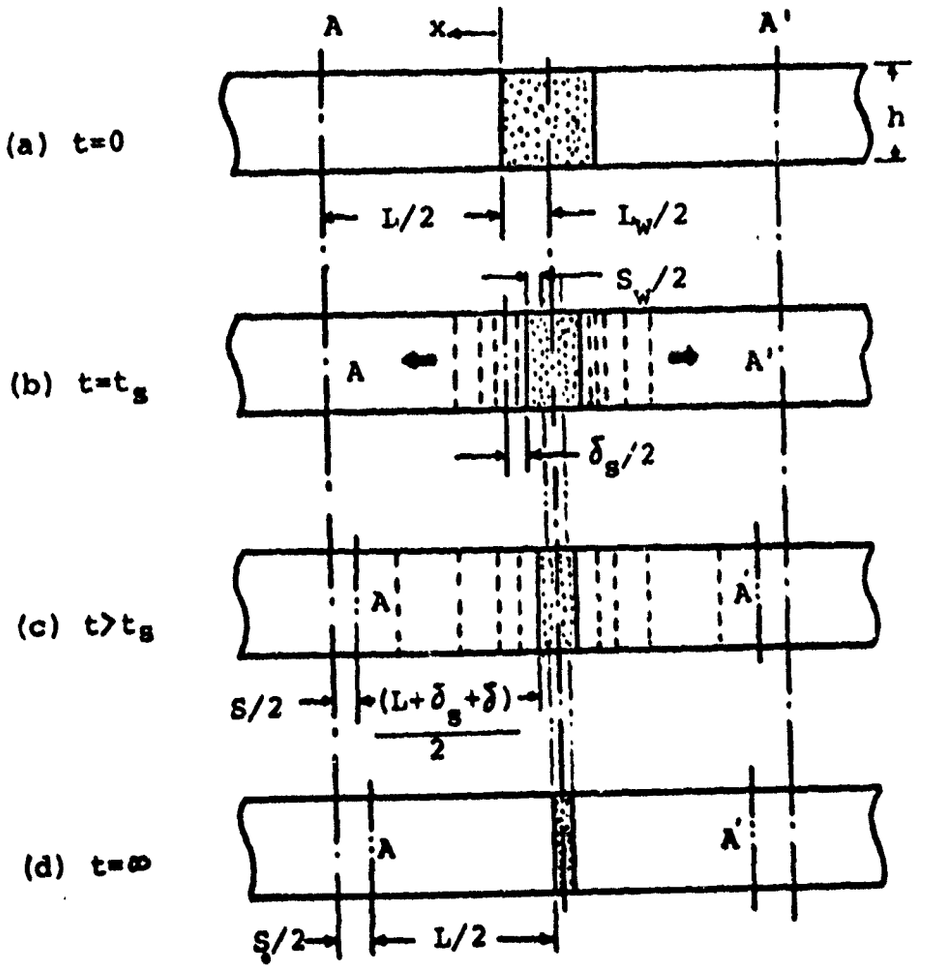

Fig. 3.1 Schematic Presentation of Transverse Shrinkage of a Butt Weld in a Single Pass

with a consequent contraction of the weld metal. During this period the points of sections A and A' do not move (Fig. 3.1b).

When the weld metal begins to resist the additional thermal deformation of the base metal, points of sections A and A' begin to move in response. This starting time of the movement of A and A' is indicated by t_s.

The various thermal deformations of both the weld and base metals are defined as follows:

δ_s : thermal expansion of the base metal at $t = t_s$.

δ : additional thermal deformation of the base metal caused in $\overline{AA'}$ at $t > t_s$.

S_W : thermal contraction of the weld metal at $t > t_s$.

The above deformations can be calculated by the following relations:

$$\delta_s = 2\int_0^{L/2} [\alpha(T) \cdot T(t_s, x) - \alpha(T_o) \cdot T_o]dx \qquad (3.1)$$

$$\delta = 2\int_0^{L/2} [\alpha(T) \cdot T(t, x) - \alpha(T) \cdot T(t_s, x)]dx \qquad (3.2)$$

$$S_w = [\alpha(T_M) \cdot T_M - \alpha(T_o) \cdot T_o] \cdot L_w \qquad (3.3)$$

where

$\alpha(T)$ = thermal expansion coefficient

$T(t, x)$ = temperature

T_M = melting temperature

T_o = initial and final (room) temperature.

Using the above results, the transverse shrinkage can now be calculated from:

$$S = \begin{cases} 0 & \text{for} \quad 0 \leq t \leq t_s \\ -\delta + S_w & \text{for} \quad t > t_s \\ \delta_s + S_w & \text{for} \quad t = \infty \end{cases} \qquad (3.4)$$

Thus we may conclude that the final transverse shrinkage depends on the thermal expansion of the base metal at $t = t_s$ and the thermal contraction of the weld metal.

Investigating the above conclusion further we may use the following experimental data:

Material : aluminum, 2219 - T87

Heat Input : 16,100 joules/in

Plate Thickness : 0.25 in.

Root Gap : 0.1 in.

Shrinkage : 0.026 in.

Using a constant thermal expansion coefficient, the thermal contraction of the weld metal can be estimated from equation (3.3):

$$S_w = 0.1 \times 17 \times 10^{-6} \times (1220 - 70) = 0.002$$

This means that S_w is less than 8% of the total shrinkage. Therefore, the thermal expansion of the base metal caused at $t = t_s$ is the most important factor in the final shrinkage of a single-pass butt weld in a free joint.

Effect of Plate Thickness

If we use the analytical method of temperature distribution prediction for a welded plate, as discussed in Section 2.1, and make the following assumptions:

a. Constant thermal expansion coefficient

b. Thermal radiation neglected and

c. Thermal contraction of weld metal neglected

we come up with the following formulas for the transverse shrinkage:

(1) for a thin plate

$$S = \frac{Q}{c\rho h} erf(\beta_s) \qquad (3.5)$$

(2) for a thick plate

$$S = \frac{Q}{c\rho 2\pi\lambda t_s}\left[1 + 2\sum_{n=1}^{\infty} e^{-\frac{(nh)^2}{4\lambda t_s}}\right] erf(\beta_s) \qquad (3.6)$$

where $\beta_s = \frac{L}{4\pi\lambda t_s}$

Q = heat input

c = specific heat

ρ = density

λ = thermal diffusivity

h = plate thickness

Equation (3.5) indicates that the final shrinkage decreases linearly with increasing plate thickness. Figure 3.2, which shows experimental results obtained by Matsui,[22] confirms the above statement. The figure also shows that in a thicker plate transverse shrinkage starts earlier, but the final shrinkage is smaller.

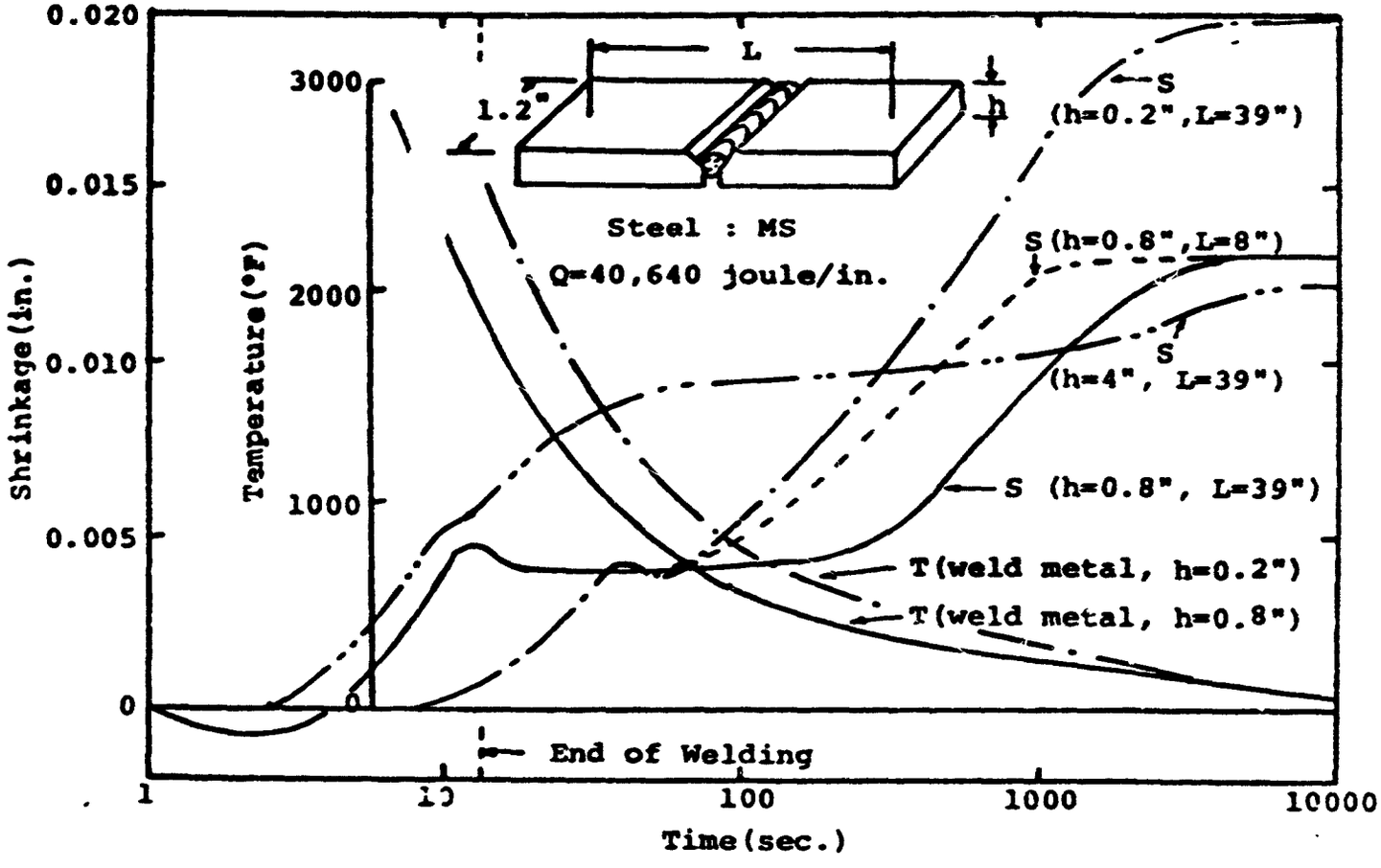

Fig. 3.2 Transverse Shrinkage During Welding and Cooling for Various Plate Thicknesses(h) and Measuring Distances(L) in Free Butt Joints(11)

Effect of Restraint

Watanabe and Satoh[20] performed a series of experiments on various degrees of restraint. They proposed an empirical formula for transverse shrinkage in restraint butt welds, as shown in Figure 3.3a. It can be seen that the final transverse shrinkage decreases as the degree of restraint increases.

Matsui measured the stresses in weld metals for fixed butt welds. The weld depth for all tests was almost identical. The degree of restraint is higher as plates become thicker. Figure 3.3b shows the changes of stresses during welding and cooling. The yield stress of the material used was 40 ksi at room temperature. The stresses of two of three tests exceeded the yield stress.

Effect of Materials

The amount of transverse shrinkage will be different for various materials because of different material properties related to equations (3.5) and (3.6). For example, aluminum alloys, in comparison with steel, have more shrinkage because of higher heat conductivity and thermal expansion coefficient.*

Phase transformation, present in ferrous materials, plays also an important role. Matsui[22] has proposed that the expansion due to phase transformation should be subtracted from the estimated shrinkage in order to predict the real shrinkage (Fig. 3.4). As one can see from the figure, the actual shrinkage in 9% nickel steel was about 70% of the extimated shrinkage by means of eqn. (3.6).

Effect of Multipass Welding

Kihara and Masubuchi[24] conducted empirical studies on transverse shrinkage during multipass welding of constrained butt

* See pages 8 and 9 of WRC No. 174

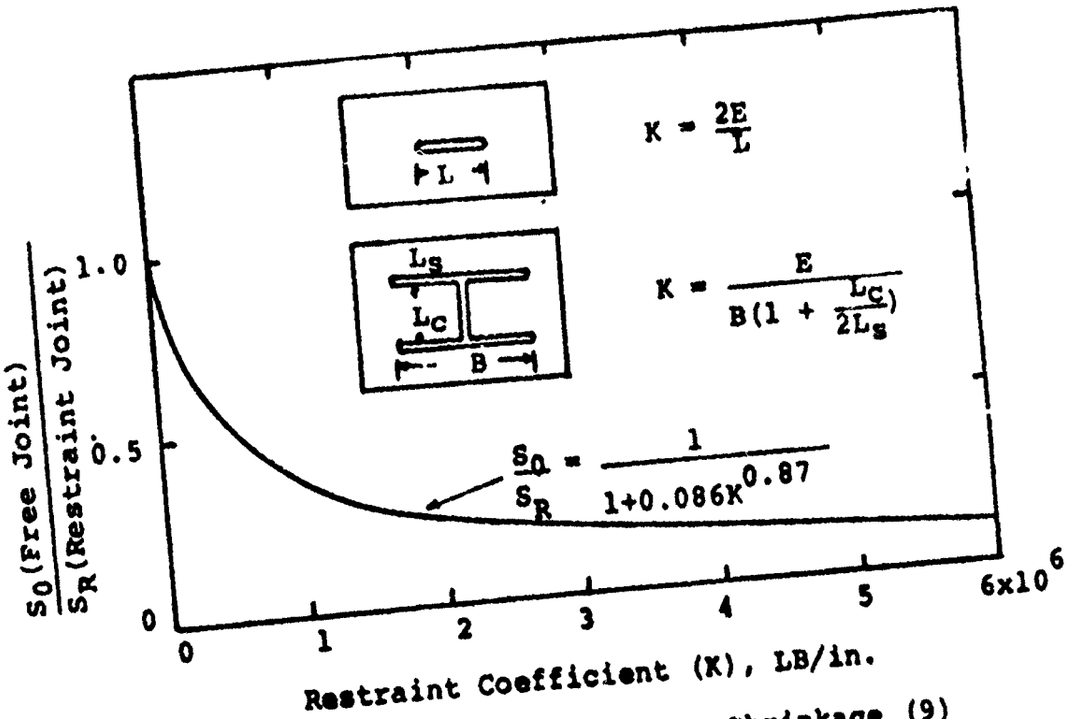

(a) Effect of Restraint on Transverse Shrinkage (9)

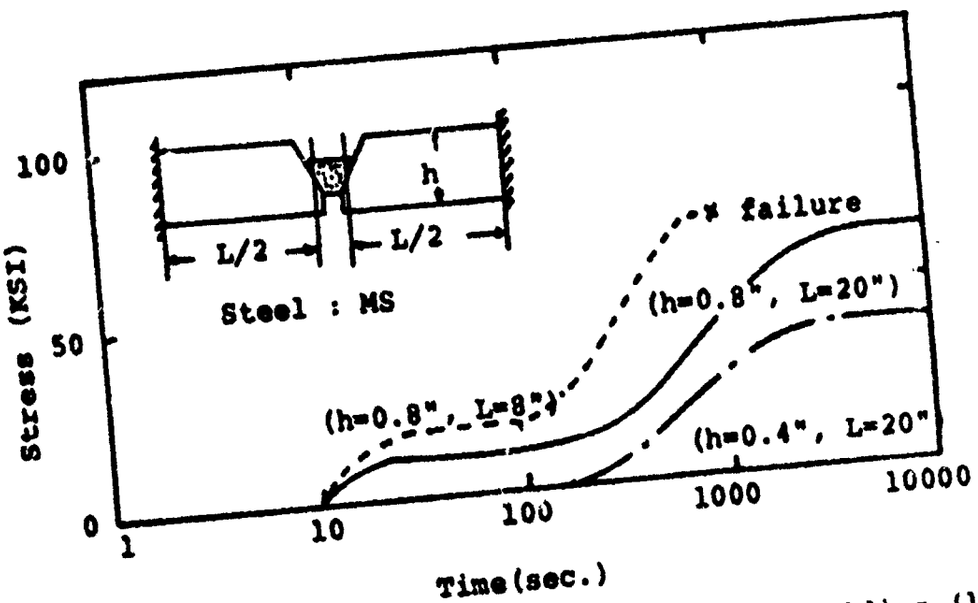

(b) Stresses in Weld Metals in a Single Pass Welding (11)

Fig. 3.3 Effects of Restraint on Transverse Shrinkage and Stress in Butt Welds (9), (11)

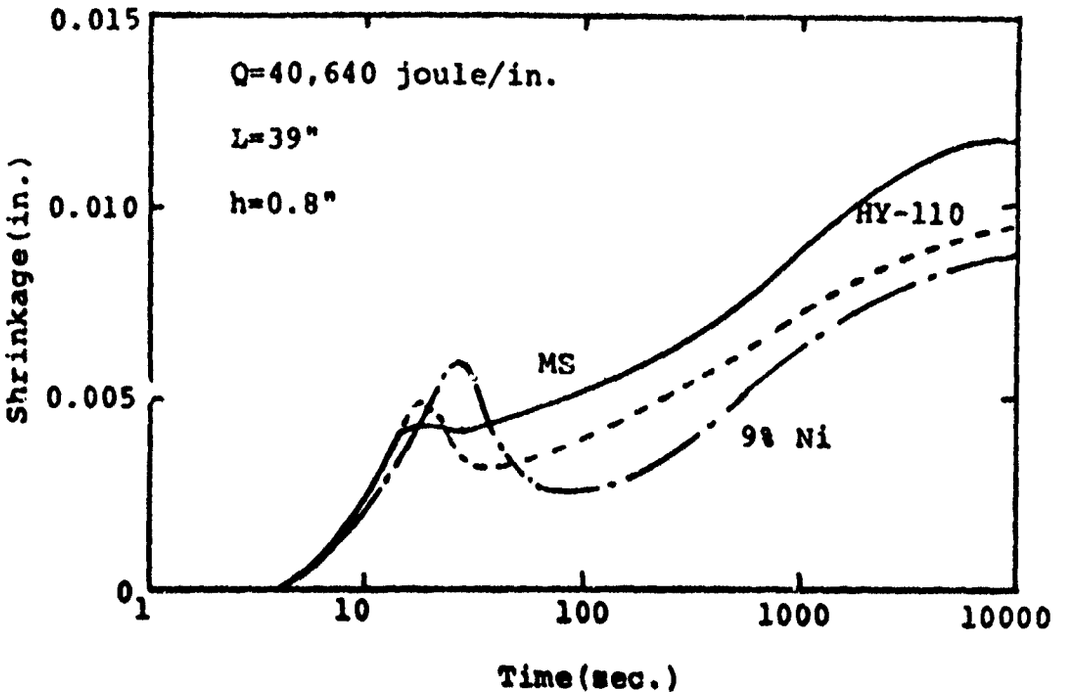

(a) Transverse Shrinkage During Welding and Cooling

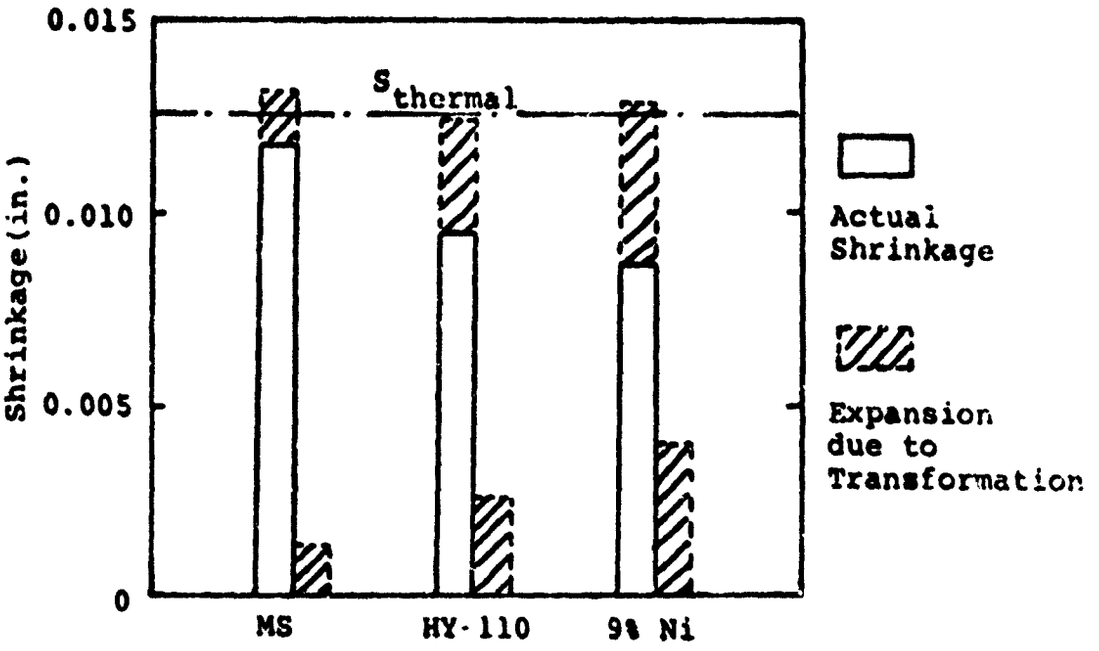

(b) Final Transverse Shrinkage

Fig. 3.4 Effects of Phase Transformation on Transverse Shrinkage (11)

joints in carbon steel. Figure 3.5 shows the increase of transverse shrinkage in multipass welding. It can be seen that the rate of shrinkage increase diminishes during later passes. This happens because the resistance that previous welds give against the thermal expansion of the base metal increases as the weld becomes larger.

Effect of Welding Length

The mechanism described above is based on a short weld length. The weld length in actual structures is, however, of the order of 10 to 20 feet. This makes the transverse shrinkage even more complicated, because of the influence of rotational distortion and nonuniform constraint.

3.2 Reduction of Transverse Shrinkage

3.2.1 Previous Investigations

Kihara and Masubuchi[24] found that a linear relationship existed between transverse shrinkage and the logarithm of the weight of the weld metal deposited. On the basis of this relationship Masubuchi[24] has proposed a methodology for reduction of transverse shrinkage. This is shown in a schematic diagram in Figure 3.6 and can be analysed as follows:

Method 1: Decrease the total weight of weld metal, as shown by arrow 1. The amount of shrinkage changes from B to C. (Use the narrow gap welding process developed at Battelle).

Method 2: Decrease the tangent of the line $\bar{A}B$, as shown by arrow 2. The amount of shrinkage changes from B to D. (Make the root gap narrower).

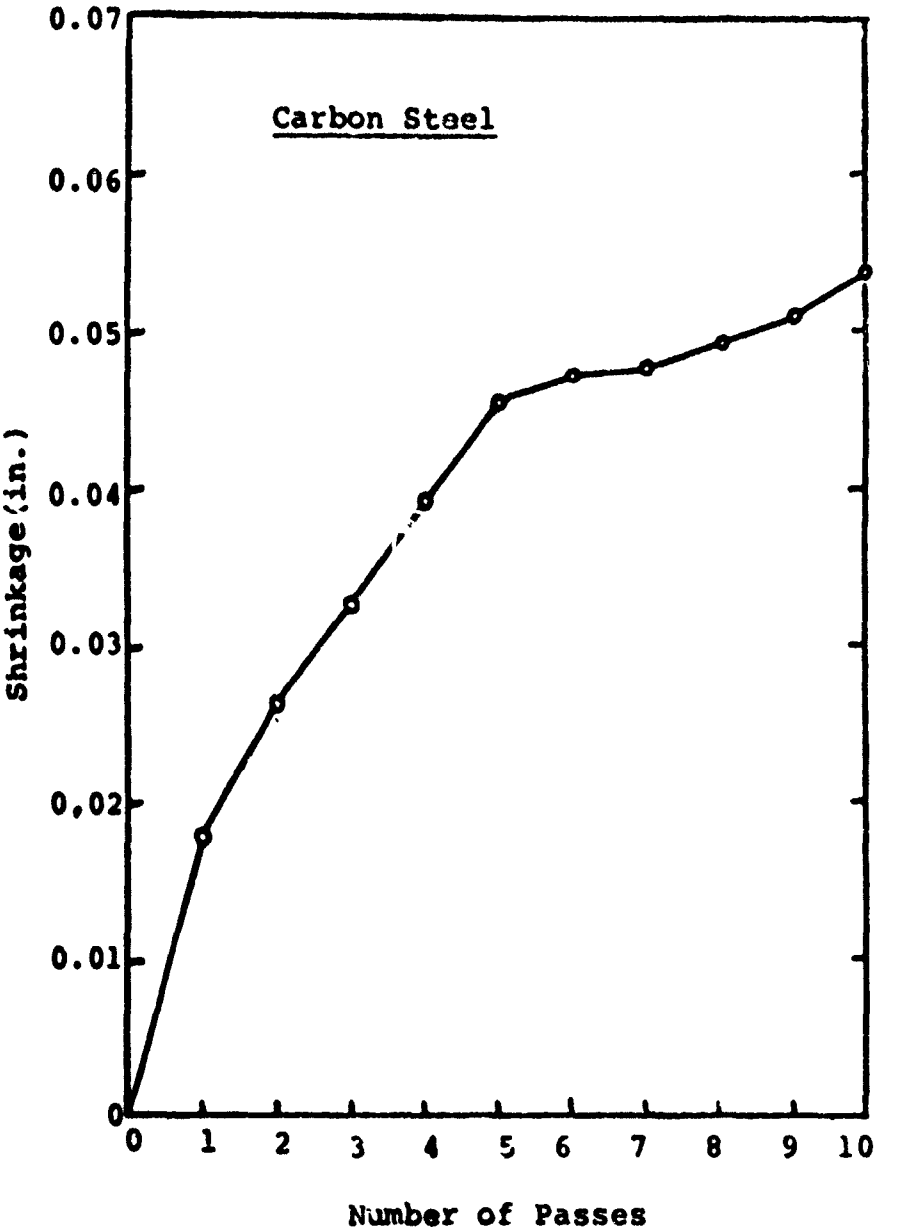

Fig.3.5 Increase of Transverse Shrinkage in Multipass Welding of a Constraint Butt Joint (13)

Method 3: Move the shrinkage for the first pass from A to A', as shown by arrow 3. The amount of shrinkage changes from B to E. (Use a larger diameter electrode).

Method 4: Minimize shrinkage caused in the first pass from A to A" and decrease the tangent of $\overline{AB}$, as shown by arrow 4. The amount of shrinkage changes from B to F. (Increase the degree of restraint).

3.2.2 Study Made at M.I.T.

Iwamura[23] conducted a study at M.I.T. on the effect of chilling and restraining on transverse shrinkage of butt welds in thin aluminum plates. His study included a theoretical analysis as well as a series of experiments.

Theoretical Analaysis

His theoretical analysis included two kinds of butt joints, one free and the other H-type restraint as shown in Figure 3.7. The analysis included both heat conduction and thermal deformation of models with short weld lengths.

The heat conduction analysis was done for one-dimensional and two-dimensional models, in an effort to include the chilling effect in some of them. The thermal properties of the material were assumed temperature independent.

The thermal deformation analysis was done using elasto-plastic theory and the load increment method. No consideration of mechanical strain was done for the free butt joint, since transverse shrinkage is the result of deformation due to thermal strain only, as mentioned in 3.1. For the restraint joint only stresses σ_x are considered (1-D analysis). Weld metal is not taken into account

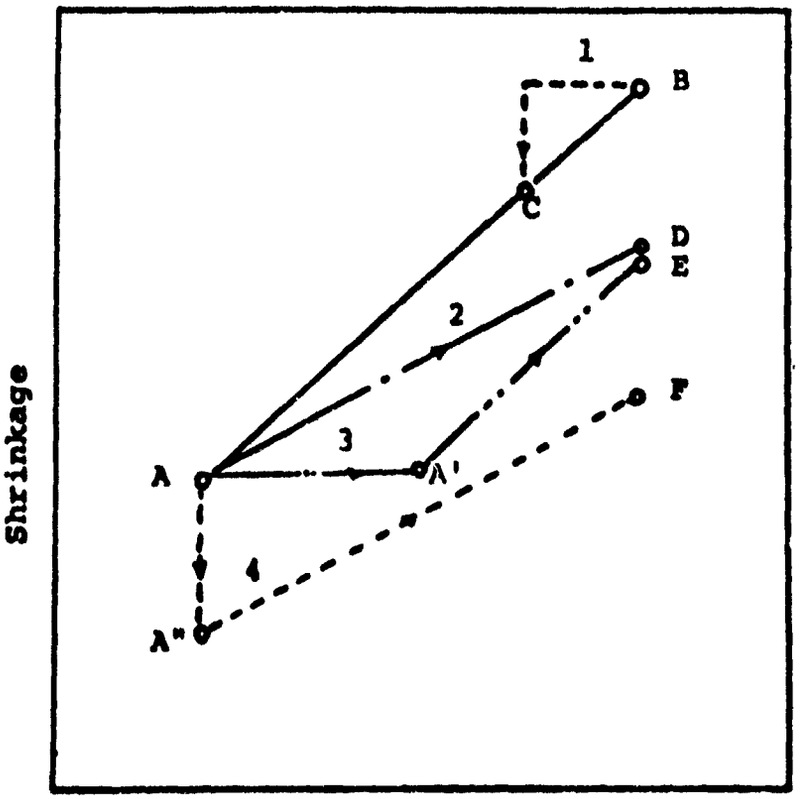

Fig. 3.6 Schematic Diagram Showing Four Methods of Reducing Transverse Shrinkage of Butt Welds (14)

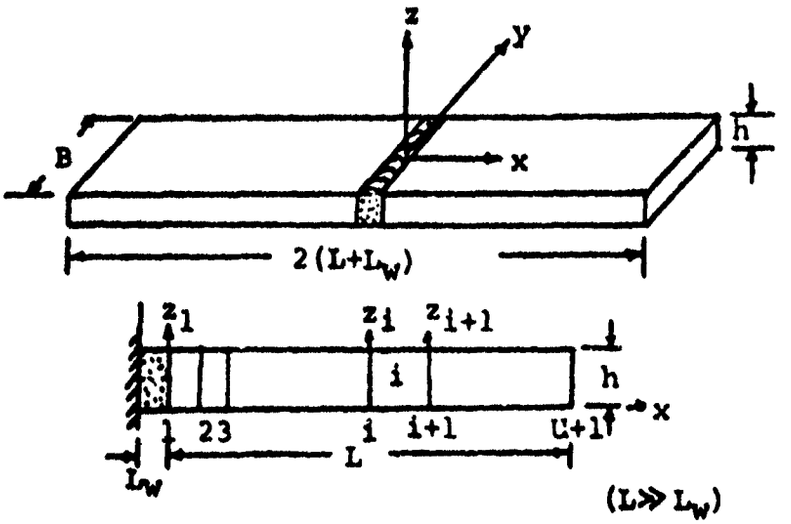

(a) Free Butt Joint

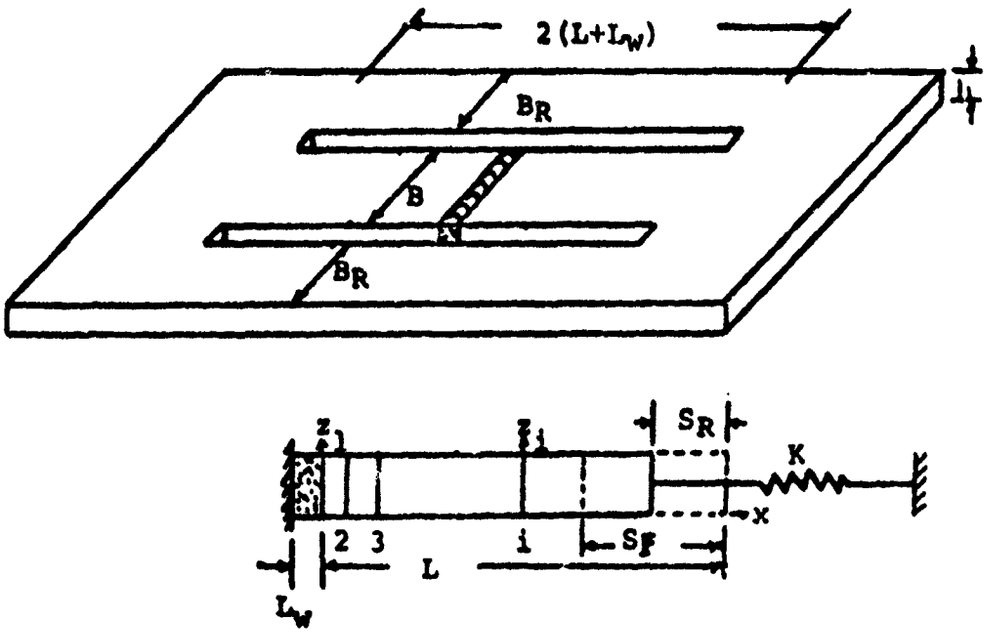

(b) H-Type Restraint Butt Joint

Fig. 3.7 Models for Theoretical Analysis

in the analysis. Temperature dependent material properties are used.

Detailed description of the analysis can be found in his thesis, where a computer program is also included to perform the calculations.

Experimental Analysis

A series of eight experiments was performed measuring temperature, strain and transverse shrinkage changes during welding. Material used was 6061-T6 aluminum. The plates were 1/4 in. thick. Weld length was 4 in. for all specimens, both the free butt joint and the H-type restraint ones. Four specimens two of each type, were chilled using dry-ice. There was also an effort to prevent angular change during welding. An automatic GMA welding machine was used with 200 amp., 25 V, 0.25 in./sec and heat input of 20,000 joules/in.

A description of the test specimens in shown in Figure 3.8, where locations of strain gages and thermocouples are indicated. Figure 3.9 provides information about the constraining and chilling equipments.

Analysis of Results

The following table lists the designation of tests included in the discussion to follow:

	Joints	
Cooling	Free	Restraint
Cooled in the air	FN-1	RN-1, RN-3
Cooled with dry-ice	FC-1	RC-1

6061-T6 Aluminum alloy (1/4" thick)

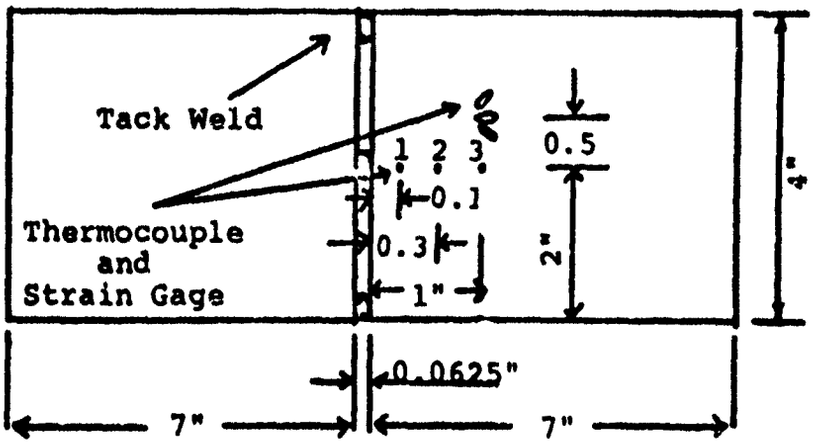

(a) Free Butt Joint

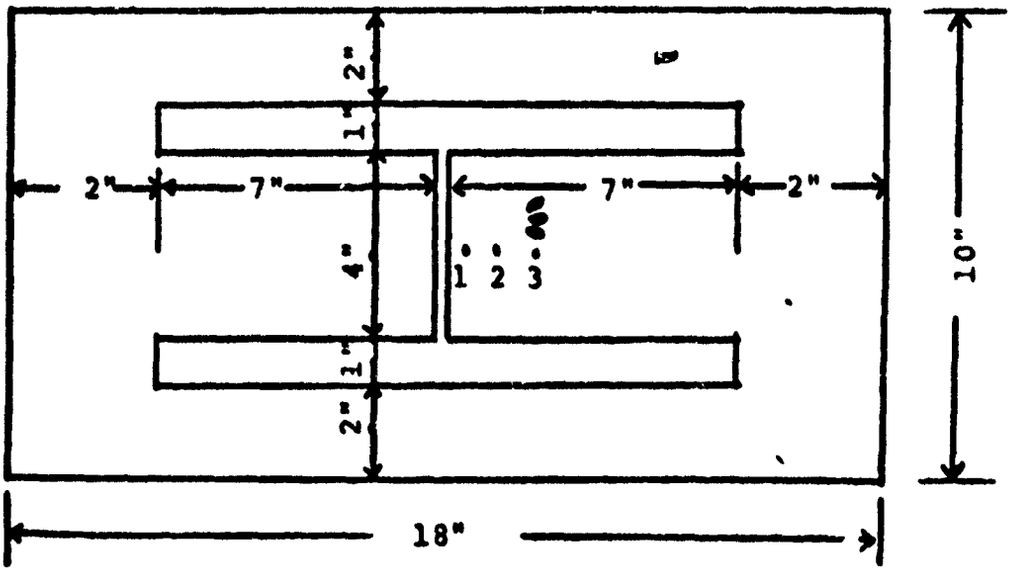

(b) Restraint Butt Joint

Fig. 3.8 Dimensions of Specimens and Locations of Measuring Temperature and Strain

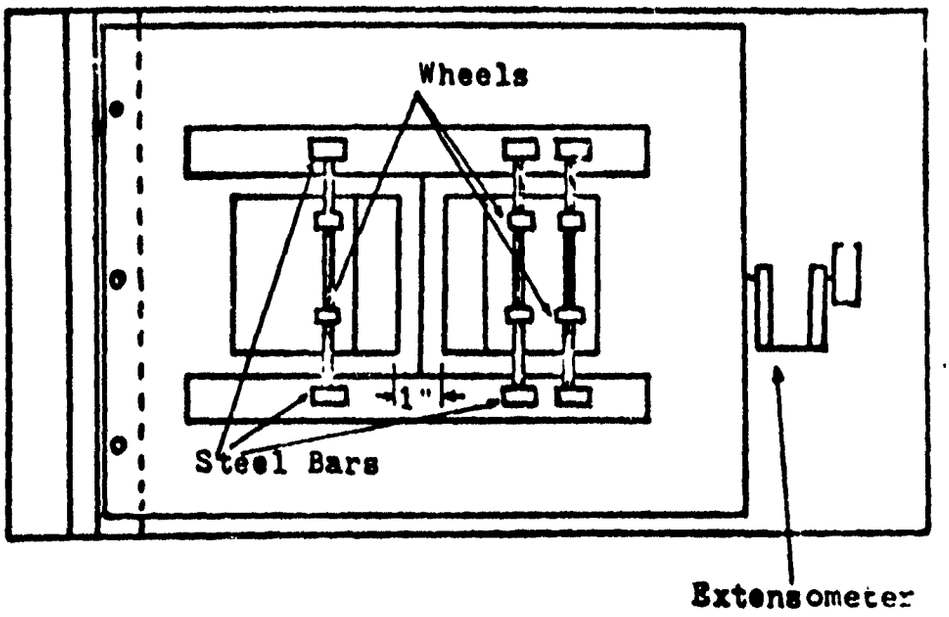

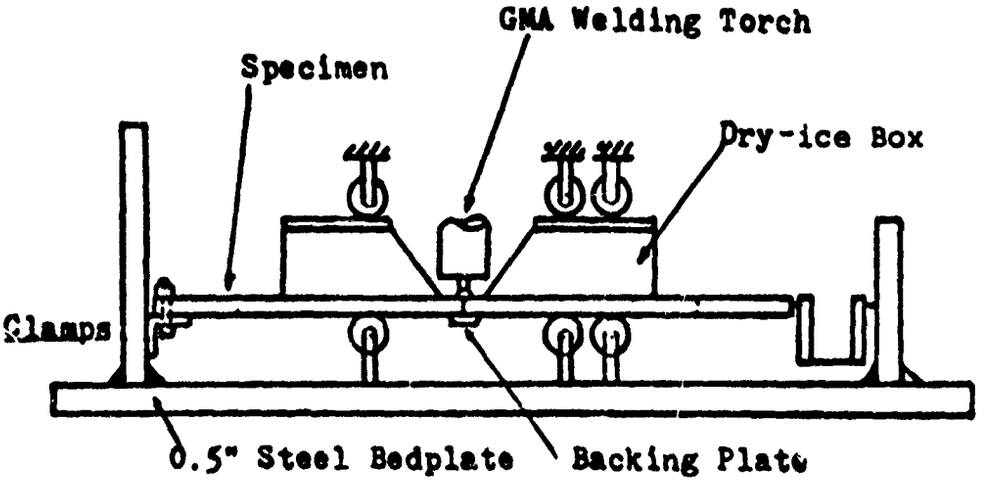

Fig. 3.9 Constraining and Chilling Equipments

Figures 3.10 through 3.14 show changes of temperatures and shrinkage for some of the tests. In general, the plate expanded after the start of welding, and the expansion increased until the arc passed the center. Shrinkage occurred after diminishing of the arc. The amount of expansion was relatively small in comparison with the final amount of shrinkage. The increasing rate of shrinkage decreased as time passed. However, in the case of chilling, shrinkage occurred during welding. As for the final amount of shrinkage, almost identical results were obtained in both cases of chilled and non-chilled.

Figure 3.15 shows the temperature distribution in both chilled and non-chilled tests. From this it can be seen that chilling with dry-ice promoted heat transfer or radiation (cooling rate), but affected a little the temperature distributions during welding.

Table 3.1 shows the final amounts of shrinkage in experiments and calculations, using the computer program developed. From the table it can be seen that the amount of final shrinkage of free joints was about 0.02 in. In restraint joints, the amount of shrinkage was about 0.014 in. Thus, restraint reduced the amount of shrinkage by about 30%. It is also worth noticing that the amount of released shrinkage was almost equal to that of free joints.

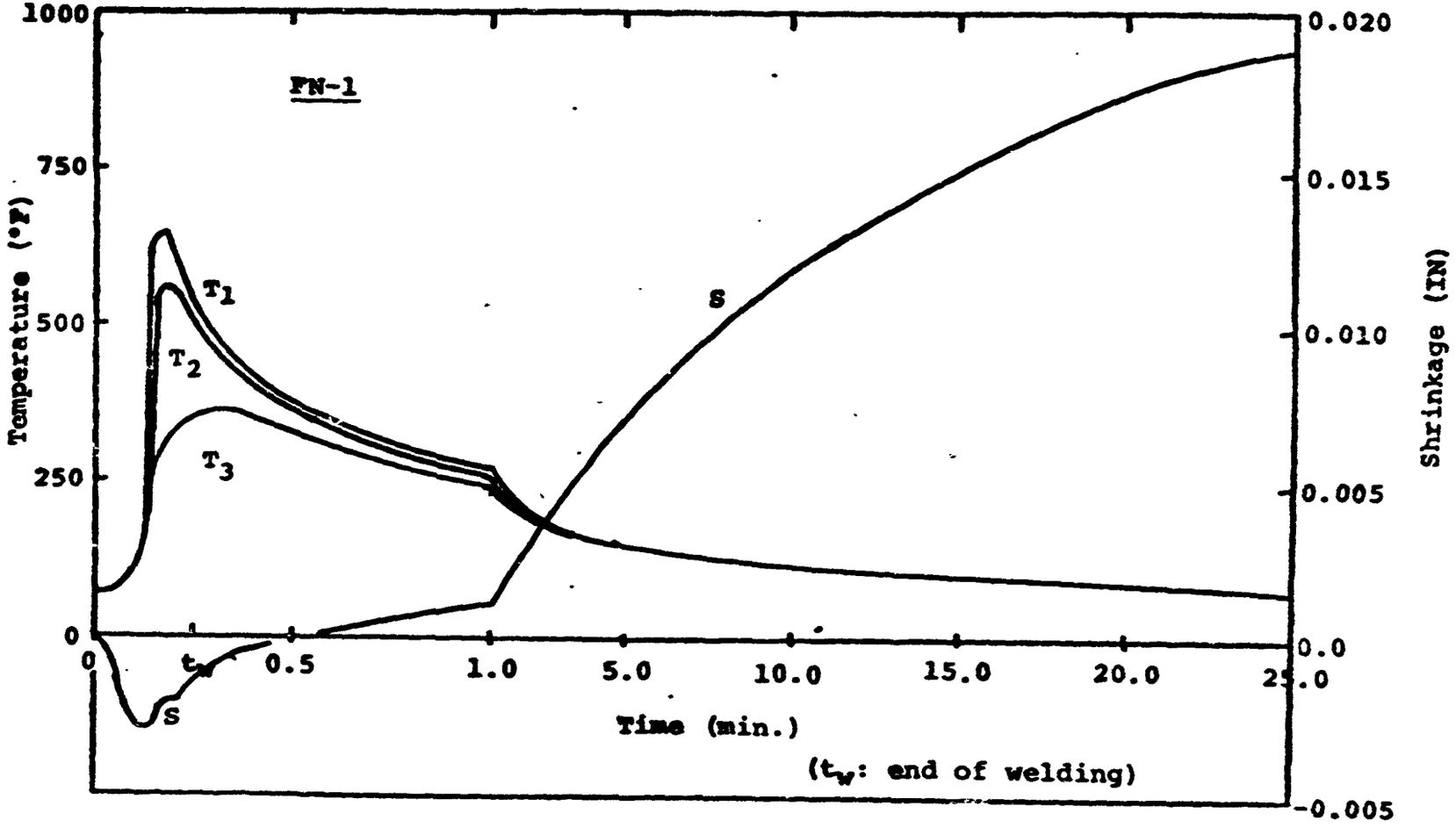

Fig. 3.10 Transverse Shrinkage and Temperature (FN-1)

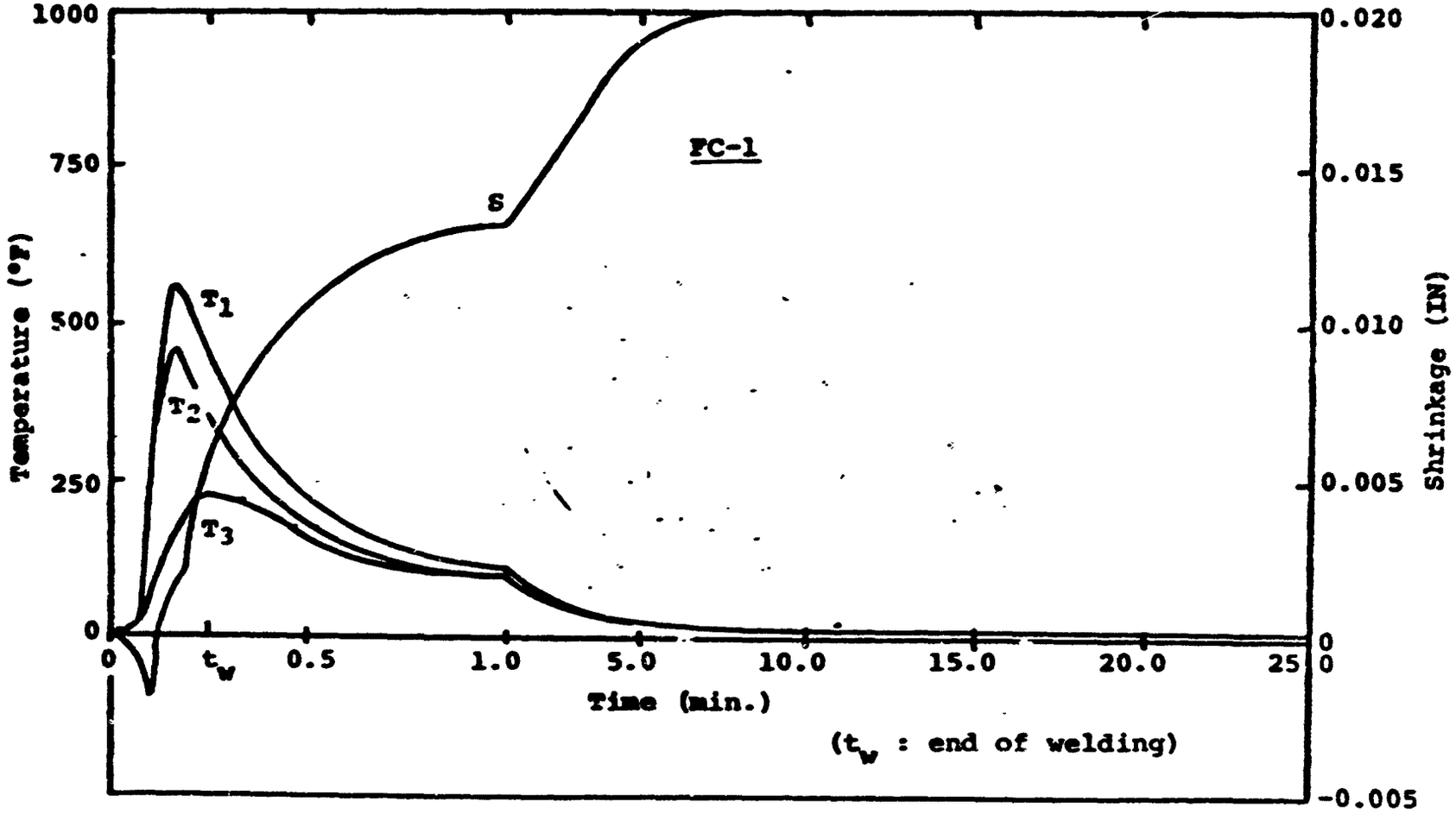

Fig. 3.11 Transverse Shrinkage and Temperature (FC-1)

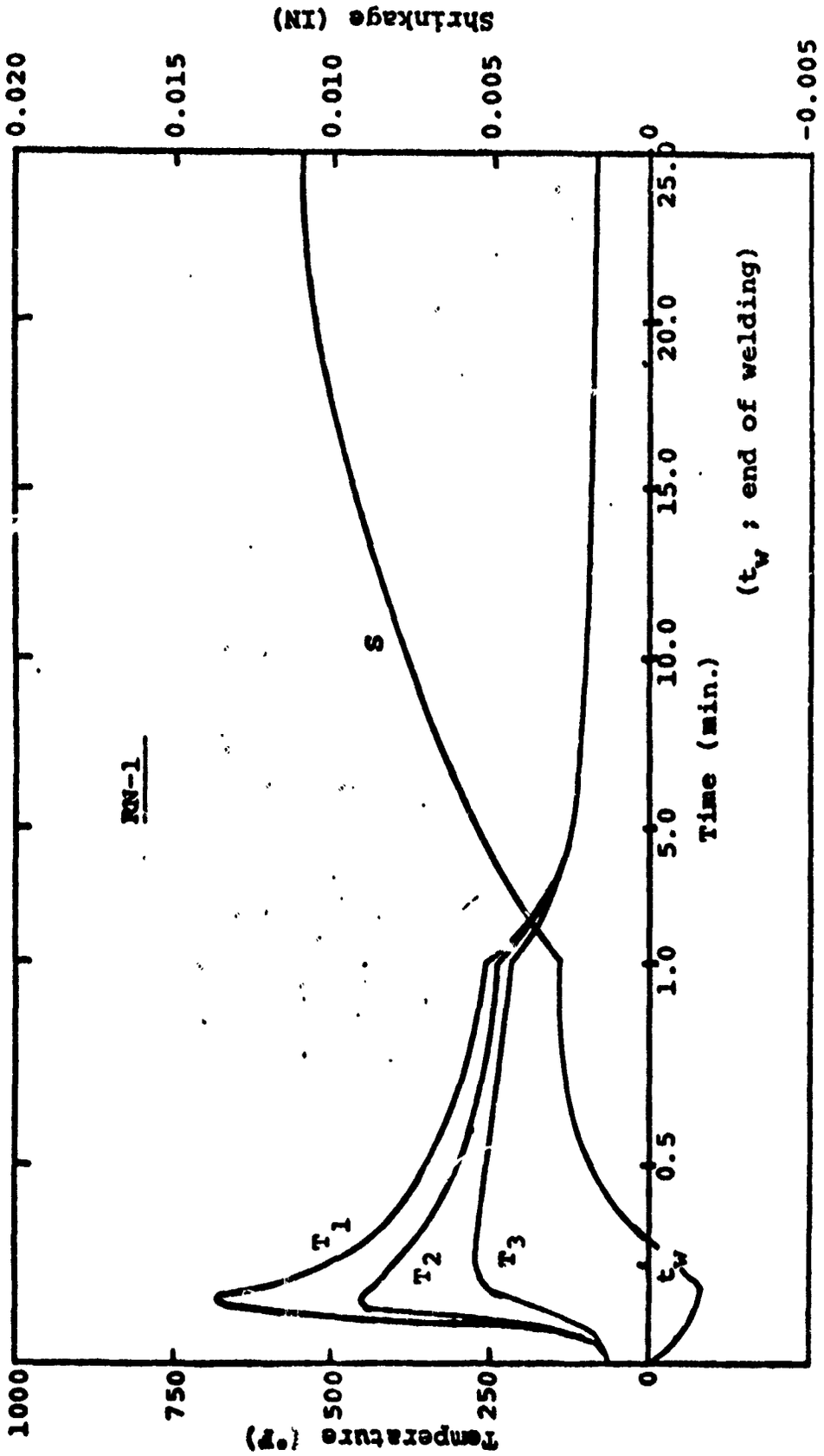

Fig.3.12 Transverse Shrinkage and Temperature (RN-1)

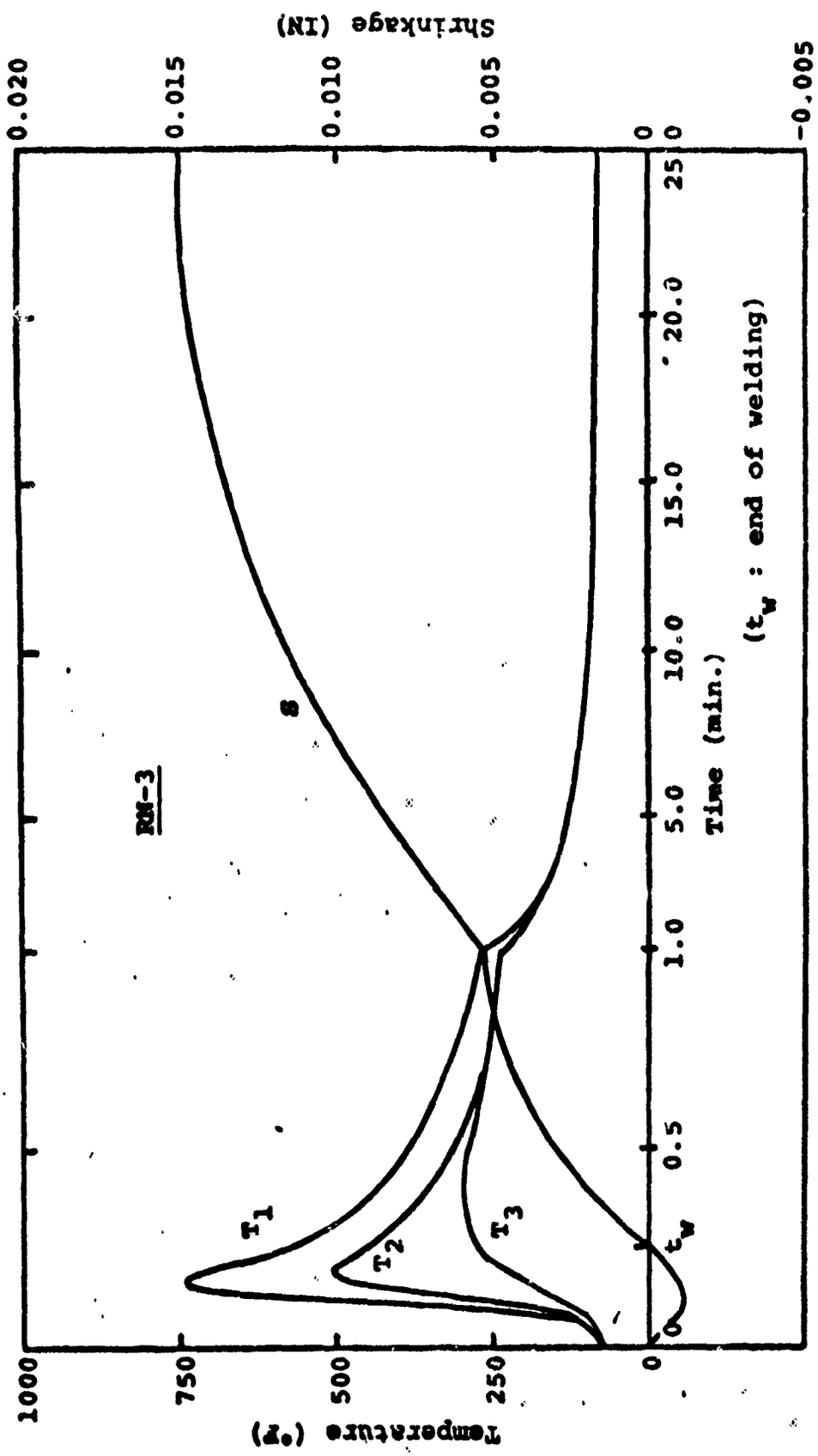

Fig. 3.13 Transverse Shrinkage and Temperature (RN-3)

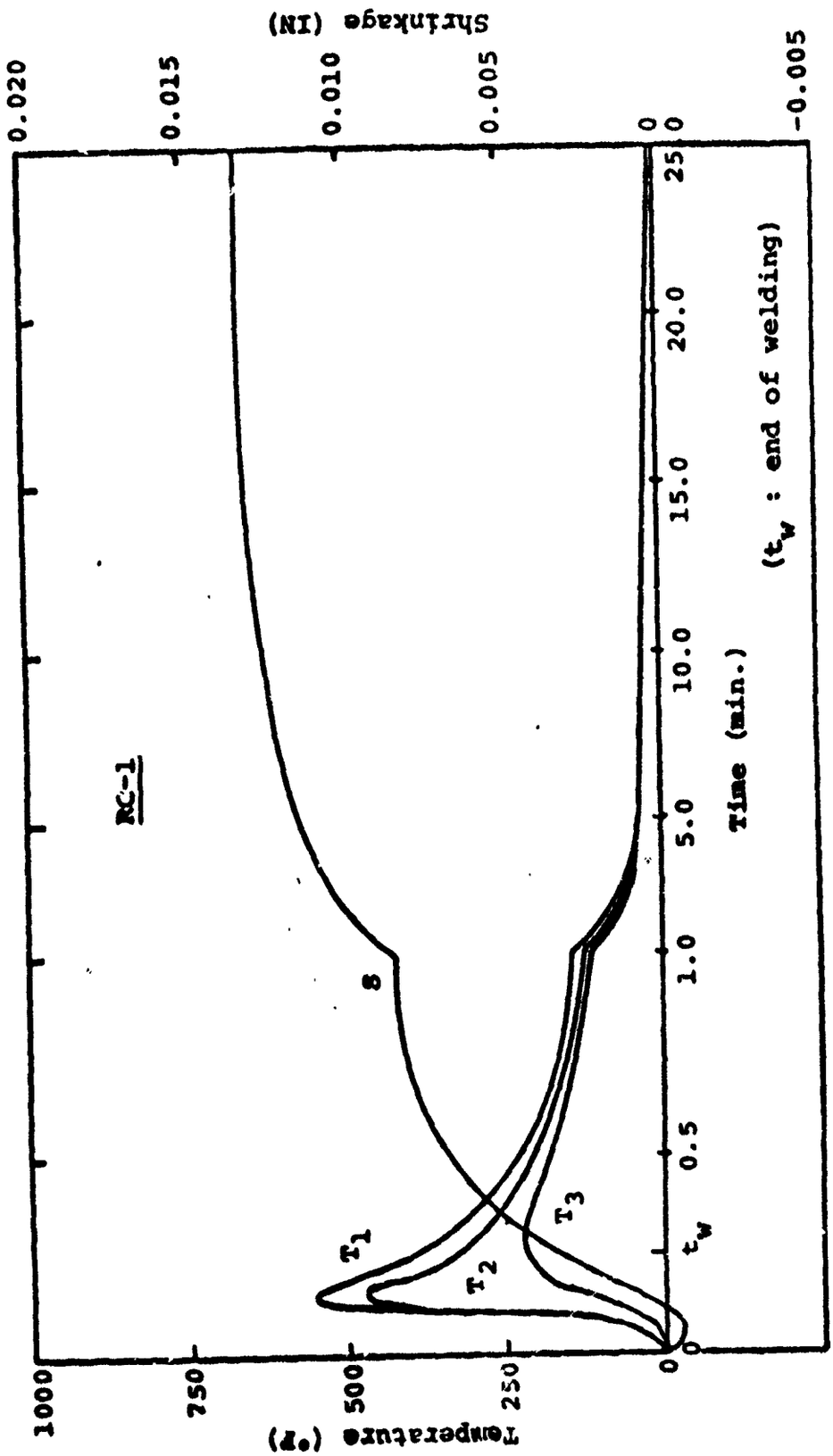

Fig. 3.14 Transverse Shrinkage and Temperature (RC-1)

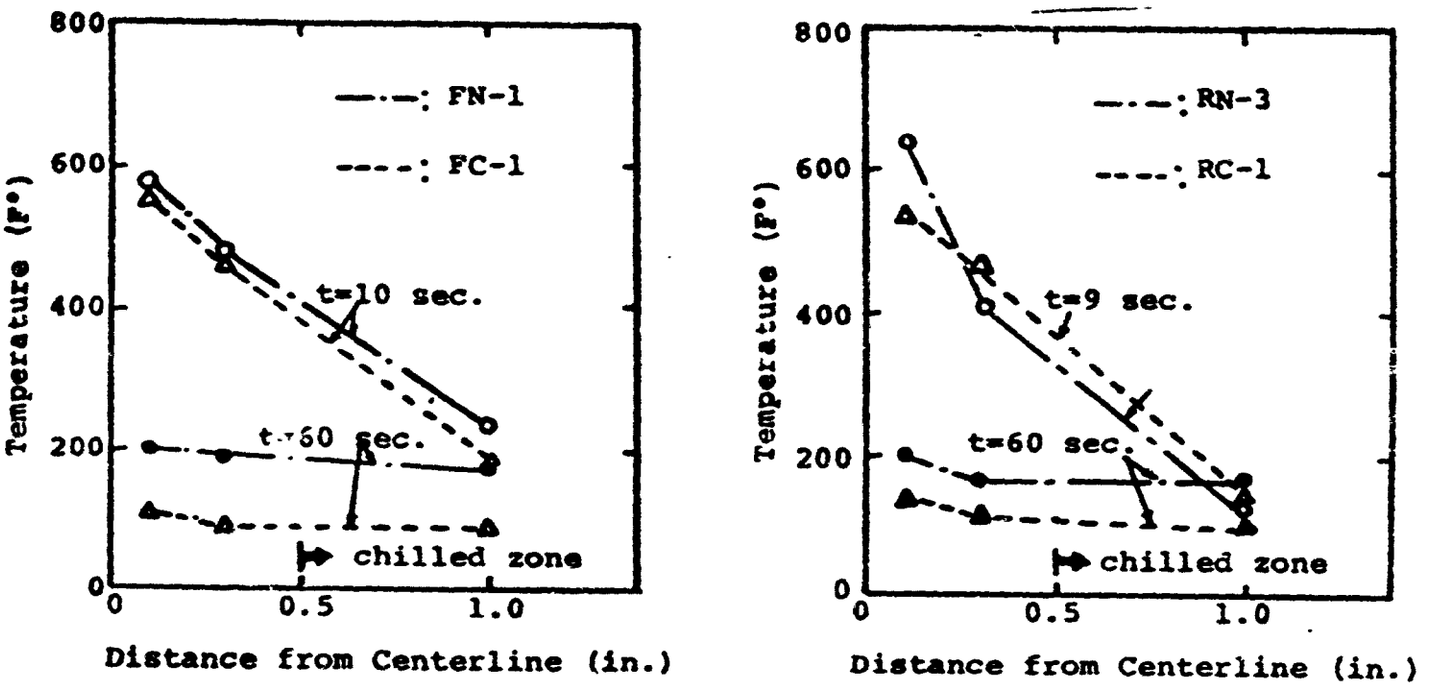

(a) Fee Joint

(b) Restraint Joint

(Temperature of FN-1 and RN-3 were adjusted to 0°F base)

Fig. 3.15 Temperature Distribution

Table 3.1 Final Amounts of Shrinkage in Experiments and Calculations

Joint	Cooling	Experiment	Numerical Calculation
Fee	non-chilled	0.0189 (0.0218*)	0.0204
	chilled	0.0200 (0.0218*)	0.0204
Restraint	non-chilled	0.0110 (0.0126*, 0.0196**) 0.0150 (0.0162*, ————)	0.0136 (0.0204**)
	chilled	0.0132 (0.0138*, 0.0188**)	0.0136 (0.0204**)

* : modified shrinkage by adding the expansion caused to the measured shrinkage

** : relaased shrinkage

4. LONGITUDINAL DISTORTION OF WELDED ALUMINUM BEAMS

Longitudinal distortion is defined as the distortion in a plane through the weld line and perpendicular to the plate. This kind of distortion is of special interest in the cases of T bars and I built-up beams.

Many investigations have been carried out in the past in an effort to collect experimental results on longitudinal distortion of various structures. However, more of the results obtained concerned steel structures. During the past two years M.I.T. researchers conducted series of experiments on aluminum welded beams and gathereduseful information on the effects of various parameters on longitudinal distortion. At the same time analytical studies were carried out, using both one-dimensional and finite element techniques, and comparing the results obtained with the experimental ones.

In this section we will try to summarize all the efforts made so far in both the analytical and the experimental areas.

4.1 Previous Investigations

Sasayama, et al.[25] investigated longitudinal distortion of steel due to fillet welding in several kinds of T bars and I beams. Figure 4.1 shows the experimental results obtained. In a T bar, the deformation gradually increases as the welding progresses (Fig. 4.1a). On the other hand, the phenomena are somewhat different in the fabrication of an I beam. In an I beam (Fig. 4.2b), the

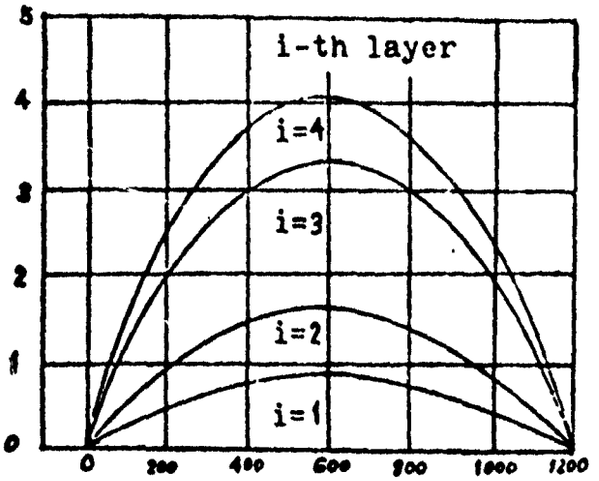

(a) 100 X150 T-BAR

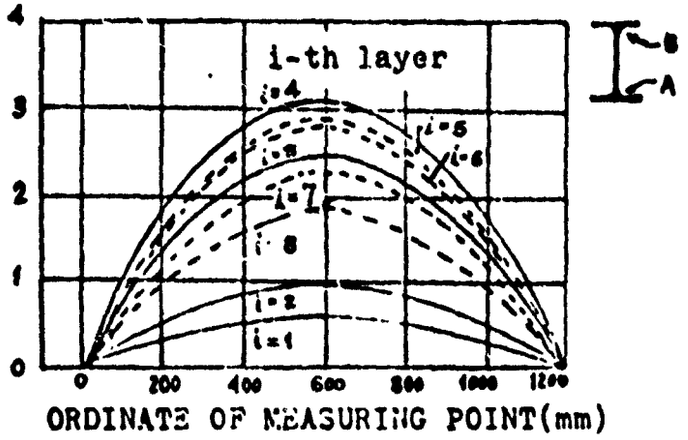

(b) I-BEAM,CONTINUOUS WELD BOTH SIDE OF FILLET: 1ST-4TH LAYER WELD A; 5TH-8TH LAYER WELD B

FIG. 4.1 LONGITUDINAL DEFLECTION OF STEEL DUE TO FILLET WELDING

deformation increases with the welding of the underside fillet, and it decreases with the welding of the other side. However, as the deformation due to the welding of the second fillet is generally smaller than that of the first, the residual deformation remains, even when the weight of the deposit metal of both fillet welds is equal and the geometry of the joint is symmetric.

This occurs because the effective resisting area of the joint differs between the two. That is, the upper flange does not effectively constrain the deformation during the welding of the underside of the fillet, since the upper flange is only tack welded to the web plate. On the contrary, both flanges effectively constrain the welding of the upper side fillet, since the lower flange has already been welded to the web.

The relation between the weight of electrode consumed per weld length and the apparent shrinkage force (P_x^*) is shown in Figure 4.2. The apparent shrinkage force is taken from the relation with the curvature of longitudinal distortion ($\frac{1}{R}$). The following formula was proposed from the experiment:

$$(\frac{1}{R}) = \frac{P_x^* \ell^*}{EI} \qquad (4.1)$$

where, ℓ^* = distance between the neutral axis of the beam and the weld line.

I = moment of inertia about the neutral axis.

E = Young's modulus.

Ujiie, et al.[26] investigated distortion in aluminum structures. They proposed twin-GMA double-fillet welding as a method to reduce longitudinal distortion. The method seems to be effective

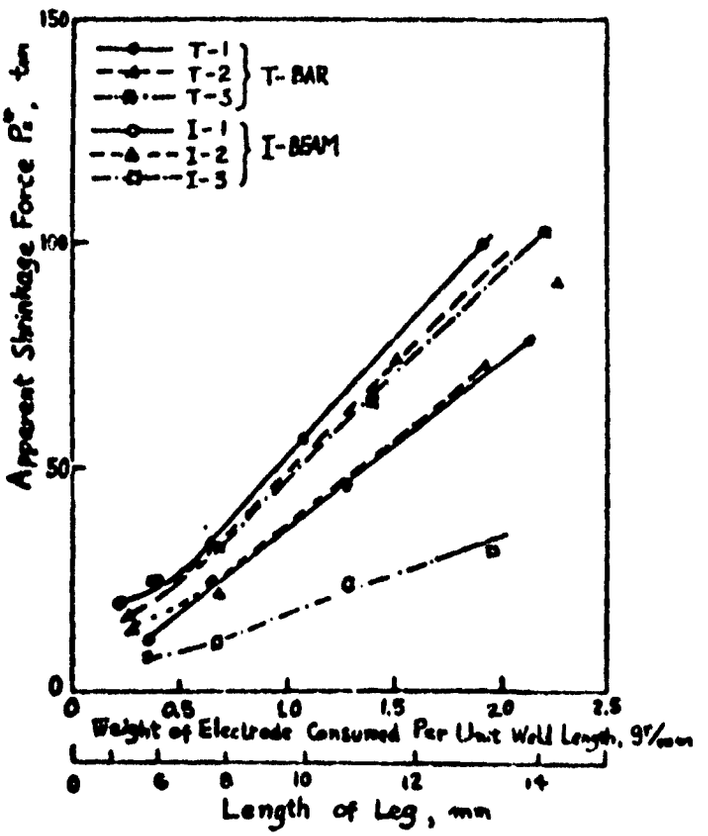

FIG. 4.2 APPARENT SHRINKAGE FORCE OF STEEL DUE TO FILLET WELDING

if used for T bars thicker than 20 mm (0.787 in.).

4.2 Experimental Investigation at M.I.T.

Yamamoto[27] conducted a series of experiments at M.I.T. trying to analyze the longitudinal distortion mechanism in a built up beam, to provide experimental data for the development of a computer program on longitudinal distortion, and to investigate a method of reducing longitudinal distortion. Experiments were performed in the following phases:

(1) Simple rectangular plates were welded or heated along one edge by automatic GMA or GTA (no filler wire) welding processes.

(2) T-section beams with the same web depth as the plates of the previous phase were welded by automatic GMA welding process under the same supporting condition used in phase (1).

(3) A clamped T-section beam was welded by the automatic GMA welding process.

The material used in the experiments was the aluminum-magnesium structural alloy 5052-H32, strain hardened and non-heat treatable. Filler wired 4043 and 2319 were used, the selection based on ease of welding and material on hand.

The plates used were 1/2 in. thick and 4 feet long, so that two-dimensional characteristics could be obtained. Welding conditions were changed during the various passes so that good penetration and the minimum weld length for adequate joint strength could be obtained.

Figure 4.3 shows a typical test specimen. It also provides dimensions as well as strain gage and thermocouple locations. Figures 4.4 and 4.5 show the general arrangement of the experimental equipment for the simply supported and the clamped test specimen respectively.

Similar trends were observed in the development of longitudinal deflection of the simple rectangular plates using GMA and GTA. Convex deflections were observed during the welding process, while concave deflections resulted during the cooling stage (see Fig. 4.6). Upon comparison of GMA and GTA (no filler wire) it was found that the effect of deposit metal in increasing the longitudinal distortion can be estimated at about 10%, assuming that thermal input is proportional to the maximum deflection.

Yamamoto[27] contained in his thesis an exhaustive list of data concerning temperature distribution, strains and stresses measured during the experiments. The collection of this data was mandatory, so that a comparison with predicted results from analytical formulations of the problem could be obtained. The interested reader is referred to this thesis for further information.

Figure 4.7 shows the longitudinal deflection at midlength of a typical T-section beam as measured during the experiments.

Yamamoto[27] tried to relate the experimental results with an analytical method for predicting the longitudinal deflection. Modelling the simple beam welded at its edge by a simply supported beam with the shrinkage force P_x^* applied at the welded edge as an external force, he found that the deflection y is given by:

$$Y = \frac{M_o L^2}{4EI_u{}^2}\left[1 - \frac{\cos(u - kx)}{\cos u}\right] \qquad (4.2)$$

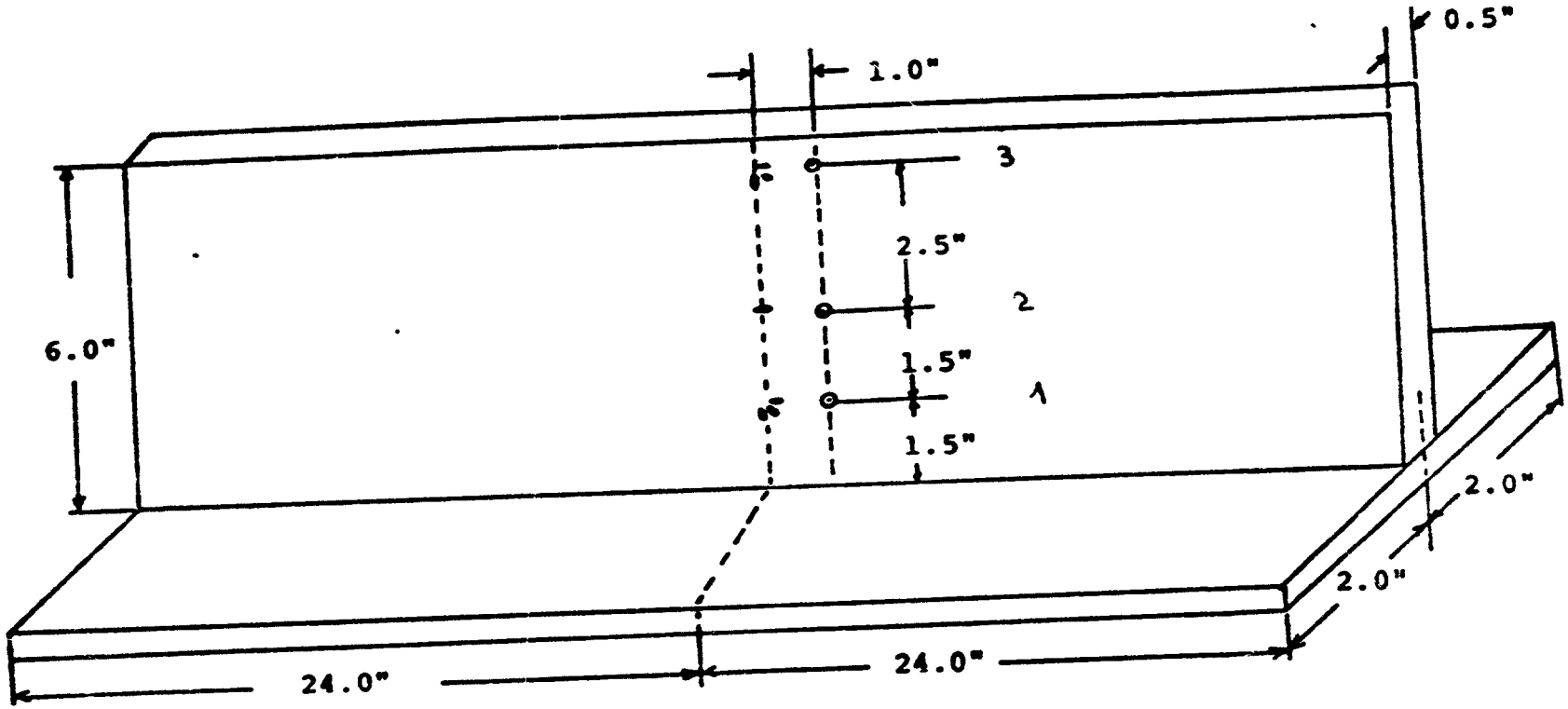

: ROSETTE STRAIN GAGE FAER-18RB-12S13L

: SINGLE STRAIN GAGE FAE-25-12S13

: THERMOCOUPLE

FIG.4.3 ARRANGEMENT OF THE STRAIN GAGE AND THERMOCOUPLE FOR T-SECTION BEAM

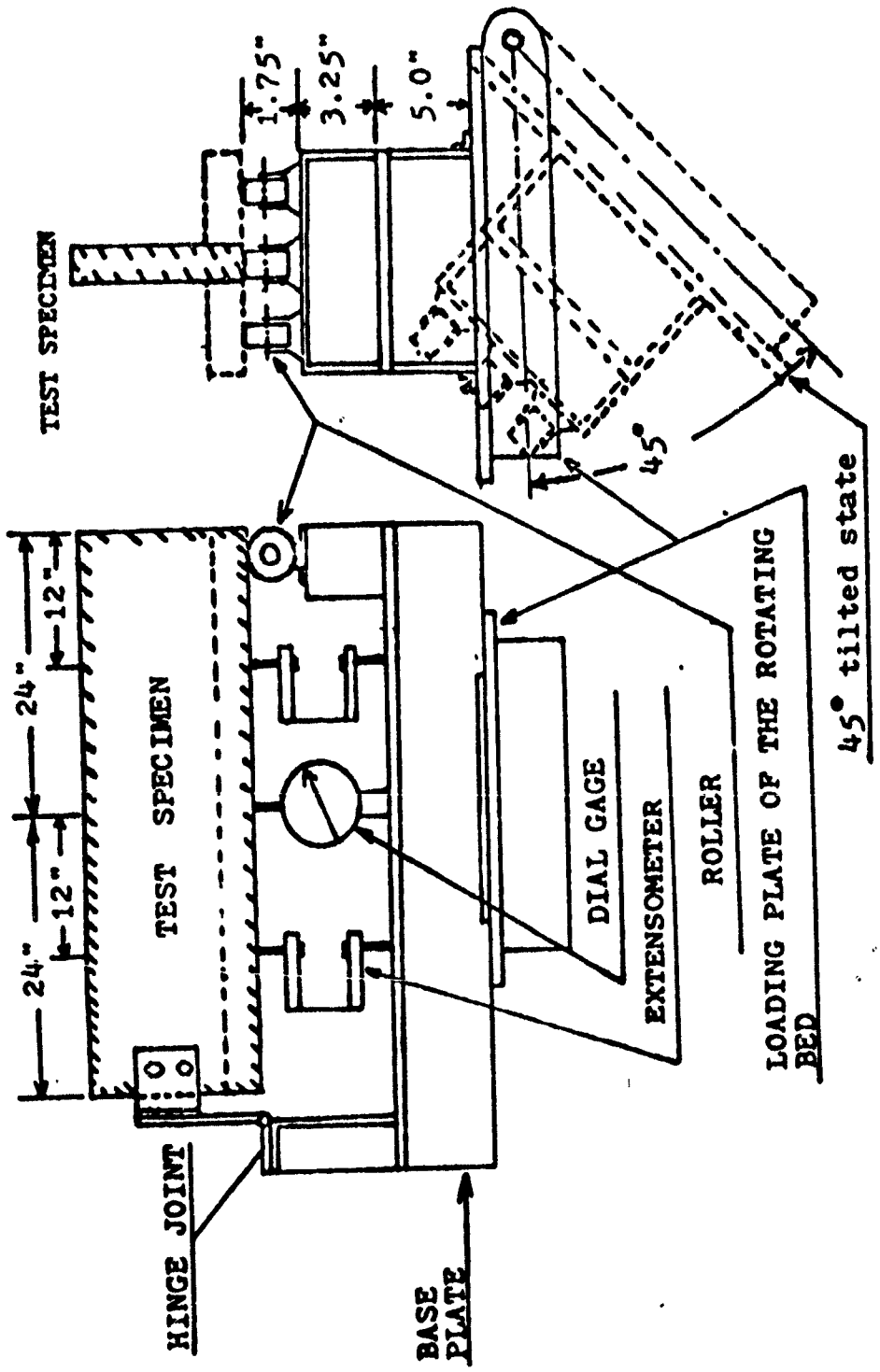

FIG. 4.4 GENERAL ARRANGEMENT OF THE EXPERIMENTAL EQUIPMENT FOR SIMPLY SUPPORTING TEST SPECIMEN.

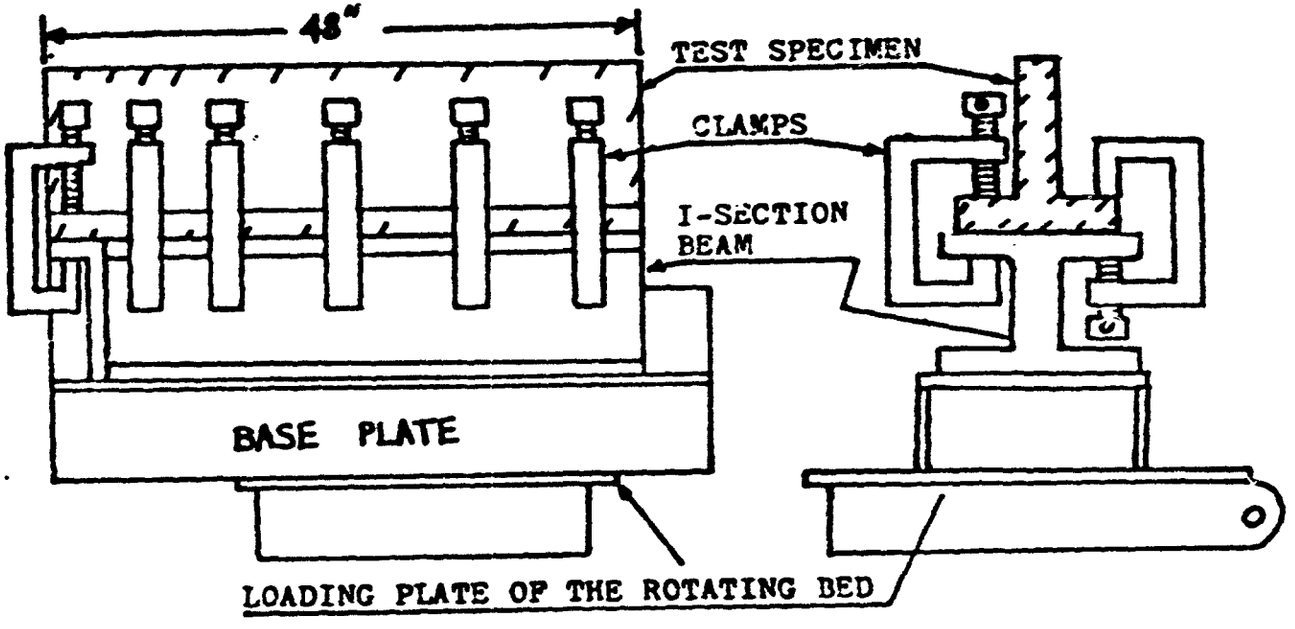

FIG. 4.5 GENERAL ARRANGEMENT OF THE EXPERIMENTAL EQUIPMENT FOR CLAMPED TEST SPECIMEN.

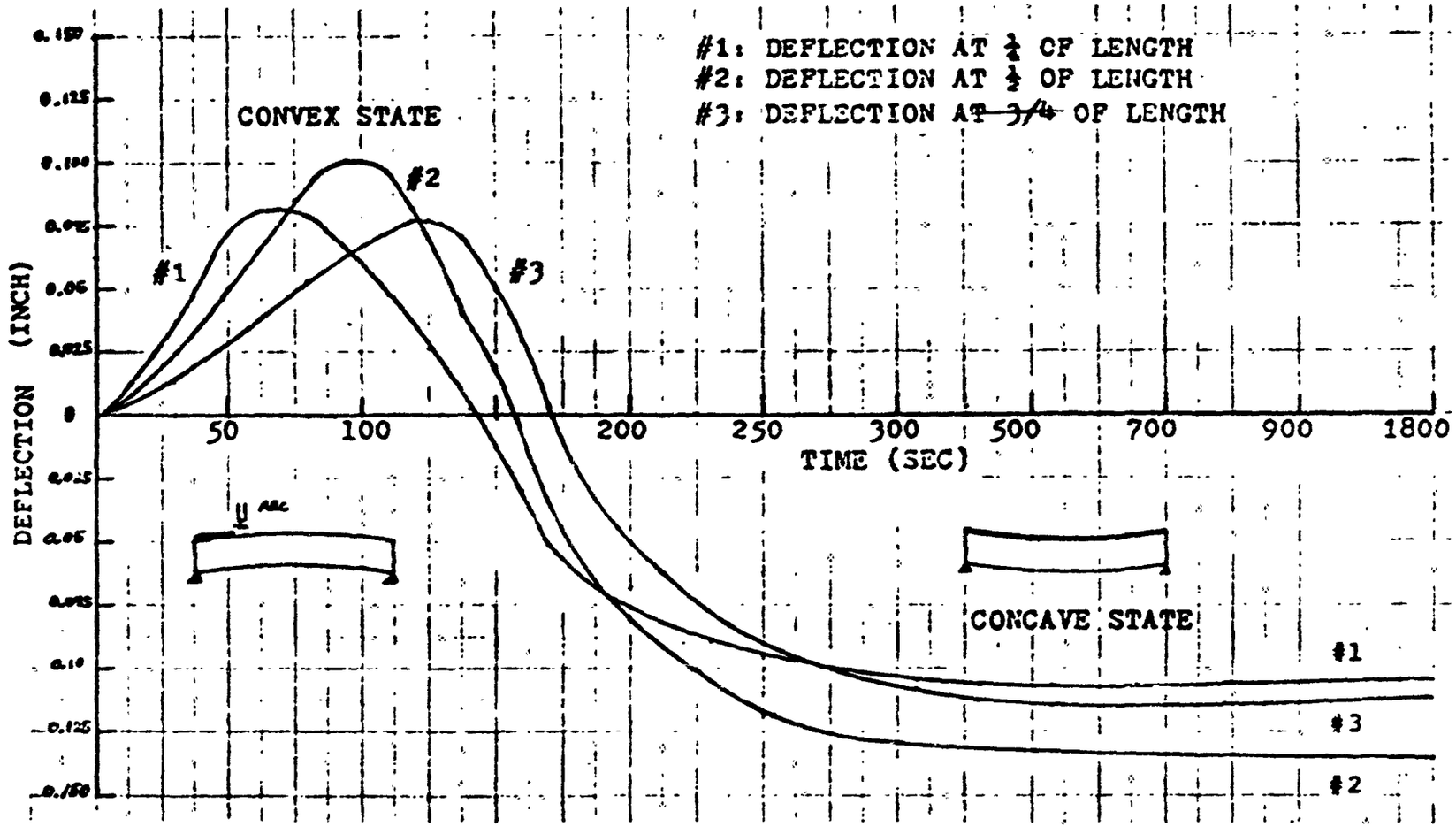

FIG. 4.6 — LONGITUDINAL DEFLECTION AT DIFFERENT LONGITUDINAL POINTS (MIG-WELD)

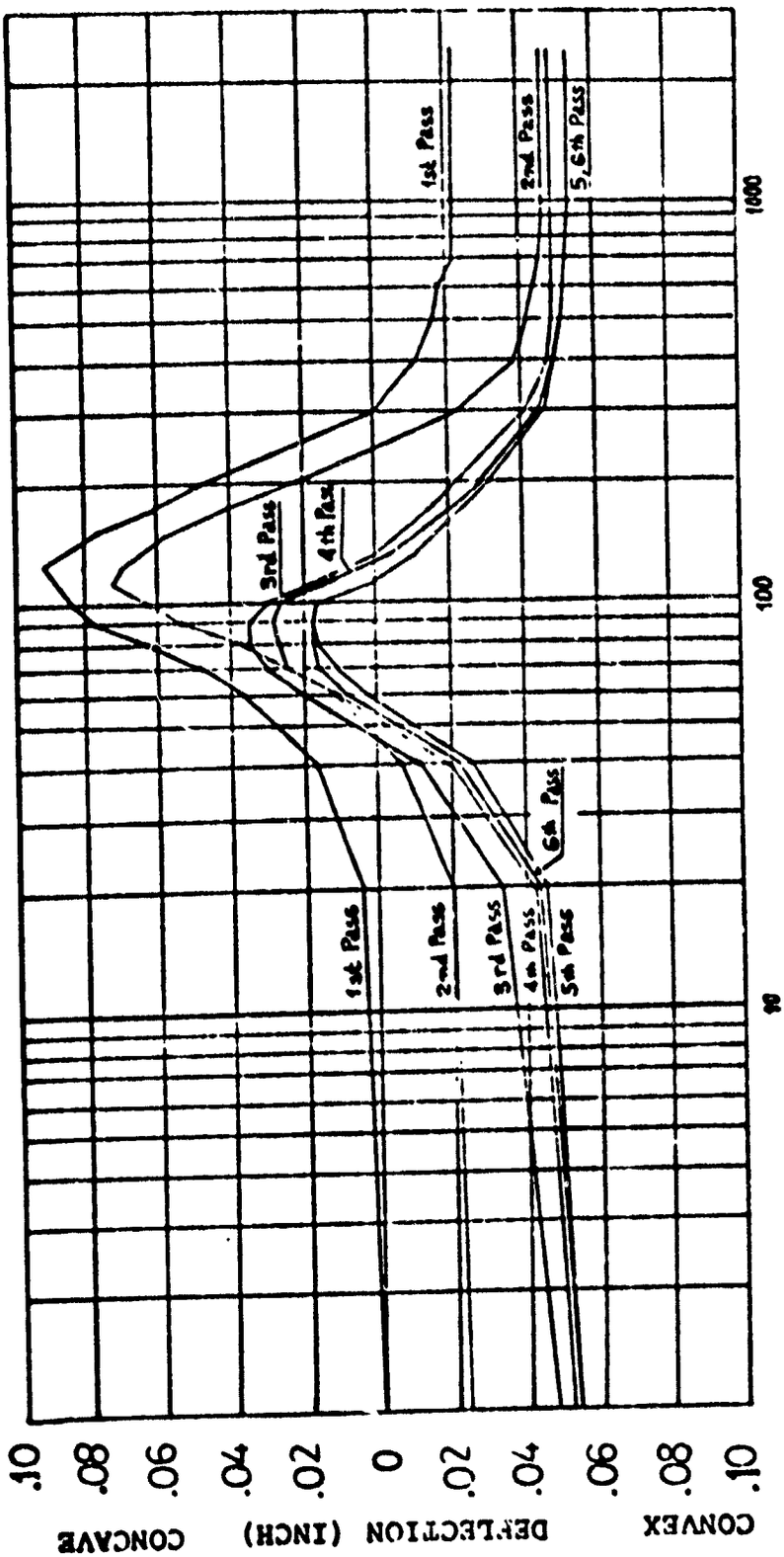

FIG. 4.7 THE LONGITUDINAL DEFLECTION AT MIDLENGTH OF T-SECTION BEAM (6"WEB PLATE HEIGHT)

where:

$$u = \frac{kL}{2}$$

$$k = \left(\frac{P^*_x}{EI}\right)^{1/2}$$

$$M_o = - L_{na} \cdot P^*_x \qquad (4.3)$$

L_{na} = distance between the neutral axis of the beam and the weld line

L = beam length

I = moment of inertia of beam

E = Young;s modulus

P^*_x = shrinkage force

At mid length:

$$y = - \frac{M_o L^2}{8EI} \cdot \frac{2(\sec u - 1)}{u^2} \qquad (4.4)$$

Shrinkage force is calculated for both GMA and GTA welding processes using the values:

$$I = 9 \text{ (inch)}^4; \; E = 10.2 \times 10^6 \text{ psia} ; \; L_{na} = 3 \text{ in.}$$

S_o:

$$P^*_x = \begin{cases} + 13{,}924 \text{ lbs} , \text{ for GMA} \\ + \; 9{,}025 \text{ lbs} , \text{ for GTA} \end{cases}$$

(+ sign means compression)

The stresses are then calculated using

$$\sigma = \frac{M_o}{I/y} - \frac{P^*_x}{th} \qquad (4.5)$$

where t = thickness

h = breadth

It is found:

$$\sigma = \begin{cases} 4{,}641y - 4{,}641 \text{ , for GMA} \\ 3{,}008y - 3{,}008 \text{ , for GTA} \end{cases}$$

Comparison of the stresses calculated above with the experimental ones showed good agreement everywhere, except in the region near the weld, where the discrepancy is expected due to the plastic region. Therefore, Yamamoto believes that the use of the shrinkage force obtained by the beam theory may be a useful tool in predicting longitudinal deflection.

The shrinkage force calculated above is now applied to fillet welding of a T-section beam. For a 6" x 4" T-beam, I = 21.59 in.^{4} and L_{na} = 1.7 in. Substituting these values into equation (4.4) we find:

Y_{cal} = 0.0314 in. at midlength

The corresponding experimental value was

Y_{exp} = 0.0235 in.

Thus, deflection is overestimated by approximately 33%. Yamamoto proposed the use of a modification factor to take into account the difference between the shrinkage force P_x^* of a simple beam (edge welding) and a T-section beam (fillet welding). This modification factor was based on the observation that the heat intensity of the simple beam was 1.5 times that of the fillet welding in the T-section beam, which results in a value of 2/3 for

the factor. The calculated deflection thus becomes $y_{cal} = 0.0208$ in. Comparing analytical and experimental results for other cases, too, he finally proposed the following formula, which gives a reasonable approximation of longitudinal deflection at the mid-point of a T-section beam:

$$y = - \frac{M_o L^2}{4EI} \cdot \frac{\sec u - 1}{u^2} \qquad (4.6)$$

where

$$u = \frac{kL}{2}$$

$$k = \left(\frac{P_x^* C}{EI} \right)^{1/2}$$

$$M_o = - L_{na} \cdot P_x^*$$

$C = 2/3$

P_x^* = shrinkage force calculated for an edge-welded beam.

As a result of the final stage of the experiments, it is mentioned that the clamping of the T-section beam during welding had little effect on the deflection of the beam at the completion of welding.

4.3 Computer Analysis

The complexity of the problem of longitudinal distortion of built-up beams makes the application of complete analytical methods almost impossible. Driven by this statement, Nishida[8] tried to apply both one-dimensional and finite element analyses to the problem.

One-Dimensional Analysis

In the one-dimensional analysis, only one-directional stresses are considered, namely those parallel to the fillet weld. Nishida assumes the quasi-stationary state, so that the Rosenthal solution for the temperature distribution can be used. A narrow strip element perpendicular to the weld line is cut, both edges of which are assumed to remain streight (simple beam theory assumption). Then, the stress-strain relation is:

$$\varepsilon_x = \frac{1}{E}\sigma_x + \alpha T + \varepsilon_x^P \qquad (4.7)$$

where

ε_x = total strain in x-direction

σ_x = stress in x-direction

E = Young;s modulus

α = thermal expansion coefficient (average)

T = temperature change from reference temperature

ε_x^P = plastic strain in x-direction

Since no external forces are present, the following equilibrium conditions hold:

$$\int_0^B \sigma_x A \, dy = 0 \qquad (4.8)$$

$$\int_0^B \sigma_x A \, y \, dy = 0 \qquad (4.9)$$

where B = plate width

By assuming $\tau_{xy} = \sigma_y = \sigma_z = 0$ the compatibility equation becomes:

$$\frac{\partial^2 \varepsilon_x}{\partial_y{}^2} = 0 \qquad (4.10)$$

which results in:

$$\varepsilon_x = a + by \tag{4.11}$$

Using equations (4.7) through (4.11) and an iteration procedure where plastic deformation has occurred, stress σ_x and strain ε_x can be determined.

Nishida extended the above procedure to a T-beam, treating each element separately (see Fig. 4.8) so that one-dimensional analysis can still be applied. Note that in this case an unknown reaction force R is present so that the equations become a little more complicated. A computer program is included in his thesis to carry out all the computations necessary.

Once the transient thermal strains are calculated, it is then possible to calculate the transient deflections of weld plates and built-up beams. Curvature, ρ, at a given time is equal to the quantity b in equation (4.11). Since the simple beam theory is assumed, the following relation holds:

$$\rho = \frac{d^2W(x)}{dx^2} \tag{4.12}$$

where W is the deflection in the y-direction at location x. The shape of deflection, W, can then be obtained by integrating the known ρ-curve twice along the x-direction.

The sensitivity of the results to material properties at the high temperature region was found to be great. Therefore, Nishida suggested that the precise value of high-temperature properties should be used in the above calculation.

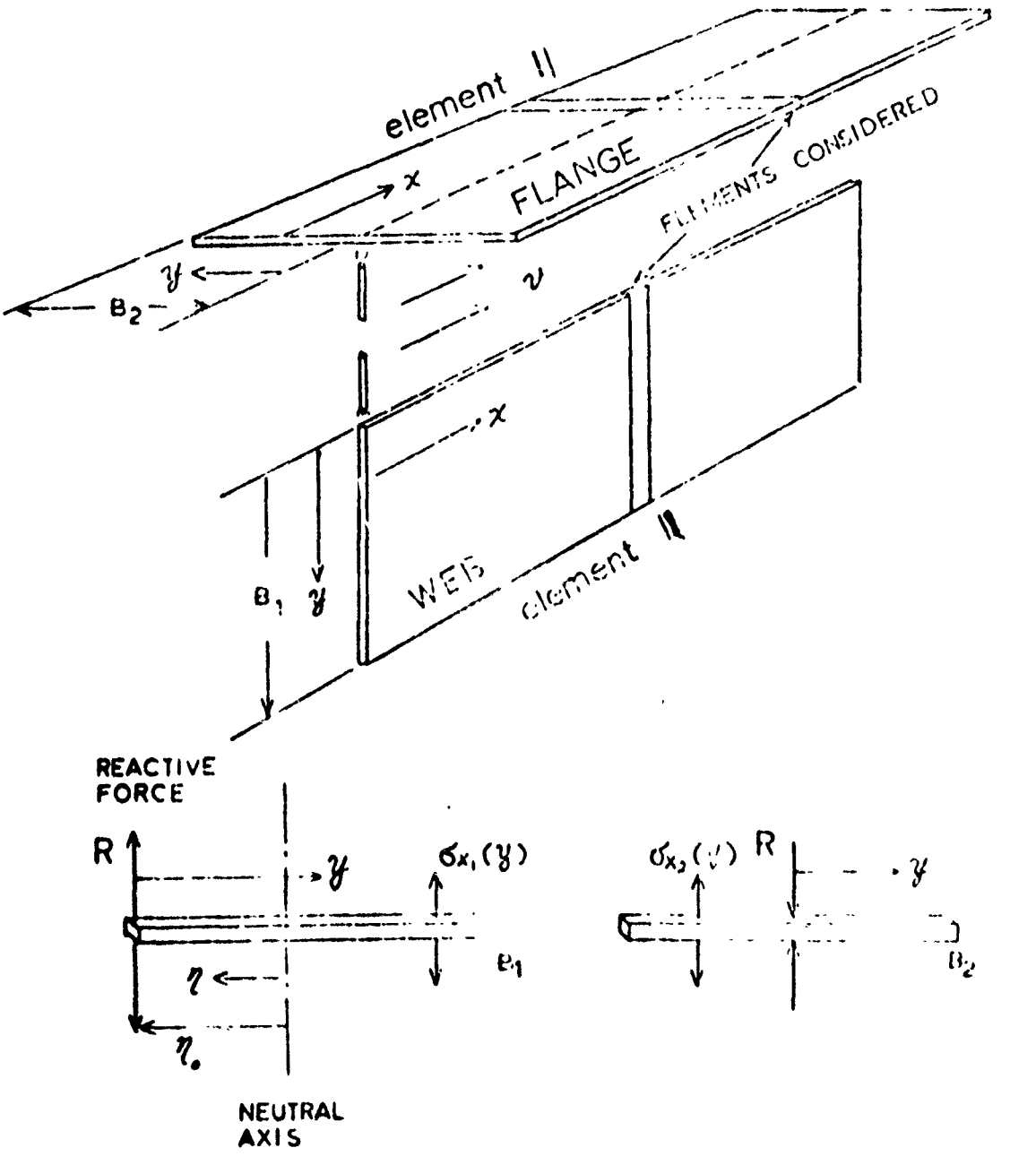

Fig.4.8 Elements of T-shaped build-up beam

Based on the above analysis, which as will be seen later was proven to be adequate for analyzing the problem of longitudinal distortion, Nishida conducted a parametric study to investigate the effect of various factors on values of residual deflection (deflection after welding is completed and the specimen has cooled to room temperature) at midlength. Figure 4.9 shows an example of this parametric study, in which the value of heat input was kept unchanged. It can be seen that when welding speed is increased while current, I, and voltage, V, are kept constant, the amount of distortion decreases rather drastically. On the other hand, when welding speed is increased while heat input is kept unchanged, residual distortion increases. There is also an indication that a welding speed exists where distortion becomes maximum.

Finite Element Analysis

The next step in improving the accuracy of the computation was to take into account the transverse stress σ_y, as well as the boundary at the finishing portion. Nishida tried to solve this two-dimensional problem using the incremental elasto-plastic finite element formulation, based on the flow theory of plasticity. The tangent stiffness method and the Huber-Mises-Hencky yield criterion were utilized. The plase transformation of steel and other metals was also taken into account, using the continuous cooling transformation diagram. A complete formulation of the method as well as the computer program developed (a modification of the second version of the M.I.T. 2-D F.E.M.) are included in Nishida's thesis.

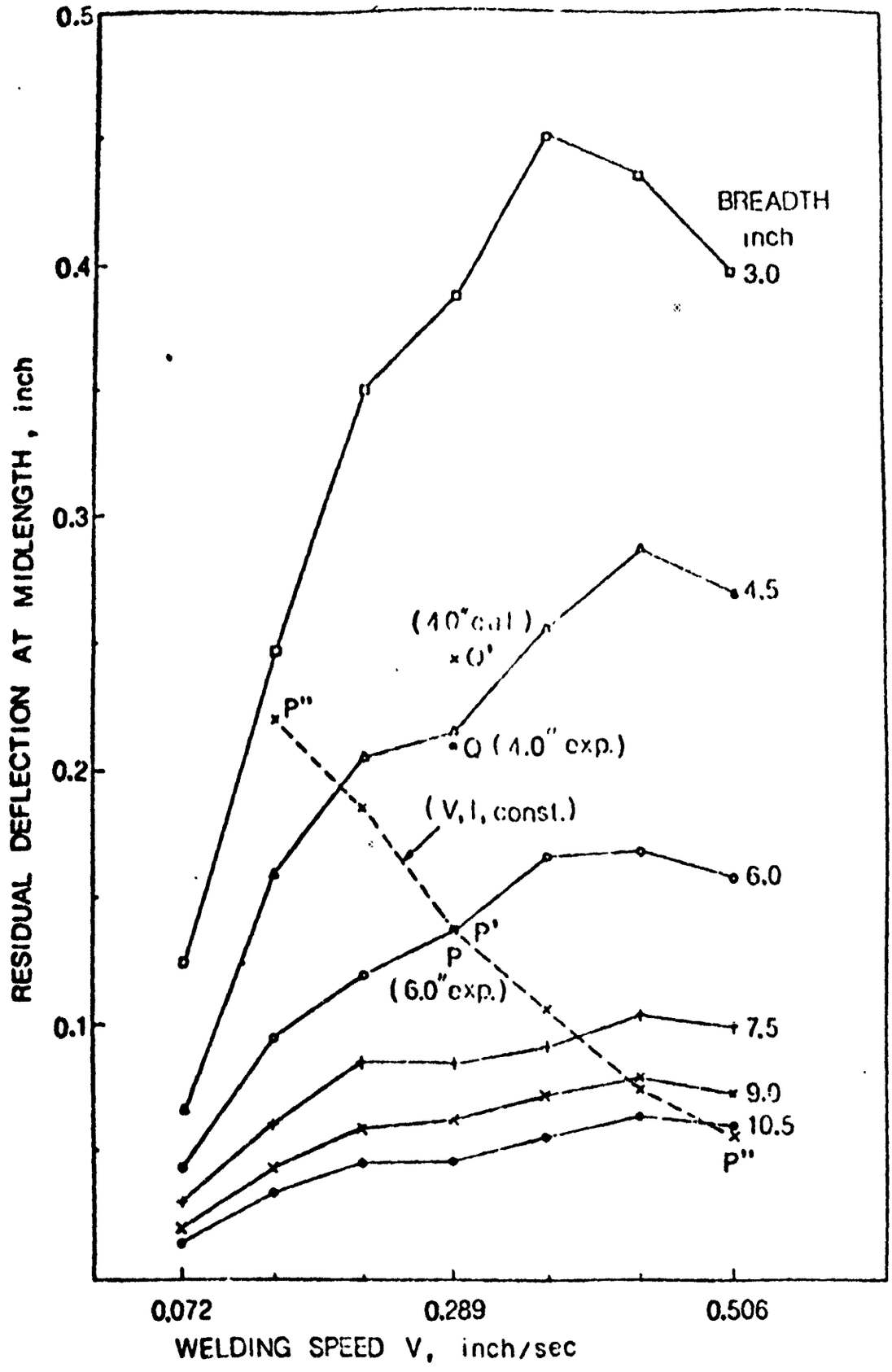

Fig. 4.9 Example of parameter study

Figure 4.10 shows comparison among deflection histories obtained by the F.E.M., the one-dimensional calculation and experimentally. One can see that the 2-D F.E.M. gives relatively poor results compared to the one-dimensional program. This suggests that an improvement of the F.E.M. program is mandatory. At the same time the current program is very expensive so that an effort for improving the mesh pattern is out of the question.

In section 7 we will come back in the discussion of the one-dimensional program, when we will deal with differential heating as a method of reducing longitudinal distortion.

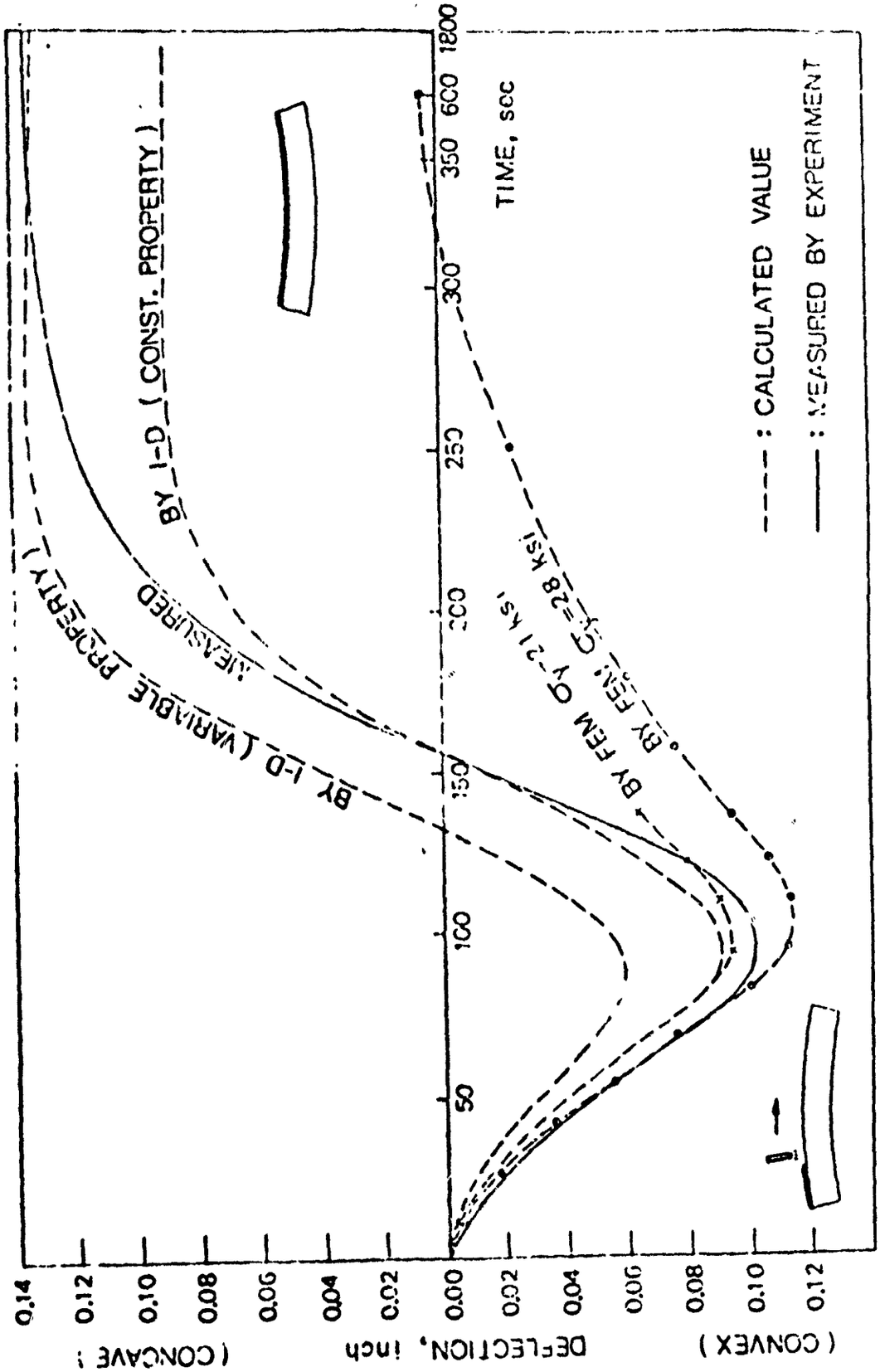

Fig. 4.10 Comparison among deflection histories by the F.E.M., the one-dimensional, and the experiment

5. OUT-OF-PLANE DISTORTION IN ALUMINUM FILLET WELDS

A typical structural component of ships, aerospace and other structures is a panel structure which is composed of a flat plate and longitudinal and transverse stiffeness, fillet welded to the bottom plate as shown in Figure 5.1. The major distortion problem in the fabrication of a panel structure is that related to out-of-plane distortion caused by angular changes along the fillet welds.

For example, corrugation failures of bottom shell plating in some welded cargo vessels are believed to be due to the reduction of buckling strength of the plating with excessive initial distortion. This subject will be discussed in detail in Section 6.

When longitudinal and transverse stiffeness are fillet welded as shown in Figure 5.1, the deflection of a panel, δ, changes in both x- and y-direction. Because of the mathematical difficulties involved in the two-dimensional analysis, most studies conducted so far are one-dimensional. A 2-D analysis, however, was conducted at M.I.T. using the finite element method.

In this section we will try to discuss the state of the art of the mathematical analysis developed at M.I.T., as well as some of the experimental results obtained.

5.1 One-Dimensional Analysis

Semi-Analytical Method

Figure 5.2 shows out-of-plane distortion in two types of simple fillet-welded structures. In both cases, the plates are narrow in the y-direction and the distortion is one-dimensional.

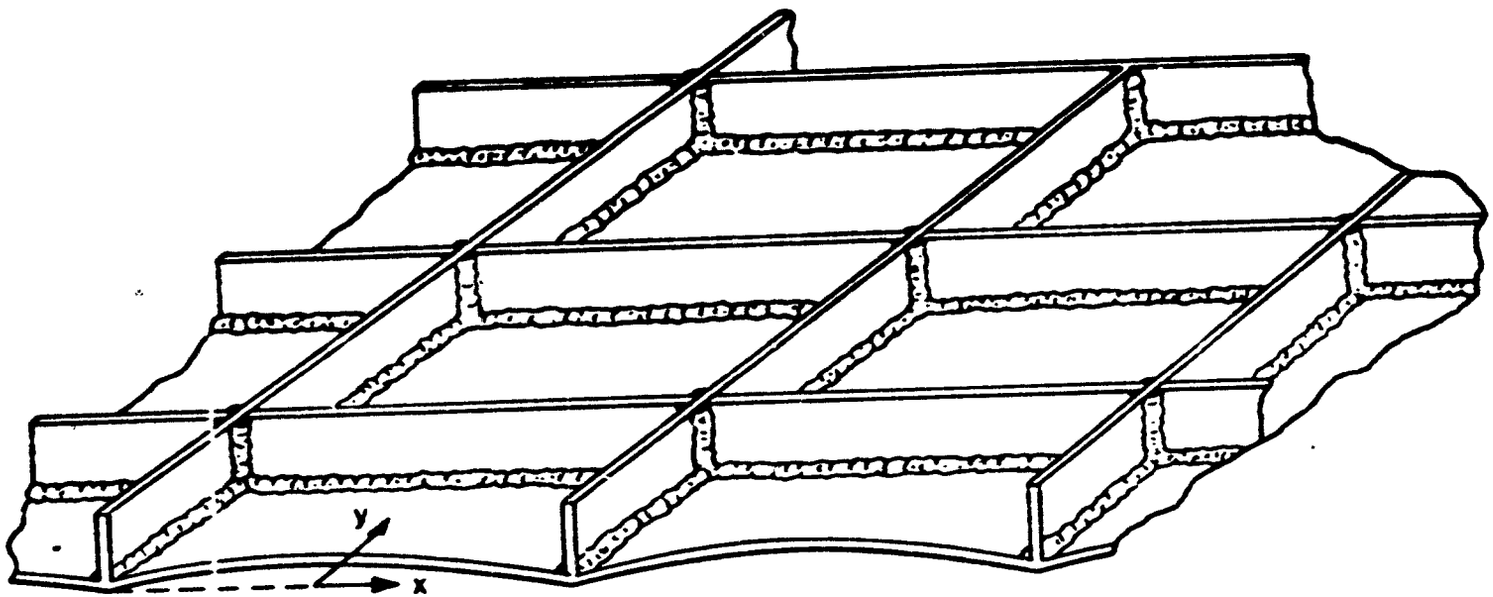

PANEL STRUCTURE WITH LONGITUDINAL AND TRANSVERSE STIFFENERS

FIG. 5.1

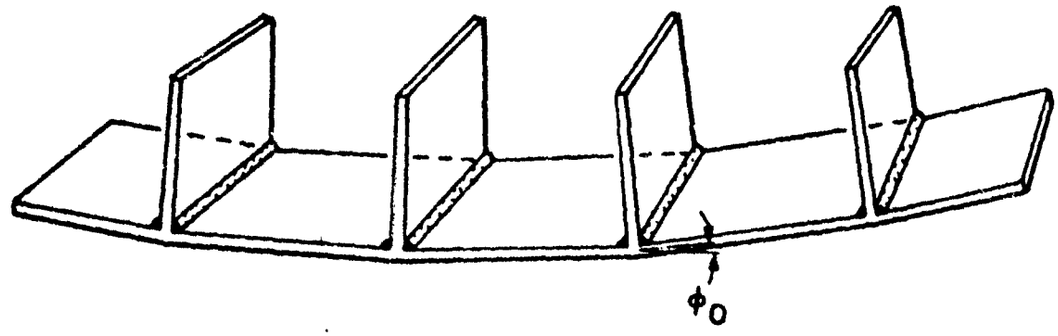

a. FREE JOINT

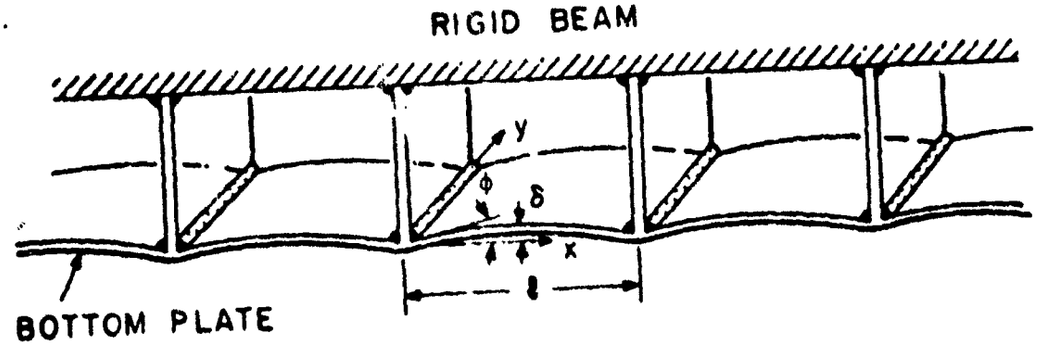

b. CONSTRAINED JOINT (FRAMED STRUCTURE)

FIG. 5.2 DISTORTION DUE TO FILLET WELDS IN TWO TYPES OF ONE DIMENSIONAL MODELS

When a fillet joint is free from external constraint, the structure simply bends at each joint to a polygonal form, as shown in Figure 5.2a. However, if the joint is constrained by some means, a different type of distortion is produced. For example, if the stiffeners are welded to a rigid beam, as shown in Figure 5.2b, the angular changes at fillet welds cause wavy, or arc-form, distortion of the bottom plate.

Masubuchi, et al.,[28] have found that the wavy distortion and resulting stresses can be analyzed as a problem of stresses in a rigid frame. In the simplest case in which the sizes of all welds are the same, the distortion of all spans are equal and the distortion, δ, can be expressed as follows:

$$\delta/\ell = [1/4 - (x/\ell - 1/2)^2] \cdot \phi \qquad (5.1)$$

where

ϕ = angular change at a fillet weld, radiums

ℓ = length of span.

The maximum distortion at the panel center ($x = \ell/2$), δ_{max}, is:

$$\delta_{max} = 1/4 \cdot \phi \cdot \ell \qquad (5.2)$$

The amount of angular change, ϕ, in a restrained structure is smaller than that in a free joint, ϕ_o. The amount of ϕ also changes when the rigidity of the bottom plate, $D = Et^3/12(1 - r^2)$, and the length of the span, ℓ, change.

In case of structures in low-carbon steel, it has been found that the following relationship exists:

$$\phi = \frac{\phi_o}{1 + 2D/\ell \cdot 1/C} \qquad (5.3)$$

where C, the so-called "coefficient of rigidity for angular changes," can be determined by welding conditions and plate thickness.

A study was conducted at M.I.T. by Taniguchi[29] to determine experimentally values of ϕ_o and C for GMA welds in aluminum. The material used in the experiments was the strain hardened, aluminum magnesium structural alloy 5086-H32, largely utilized in marine and general structural applications. As for the filler metal, the recommended Filler-5356 was used.

Figure 5.3 shows the test specimens for both the free joint and constraint joint experiments. The welding sequence and the number of passes are also indicated in the same figure. The jig assembly used to carry out the experiments is shown schematically in Figure 5.4.

Figure 5.5 shows values of ϕ_o as a function of plate thickness, t (mm), and weight of electrode consumed per weld length, w (gr/cm). It is noticeable the fact that the angular change is maximum when plate thickness is around 0.3 in (7 mm). When the plate is thinner than 0.3 inch, the amount of angular change is reduced as the plate thickness is reduced. This is because the plate is heated more evenly in the thickness direction, thus reducing the bending moment. When the plate is thicker than 0.3 inch, the amount of angular change is reduced as the plate thickness increases because of the increase of rigidity of the plate.

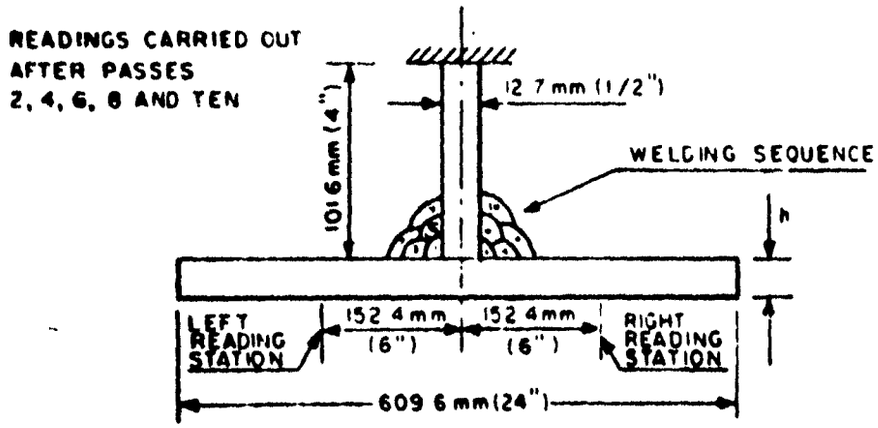

a. FREE JOINT TEST SPECIMEN

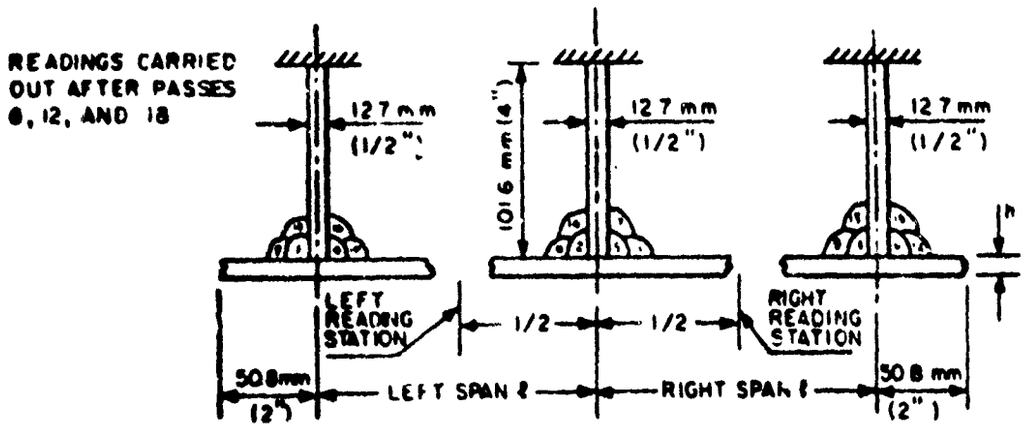

b. CONSTRAINED JOINT TEST SPECIMEN

ALUMINUM TEST SPECIMENS

FIG. 5.3

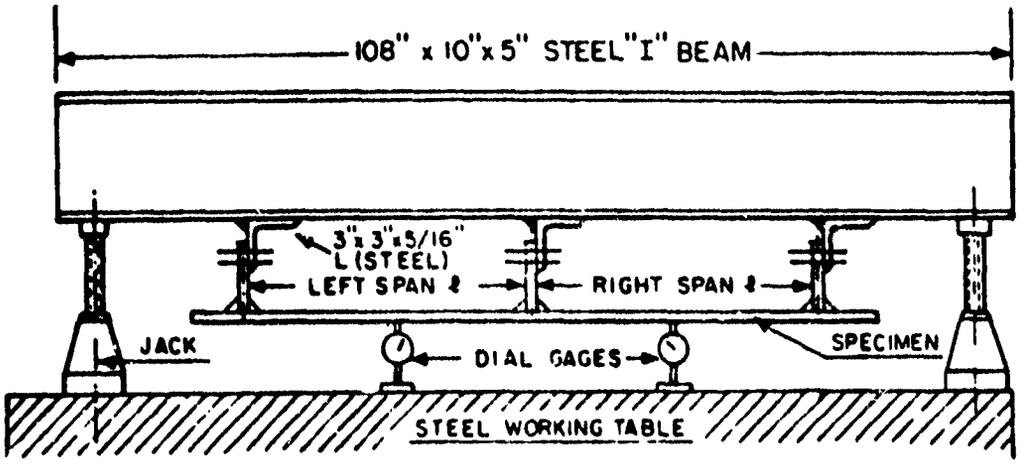

a GENERAL ASSEMBLING FOR THE EXPERIMENTS

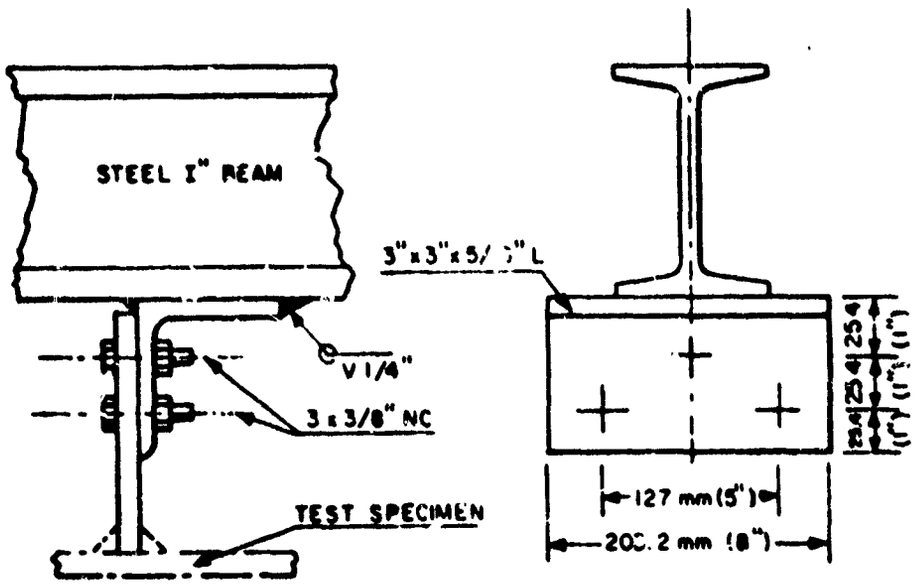

b. DETAILS OF FIXATION OF THE TEST SPECIMENS

JIG ASSEMBLING FOR THE EXPERIMENTS

FIG. 5.4

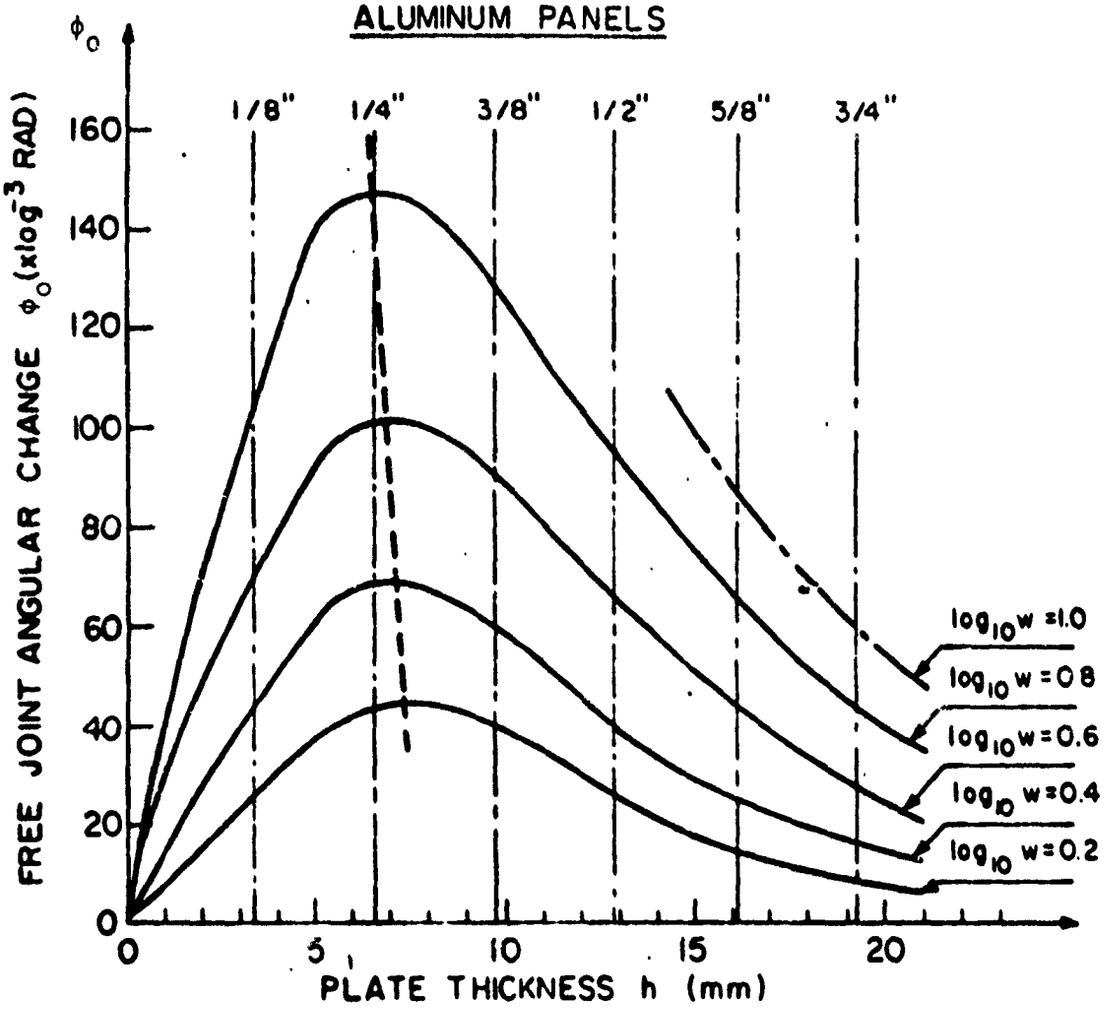

VARIATION OF FREE JOINT ANGULAR CHANGE ϕ_o IN FUNCTION OF PLATE THICKNESS "t" AND CONSTANT $\log_{10} w$ FOR ALUMINUM

FIG. 5.5

The arc form deformation in the constraint joint case, as shown in Figure 5.2b, is a consequence of the development of highly concentrated residual stresses near the weld zone, as well as of the presence of the reaction stresses which result from the constraint. The reaction stresses are observed to be uniformly distributed over the whole region of the welded joint. This can lead to the assumption that the induced bending moments at the weld joints are constant. Using this assumption and the simple beam theory, the following relation is derived:

$$\phi_{max} = \frac{M_o}{2EI} \qquad (5.4)$$

where

ϕ_{max} = maximum value of at x = 0

M_0 = induced bending moment

Figure 5.6 shows the angular changes ϕ_{max} as plotted against the plate thickness t, for constant values of $\log_{10}w$. The results obtained for the last three spans are in good agreement with what was expected from the experiments. However, the results for the case of a 16" span are somewhat surprising. It seems that in the case of shorter spans, there is some kind of combination between the reaction stresses and the effect of shrinkage of the weld fillets, resulting in an inherrent bending moment of such a magnitude so as to cause relatively larger angular distortion at the fillet welds. This argument is not at all conclusive, therefore more work should be done on this problem.

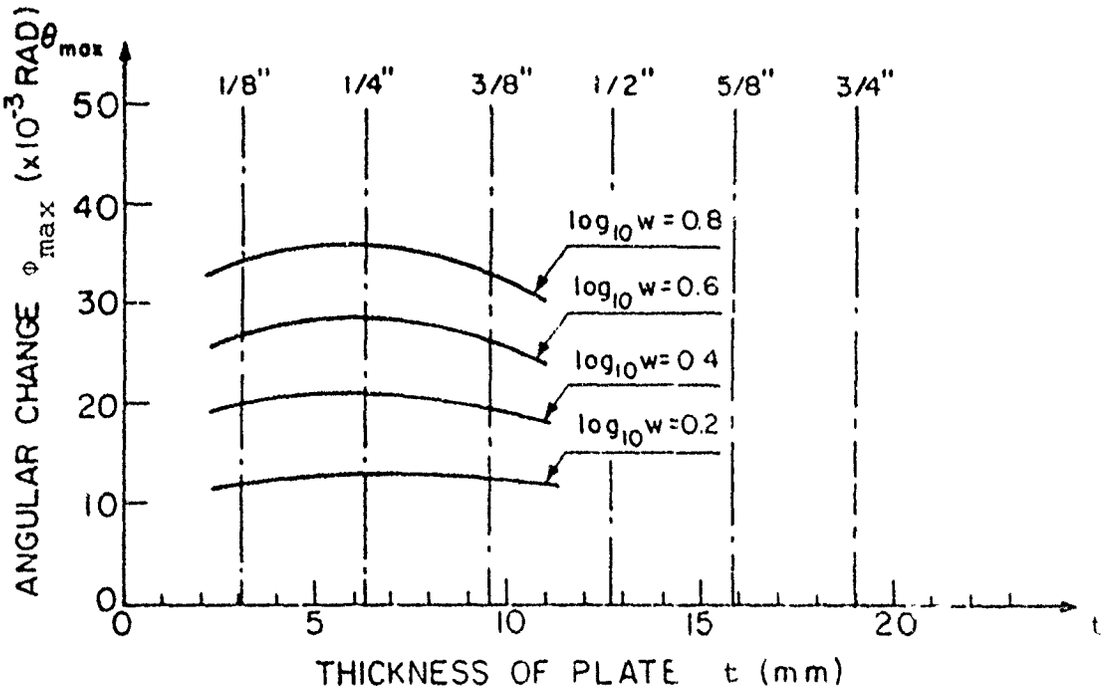

a SPAN = 406.6 mm (16")

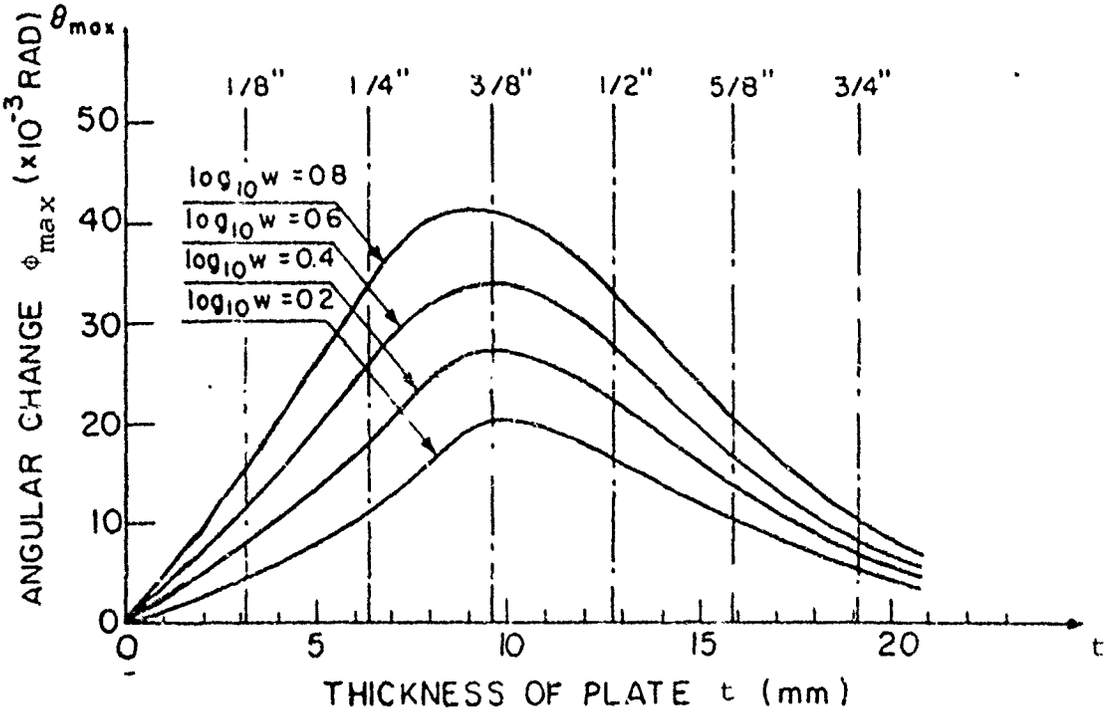

b SPAN = 508.0 mm (20")

VARIATION OF ϕ_{max} WITH "h" FOR CONSTANT $\log_{10}$w

FIG 5.6

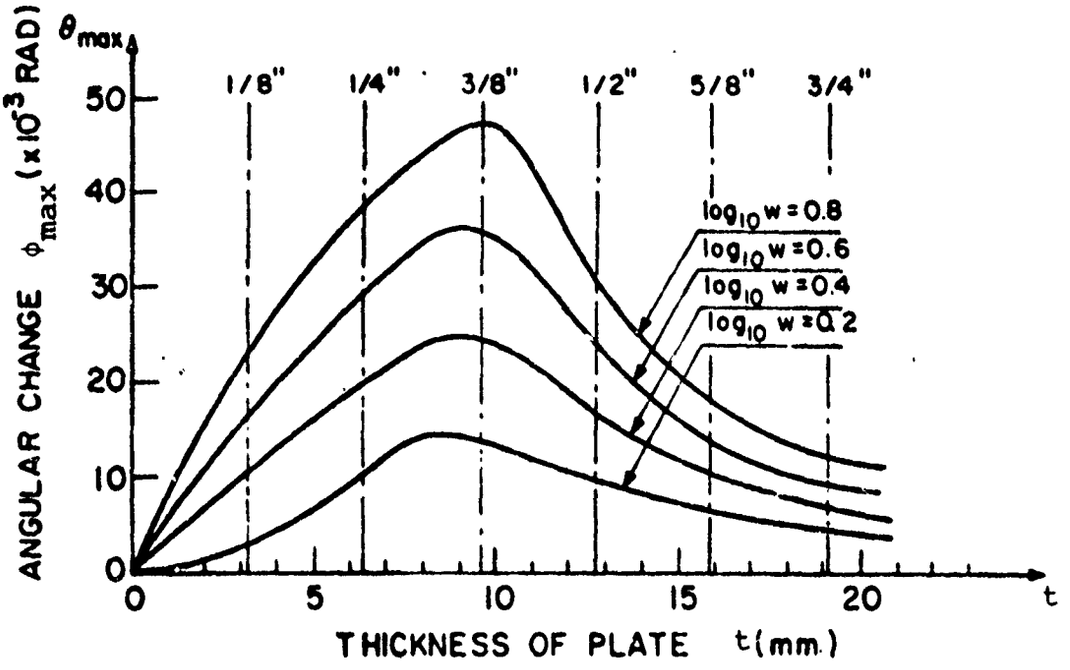

c. SPAN = 609.6 mm (24")

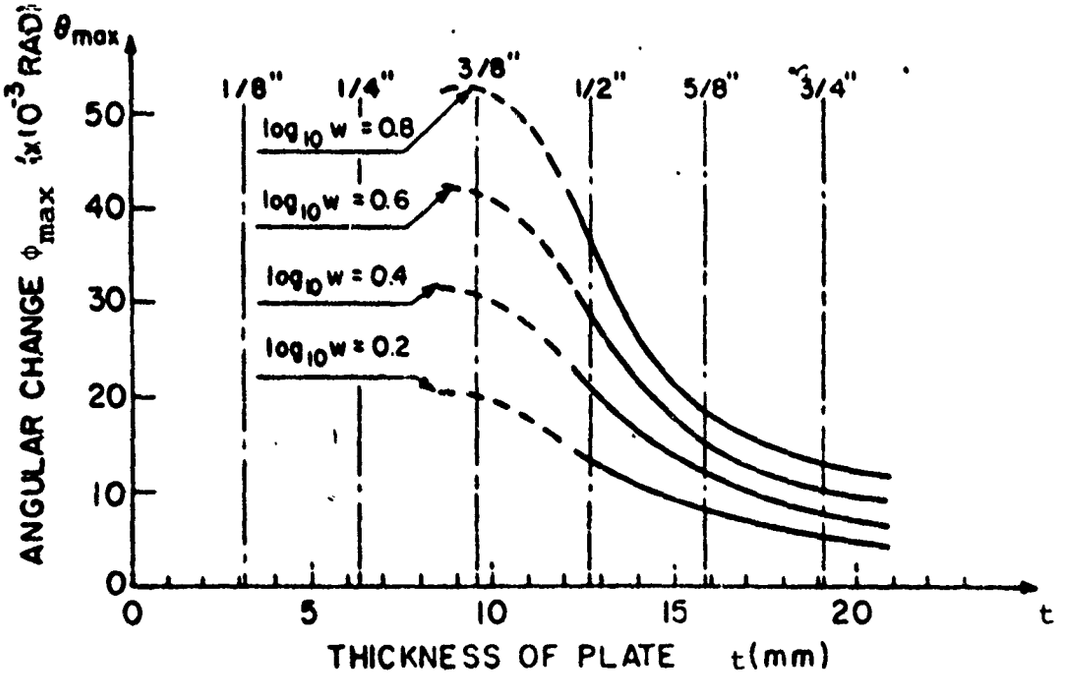

d. SPAN = 812.8 mm (32") - DASHED LINES ARE GUESSES

VARIATION OF ϕ_{max} WITH "h" FOR CONSTANT $\log_{10} w$ (CONT.)

FIG. 5.6

Doing a somewhat similar analysis with the one done by Masubuchi, Taniquchi[29] arrived at the same relation between ϕ and ϕ_o (Eq. 5.3). The coefficient of rigidity C was found using the experimental results obtained. It is shown plotted in Figure 5.7 as a function of $\log_{10}w$ and plate thickness, t.

Taniguchi carried out a regression analysis trying to obtain C in an equation form. He suggested the following equation:

$$C = 6.35t^{(2.67 - 0.065w)} \qquad (5.5)$$

which is valid for the following cases:

$1.58 \leq W \leq 6.30$ (w in q/cm)

6 mm (about 1/4") $\leq$ t $\leq$ 19 mm (about 3/4") (t in mm)

Analytical Method

It can be stated in general that the following variables are very important if the conduction of a purely analytical analysis is desired:[29]

(1) Temperature distribution throughout the thickness of the plate, due to the welding heat.

(2) Shrinkage of the welding fillet.

(3) Heat input due to welding conditions.

(4) Cooling rate of the weldment as well as of the heat affected zone.

(5) The temperature dependent mechanical and thermal properties of the material.

(6) The stiffness of the structure.

(7) The dimensions of the panel structure.

(8) Number of welding passes.

(8) Welding sequence.

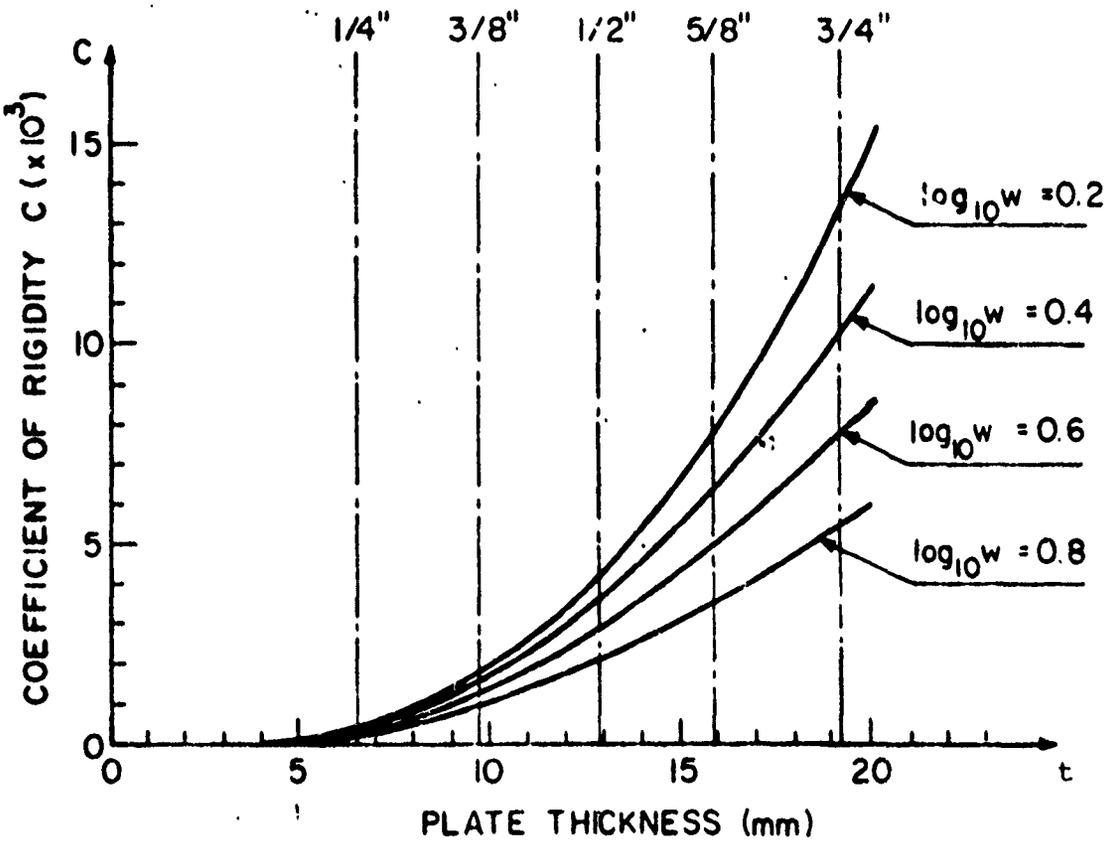

VALUES OF THE COEFFICIENT "C" PLOTTED AGAINST PLATE THICKNESS AND CONSTANT VALUES OF $\log_{10} w$

FIG. 5.7

(9) Welding process.

Taniguchi[29] conducted a theoretical analysis for the prediction of the angular change ϕ_o in free joints taking into account only the two first effects.

Table 5.1 summarizes and compares the theoretical and experimental results obtained in the analysis. Results for mild steel from previous investigations are also included. It is apparent that for both materials, the experimental values are quite above the theoretical ones, at least in the lower range of thicknesses. This disagreement is believed that is due to the many simplifications introduced in the analysis. It is felt, however, that if a more accurate analysis is conducted, a better agreement with the experiments can be achieved.

5.2 Two-Dimensional Analysis

A two-dimensional analysis was conducted at M.I.T. by Shin[30] using the finite element method. A summary of this analysis will be included here.

Equation (5.3), developed by Masubuchi[28] for the one-dimensional case, was induced by using the minimum energy principle. As was stated in Section 5.1, the amount of angular change ϕ in a constrained structure is smaller than that in a free joint, ϕ_o. This indicates that a certain amount of energy is necessary to decrease the angular change energy is necessary to decrease the angular change from ϕ_o to ϕ. If the necessary energy is represented

TABLE 5.1

VALUES OF θ_o FOR ALUMINUM AND STEEL OBTAINED FROM THEORETICAL CALCULATION AND FROM EXPERIMENTS

h (mm)	θ_o ($\times 10^{-3}$ RAD)							
	5086-H32-Aluminum				Mild Steel			
	Due to plate heating	Due to fillet shrinkage	Total θ_o		Due to plate heating	Due to fillet shrinkage	Total θ_o	
			Calc.	Exp.			Calc.	Exp.
6.350 (1/4")	0.02	8.20	8.22	42.0	5.50	8.90	14.40	38.0
9.525 (3/8")	0.55	6.90	7.45	39.0	9.15	7.10	16.25	56.0
12.700 (1/2")	1.75	5.70	7.45	26.0	11.25	5.40	16.65	36.0
15.875 (5/8")	2.50	4.70	7.20	14.0	11.10	4.30	15.40	26.0
19.050 (3/4")	2.05	3.80	5.85	9.0	8.45	3.40	11.85	19.0

$D_{f\ Al}$ = 7.52 mm (0.296") corresponding to $\log_w$ = 0.200

$D_{f\ Steel}$ = 6.10 mm (0.240") corresponding to $\log_w$ = 0.650

Fillet sizes obtained from the recommended welding conditions for aluminum and steel.

by U_w, one may write:

$$U_w = \int_0^{\phi_o - \phi} \frac{dU_w}{d(\phi_o - \phi)} \, d(\phi_o - \phi) \qquad (5.6)$$

On the other hand, the strain energy stored in the constrained plate per unit width, U_p, can be expressed, using the elastic beam theory, as:

$$U_p = \frac{D}{\ell} \phi^2 \qquad (5.7)$$

Since U_p increases and U_w decreases as the constrained angle increases, the condition for equilibrium of this system requires that the total energy $U_t = U_w + U_p$ should be minimum. Furthermore, for the simplification of the problem, the ratio of incremental welding energy change to angular change is assumed to be linear as follows:

$$\frac{dU_w}{d(\phi_o - \phi)} = C(\phi_o - \phi) \qquad (5.8)$$

From equations (5.6) and (5.8), welding energy per unit width can be expressed as:

$$U_w = \frac{C}{2}(\phi_o - \phi)^2 \qquad (5.9)$$

Accordingly, the condition of equilibrium is as follows:

$$\frac{\partial U_t}{\partial \phi} = - C(\phi_o - \phi) + \frac{2D}{\ell} \phi = 0$$

From the above, equation (5.3) is obtained.

Extending the same principle to the distortion of a rectangular plate with fillet welds along the force edges, we can express the deflection $\delta(x, y)$ at any point as:

$$\delta(x, y) = c_1 + c_2x + c_3y + \ldots \tag{5.11}$$

The strain energy stored in the rectangular plate, with length a and width b, is given then by:

$$U_p = \frac{D}{2}\int_0^a \int_0^b \left[\left(\frac{\partial^2\delta}{\partial x^2} + \frac{\partial^2\delta}{\partial y^2}\right)^2 - 2(1-\gamma)\left(\frac{\partial^2\delta}{\partial x^2}\cdot\frac{\partial^2\delta}{\partial y^2} - \frac{\partial^2\delta}{\partial x\partial y}\right)^2\right]dxdy \tag{5.12}$$

The welding energy stored in the fillet welds along the four edges is:

$$U_w = \int_0^a \frac{C_y}{2}(\phi_o - \phi_y)^2 dx + \int_0^b \frac{C_x}{2}(\phi_o - \phi_x)^2 dy \tag{5.13}$$

where, C_y and C_x are C-values of the welds parallel to the y- and x- axis respectively, and ϕ_y and ϕ_x are angular changes at welds parallel to the y- and x- axis respectively.

For equilibrium, the variation of the total energy should be zero:

$$\delta U_T = \delta U_p + \delta U_w = 0 \tag{5.14}$$

The finite element method was used to conduct the numerical analysis. Figure 5.8 shows how the rectangular plate was divided.

As an effort to verify the validity of this analysis, comparison was made of analytically determined panel distortions and experimental data obtained by Duffy.[31] Although absolute agreement of analytical and experimental results was not accomplished, the shapes of distortion were quite similar, indicating that the analysis is valid.

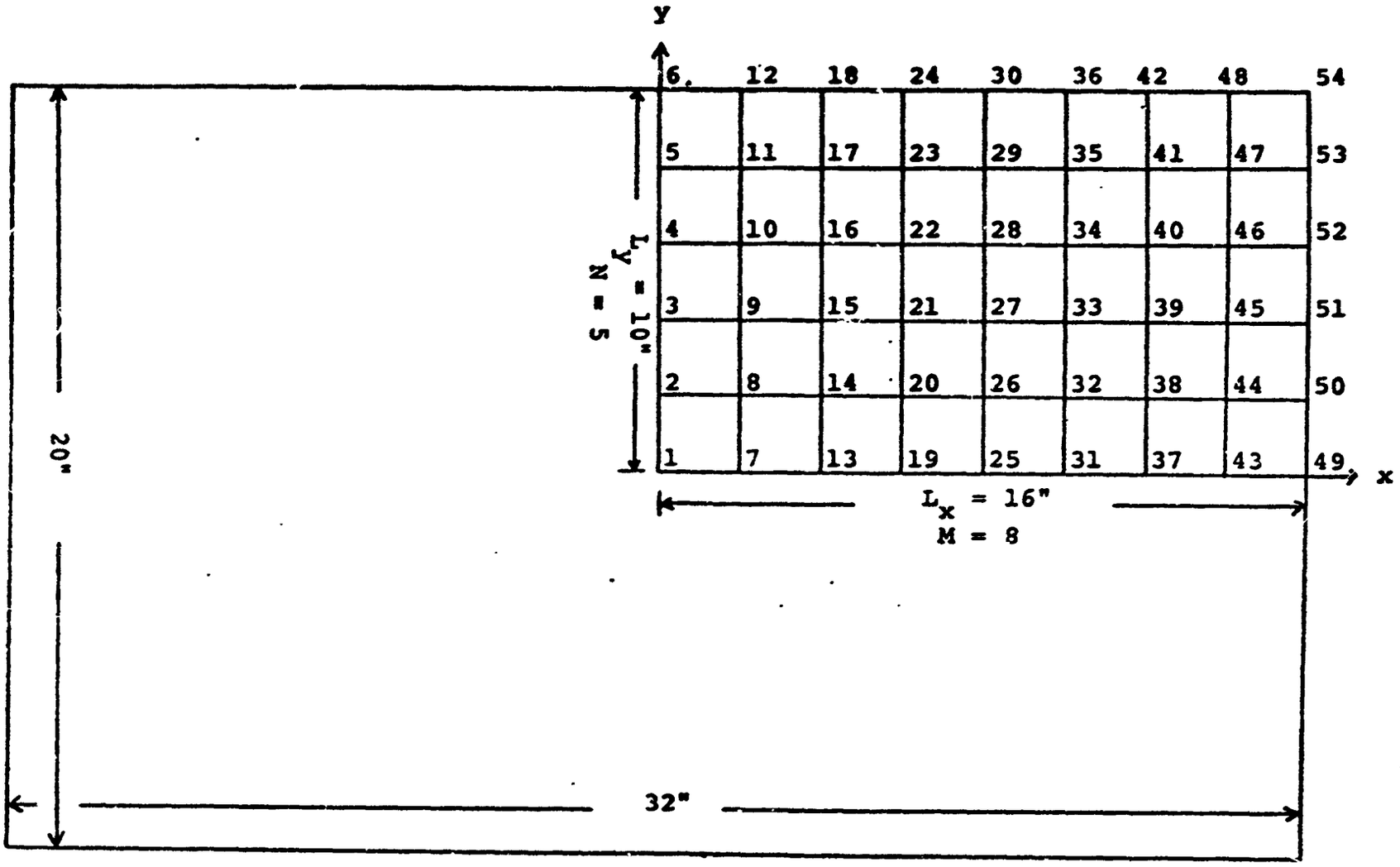

Figure 5.8 Dimensions and Element Meshes of One-quarter of the Plate for Computer Input

5.3 Out-of-Plane Distortion in Aluminum Panel Structures

A big effort was devoted at M.I.T. during the past year towards a verification and/or modification of the state of the art of out-of-plane distortion for large aluminum panel structures. V. Brito[32] conducted a series of experiments for the measurement of out-of-plane distortion of large panel structures as the ones shown in Figure 5.9. The base plate material was 5052-H32 Aluminum Low Magnesium Alloy. The welding was performed using a semi-automatic GMA welding machine and Al 4043 as filler wire. Typical dimensions of the specimens were as follows (refer to Fig. 5.9a and b):

A = B = 48 inches

a = 23 1/2, 25 5/8 in.

b = 16, 23 1/4 in.

T = 4 5/8, 5 in.

h = 3/16, 1/4 in.

H = 3/16, 1/4 in.

Some of the specimens were clamped during welding.

Brito conducted also some experiments by heating the plates before welding in an effort to reduce the distortion. His thesis contains an extensive list of the results obtained in both series of experiments.

Using both the one-dimensional and the two-dimensional analyses described in the previous sections, Brito tried to correlate his experimental results with the predicted analytical ones. Very poor agreement was found between the two, unless higher values of the rigidity coefficient C than the ones suggested by the analysis

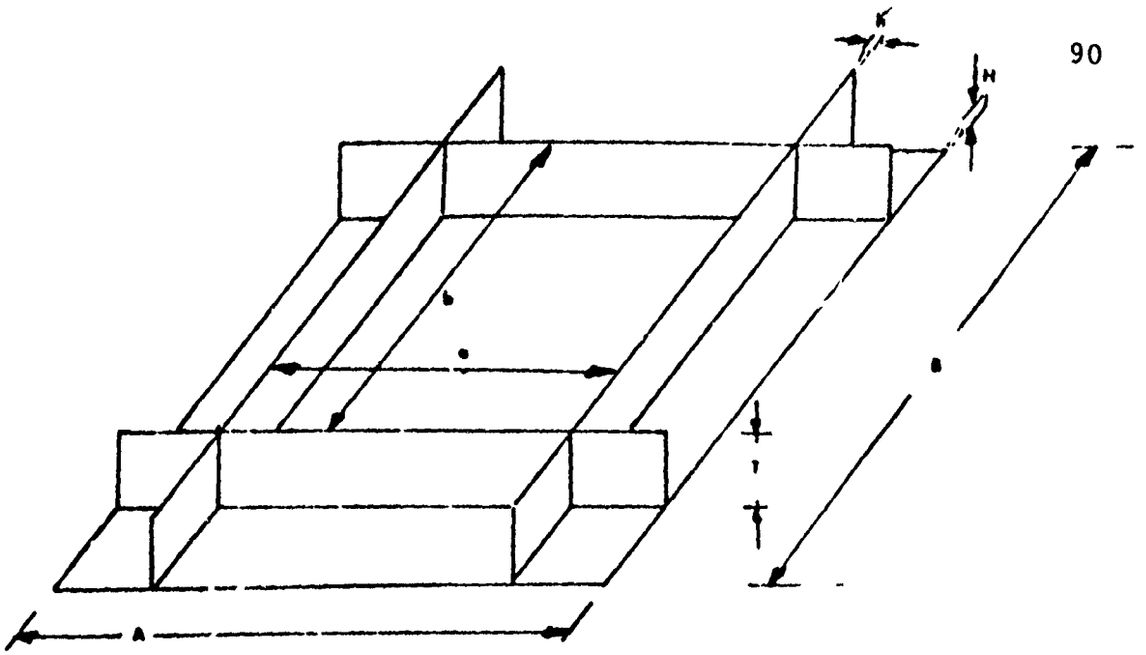

Figure 5.9a

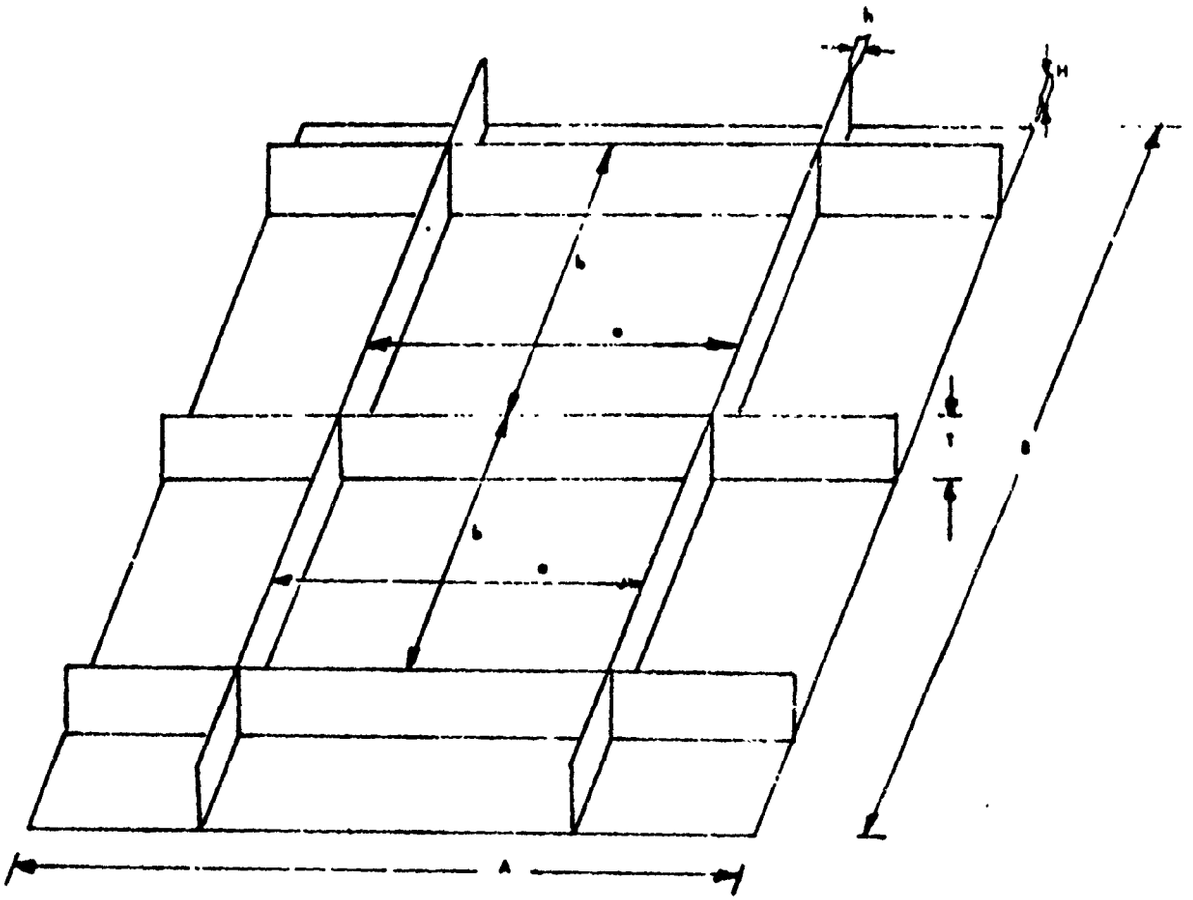

Figure 5.9b

Figure 5.9 Experiment plate dimensions and Configuration

were used.

It was decided that a modification of the two-dimensional analysis was mandatory. This was done using the concept of the induced bending moment M_c (mentioned in section 5.1) rather than the rigidity coefficient C, which was felt to be somewhat arbitrary. The plate configuration for the mathematical analysis is shown in Figure 5.10.

The merits of this approach is the fact that the induced moment M_o is independent of the stiffening space and the plate thickness. This means that the central plate deformation can be predicted, if welding parameters are known.

An equation relating the central deflection W_o and the eqivalent uniform moment M_o induced during fillet welding was developed, using the classical elastic plate theory:

$$W_o = \frac{M_o \gamma a^2}{\pi^2 D} \sum_{m=1,3,5,\ldots} (-1)^{\frac{m-1}{2}} \cdot \frac{1}{m^2}\left(\frac{\tanh \frac{m\pi\gamma}{2}}{\cosh \frac{m\pi\gamma}{2}} + \frac{\tanh \frac{m\pi}{2\gamma}}{\cosh \frac{m\pi}{2\gamma}}\right) \qquad (5.15)$$

where $\gamma = b/a$.

Figure 5.11 shows a plot of $K(\gamma)$, as defined in the figure, versus γ. The plot was done evaluating several terms of the series for various γ. It is pointed out, however, that although the method worked well for the results obtained in the aforementioned experiments, it was not checked for other plate thicknesses due to lack of available data.

Further theoretical calculations allowed the establishment of

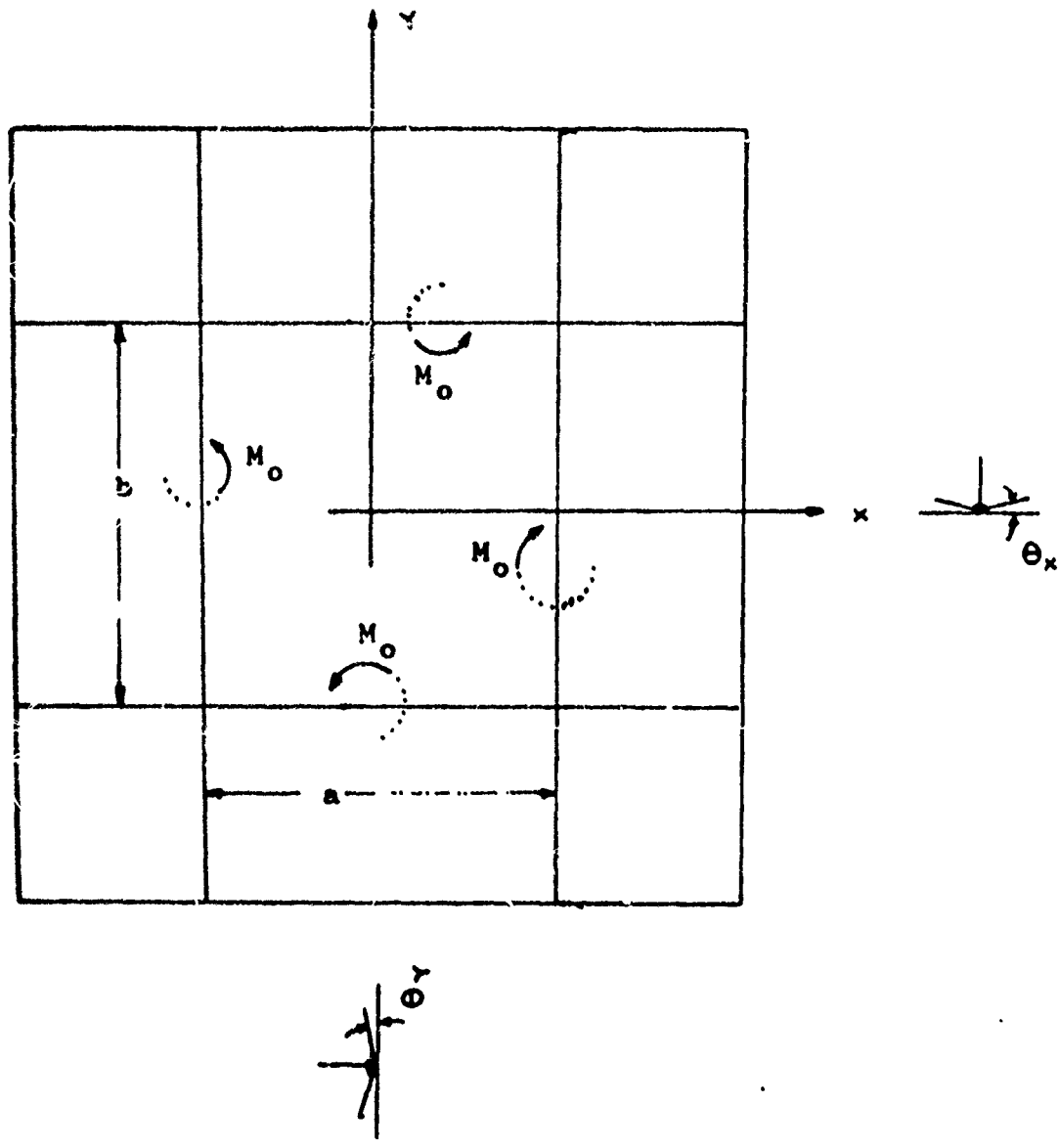

Figure 5.10 **Plate Configuration**

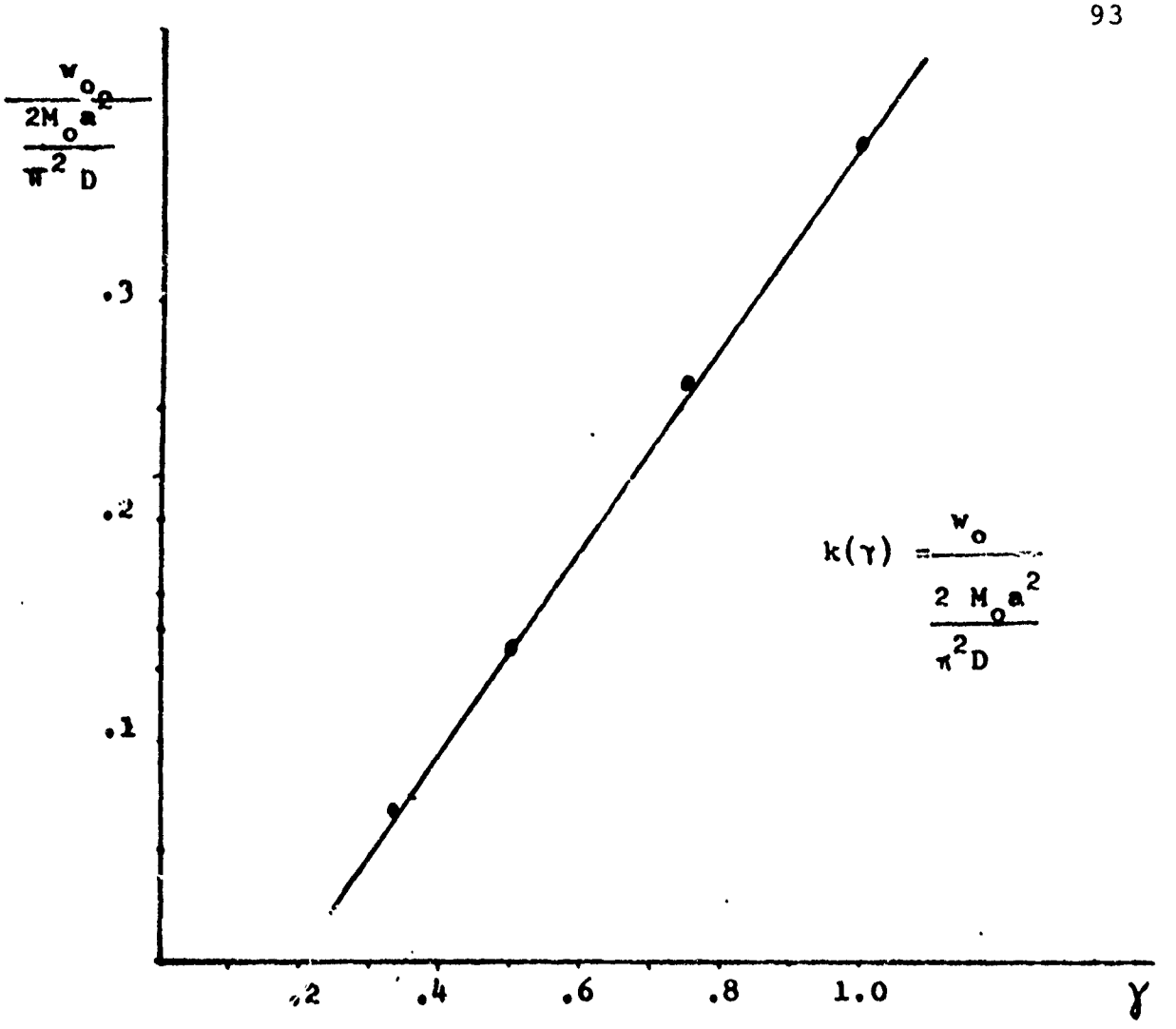

Figure 5.11 Calculation of k (γ)

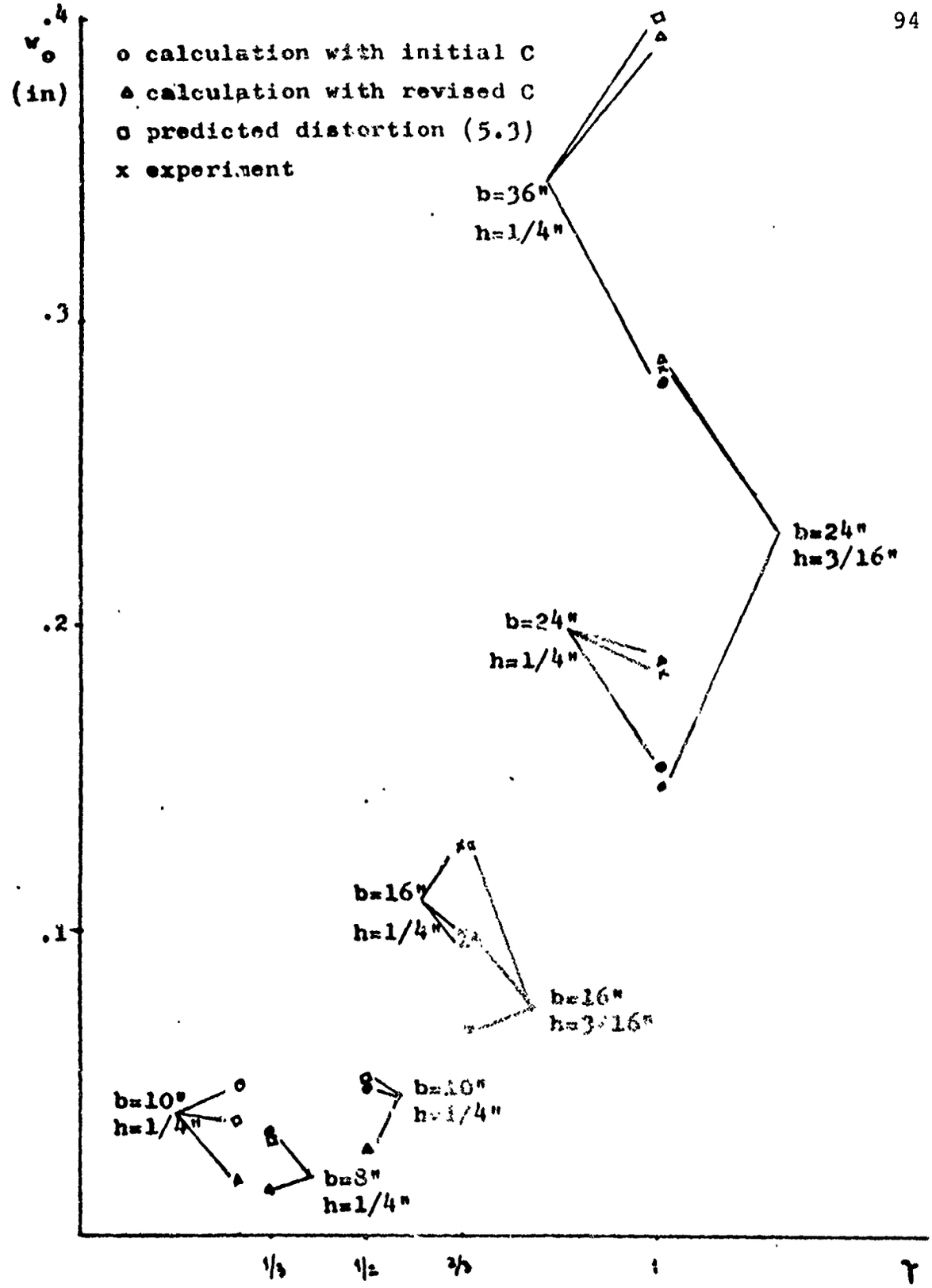

Fig. 5.12-Comparison between calculated, predicted and experimental central plate deflection

a relation between M_o and C. Using this relation, Brito recalculated the C- coefficients and from this the central deflection W_o using the finite element method discussed in Section 5.2. A closer agreement with experimental results was found, as shown in Figure 5.12.

5.4 Allowable Out-of-Plane Distortion

Figures 5.13, 5.14, and 5.15 compare results of the analysis with current Navy specifications. In these figures comparisons are made among the following:

(1) Estimate values of distortion likely to occur due to welding

(2) Initial distortion which could be allowed in order to avoid buckling of the panel under certain service conditions

(3) Distortion allowed in NAVSHIPS specifications

Figure 5.13 shows the results for steel structures with a fixed span length of 800 mm (32 inches) using various thicknesses. Figure 5.14 and 5.15 show the results for aluminum structures with span lengths of 500 mm (20 inches) and 800 mm (32 inches), respectively

Theoretically or ideally, the following should happen:

(1) The allowable distortion for buckling should be the largest among the three so that a structure which meet the Navy specifications would not buckle during service.

(2) Values of estimated weld distortion should be the lowest so that distortion which is likely to happen is less than that allowed by the specifications and is also less than the allowable distortion for buckling.

Regarding the Navy specifications for unfairness, the Navy had for many years a rather severe standards (NAVSHIPS 0900-000-1000, 1966) as indicated by broken lines in Figure 5.13. The Navy specifications have been relaxed recently as shown by solid lines in Figure 5.13 (NAVSHIPS 0900-000-1000, 1969). The new specifications also give unfairness tolerances for aluminum structures, as shown by solid lines in Figure 5.14 and 5.15.

Results of the analysis have shown that the old specifications are difficult to meet and seem to guarantee the structural integrity of the ship. The new specifications are easy to meet, but may not provide this guarantee.

Steel Structures

Figure 5.13 summarizes the results obtained for steel structures. Values of weld distortion estimated by Masubuchi (based on experiments made in Japan) and by Okerblom (based on experiments in Russia) are definitely lower than the solid lines but slightly higher than the broken lines. This means that a fabricator of a ship should have no difficulty meeting the new specifications, but they are likely to have a hard time meeting the old specifications. On the other hand, values of allowable distortion for buckling appear to be about the same as those allowed in the old specifications, but they are definitely lower than those allowed in the new specifications.

Aluminum Structures

Figure 5.14 and 5.15 summarize the results obtained on aluminum structures. A fabricator of a ship should have no difficulty

meeting the current Navy specifications. On the subject of buckling, however, the current specifications may be too relaxed.

The amount of distortion appears to depend greatly on plate thickness. When the plate is over 14 mm (9/16") or 16 mm (5/8") thick, the amount of weld distortion is much less than the allowable distortion. When the plate is less than 12 mm (1/2") or 10 mm (3/8"), however, the distortion problem becomes serious. Unfortunately the plates most widely used for light aluminum structures such as surface effect ships range from 1/2" to 1/4".

Since the results obtained on aluminum structures indicate serious problems, Professor Masubuchi discussed this subject with engineers at the Boeing Company when he visited them in June, 1975. Boeing engineers indicated that they have had serious distortion problems when fabricating aluminum structures using thin plates of 3/8" or less. Results obtained at M.I.T. seem to concur with the experience at the Boeing Company.

Figures 5.14 and 5.15 show that the amount of out-of-plane distortion can be reduced significantly by increasing the plate thickness, for example from 3/8" to 1/2". But this significantly increases the weight of the structure. One way to solve the problem is to reduce the length of span, for example, from 800 mm (32") to 500 mm (20"). Figures 5.14 and 5.15 show that in fabricating structures with plates 3/8" thick, for example, weld distortion can be reduced and the amount of allowable distortion increased by reducing the span from 32" to 20".

The results indicate that distortion analysis is important

in structural design. An optimum design must take into account structural integrity, welding fabrication, structural weight as well as fabrication cost.

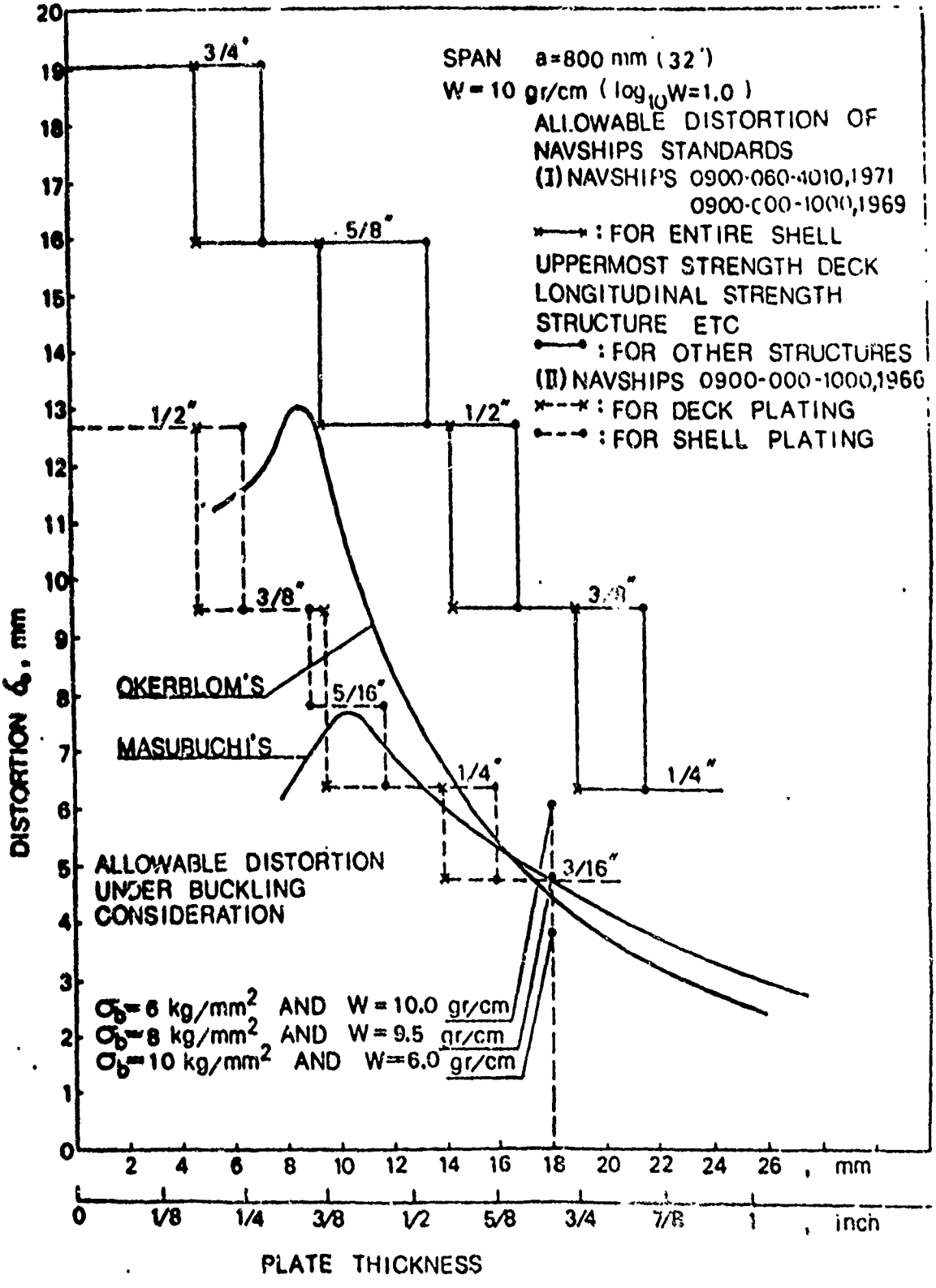

Figure 5.13 Comparison Among (1) Possible Distortion Estimated from Formulas by Masubuchi and Okerblom, (2) Allowable Distortion by Navy Specifications and (3) Allowable Distortion Under Buckling Consideration

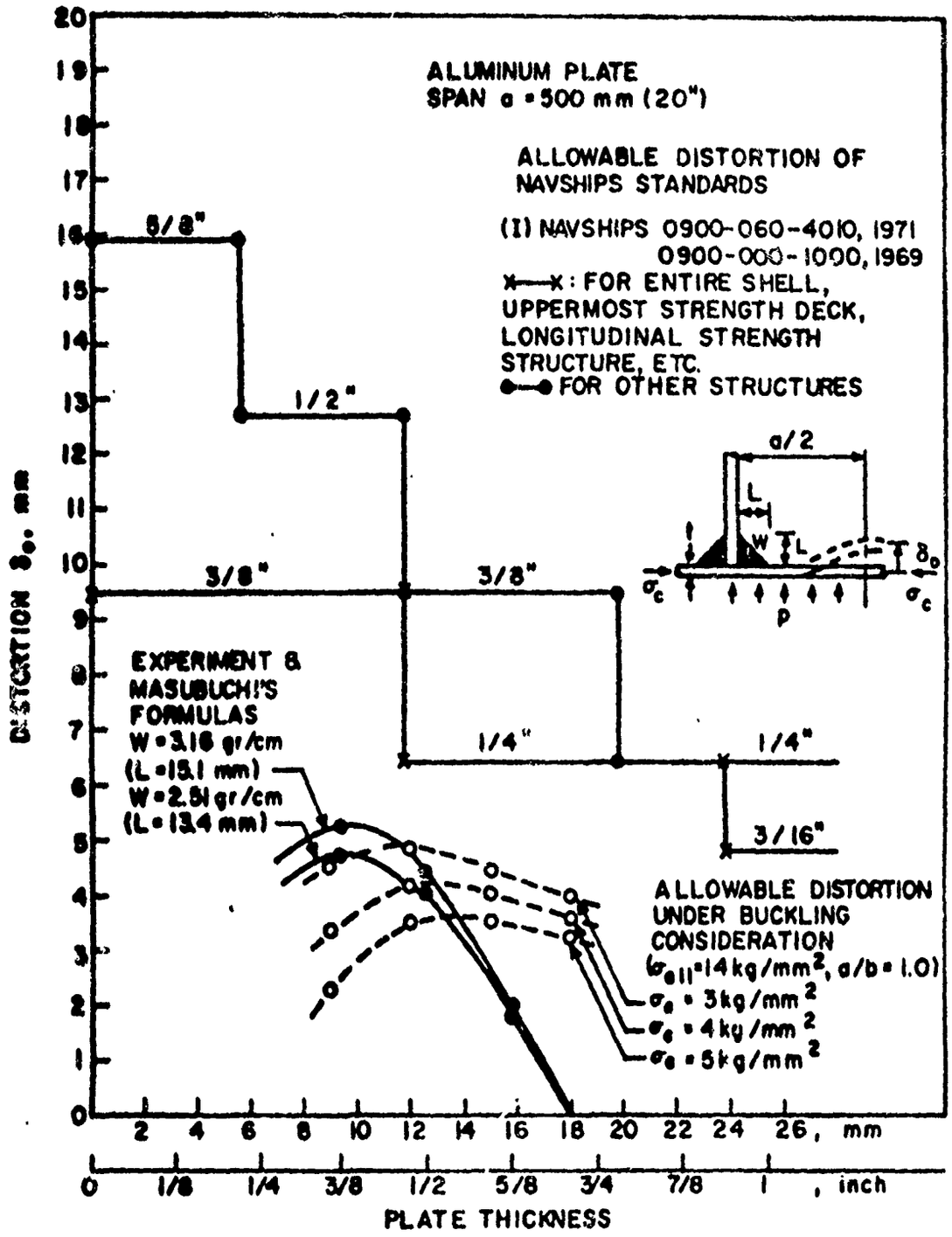

Figure 5.14 **Comparison Among (1) Possible Distortion Estimated from Formulas by Masubuchi, (2) Allowable Distortion by Navy Specification and (3) Allowable Distortion Under Buckling Consideration for Aluminum Plate of 500 mm Span**

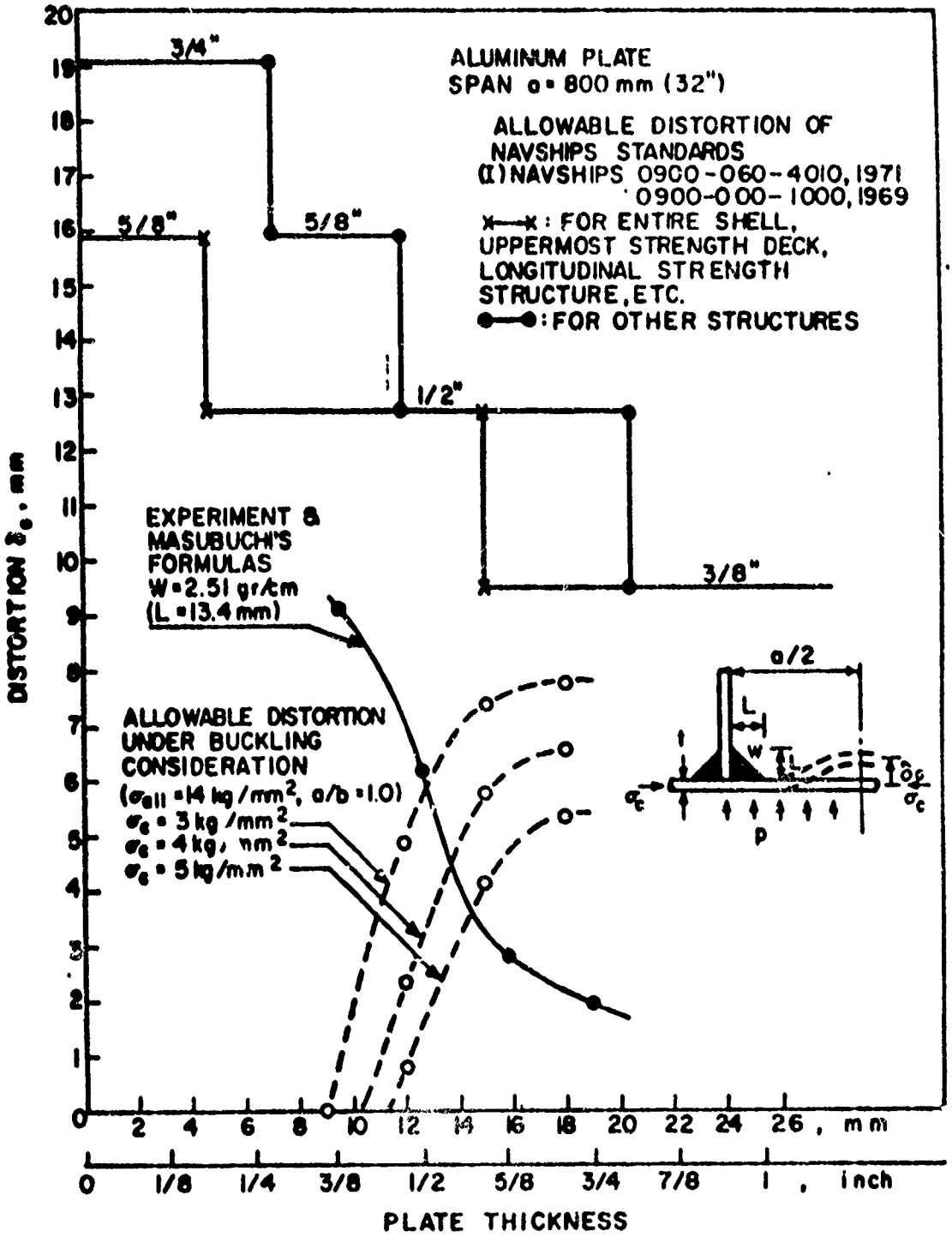

Figure 5.15 Comparison Among (1) Possible Distortion Estimated from Formulas by Masubuchi, (2) Allowable Distortion by Navy Specification and (3) Allowable Distortion Under Buckling Consideration for Aluminum Plate of 800 mm span

6. BUCKLING DISTORTION OF THIN ALUMINUM PLATES

The curves shown in Figures 5.14 and 5.15 of the previous section may imply that weld distortion decreases as the plate thickness decreases below 3/8". On the other hand, buckling becomes a serious distortion problem when thin plates are welded.

As it was explained in Section 5, this decrease in out-of-plane distortion is due to the fact that its cause, the temperature difference in the thickness direction, is almost eliminated if the plate is thin. But, if the plate is thin, it will buckle due to residual stresses only. In other workds, a welded plate will buckle even without the application of external compressive stresses, and when buckling distortion occurs, the amount of distortion is much greater than that caused by out-of-plane distortion.

Basic information about buckling distortion and its effect on the service perfcrmeance of structures can be found in references 3 and 4, written by Masubuchi. In this report we will try to summarize the investigations carried out at M.I.T. during the last years.

6.1 Analytical Investigation

A very comprehensive analytical study of buckling distortion was carried out by Pattee[33] in an effort to determine the critical load of a plate, i.e. the load necessary to maintain a slight buckle in a plate, for various boundary conditions.

For simplicity he assumed the presence of a uniform tension

zone of magnitude T_T and width 2R around the weld and a uniform compression zone of magnitude T_C away from the weld. If the width of the plate is 2b, then the equilibrium condition can be written as:

$$T_T \cdot R = -T_C \cdot (b - R) \qquad (6.1)$$

A second assumption was the symmetric distribution of stress about the weld line. He also assumed that superposition of elastic stresses is possible and that stresses are applied instantaneously throughout the plate and are uniform in the x-direction (parallel to the weld line).

Assuming that neither lateral loads nor body forces act on the plate and considering uniaxial compression only, the governing equation is:

$$\frac{\partial^4 w}{\partial y^4} + 2\frac{\partial^4 w}{\partial x^2 \partial y^2} + \frac{\partial^4 w}{\partial x^4} = \frac{N_x}{D}\frac{\partial^2 w}{\partial x^2} \qquad (6.2)$$

where w = deflection (in)

D = flexural rigidity of the plate = $\frac{Eh^3}{12(1 - \nu^2)}$

E = Young's modulus of elasticity

ν = Poisson's ratio

h = plate thickness (in)

N_x = mid-plane load (lbs/in)

Equation (6.2) can be solved either by assuming a solution of the form

$$w = f(y) \sin\frac{m\pi x}{a} \qquad (6.3)$$

or by using the so called "energy method."

Pattee solved the equation for the four boundary conditions shown in Table 6.1. The same table shows the "real-life" situation which can be approximated by these boundary conditions. The critical compressive load was found for each case for both uniform compression and residual stress situations. The computer programs used for the calculations can be found in Reference (33)

For case 1 (four edges simply supported) and uniform compression the critical load was found to be:

$$(N_x)_{cr} = \frac{\pi^2 D}{a^2}\left(m + \frac{1}{m}\frac{a^2}{b^2}\right) \qquad (6.4)$$

$$(\sigma_x)_{cr} = \frac{(N_x)_{cr}}{h} \qquad (6.5)$$

where a = plate length

b = plate width

h = plate thickness

m = number of half-waves into which the plate buckles

For any given aspect ratio (a/b) there is some value of m which causes N_x to be a minimum. These two numbers are referred as the "critical values."

Results for the other cases could not be given as a closed form solution and so an iterative procedure using the computer programs mentioned before was followed.

In all cases the magnitude of the compressive component of the residual stress was found to be larger than the magnitude of the uniform critical load. This makes intuitive sense, since the compressive residual stress must overcome the effect of the tensile zone. However, in case 3 (loaded edges simply supported, opposite edges clamped and free), little difference was found

BOUNDARY CONDITIONS	ANALOGS
1. 4 edges simply-supported	1. Butt-welded plates which are large in both directions
2. loaded edges simply-supported opposite edges free and free	2a. Long, narrow unrestrained plates 2b. The unclamped test plate
3. loaded edges simply-supported opposite edges clamped and free	3a. The "outboard" section of a stiffened panel. 3b. The partially unclamped test plate
4. loaded edges simply-supported opposite edges clamped and clamped	4a. Plate clamped during welding 4b. Sections of stiffened plates between stiffeners

Table 6.1 Boundary conditions and their Analogs

between the critical uniform and residual loads. This also makes sense since the tensile zone is next to the clamped edge and does not have much "leverage."

As for the effect of tensile zone width, it was found that the critical stress rises as the zone width increases. This is because the compressive forces must overcome the additional influence of the tensile zone. In this sense it would seem that increasing the welding heat input (which increases the tensile zone width), the critical buckling load of the plate would rise. On the other hand, however, it is known that, decreasing the heat input, the stress level is lowered and, hence, buckling is prevented. Therefore, one may conclude that an increase of the welding heat input does not help, because the compressive stresses generated grow faster than the critical stress.

It is well established that, for a given plate, critical dimensions exist which will prevent buckling. However, one should be very careful in utilizing this fact. A problem in buckling has five variables, namely plate material, length, width, thickness and critical stress. It is necessary to specify four of these in order to find the fifth or three in order to find a ratio between the other two (e.g. aspect ratio).

A normal design sequence will define material choice and plate dimensions first. Then a critical stress will be found. If one wishes to know another variable's value, one must predict the welding stress. This becomes an iterative procedure best suited to preliminary design.

The main reason for caution is a misinterpretation of what critical dimensions will allow. One might suppose that any smaller length or width and any greater thickness is always good. This is not entirely true.

The critical load, for uniform compression, can be calculated by the general formula

$$(N_x)_{cr} = k\frac{\pi^2 D}{b^2} \qquad (6.6)$$

where k is a function of a/b and the boundary conditions. As the width decreases, the critical stress rises. Hence, one can make b so small relative to the length that the plate behaves like a beam; and it is well known that beams are not so stiff as plates.

If the length is decreased, the critical load will also rise, but not greatly. Also, increasing the plate thickness is always safe, but not necessarily economical.

6.2 Experimental Investigation

Pattee[33] conducted a series of experiments to determine the buckling behaviour (during and after welding) of variously dimensioned aluminum plates with a number of different boundary conditions. Material used was the 5052-H32 aluminum alloy. 18 specimens were tested with thickness of 1/16", 1/8" and 3/16". All specimens were 6 feet long, with widths 1, 2 and 4 feet. Two specimens were tested for each combination of the above parameters. Thermocouples and strain-gages were located on each of them in order to measure temperature and strain distributions. An auto-

matic GTA system was chosen for the welding, using 5456 alloy filler wire. Since welding of thin plates can cause many problems (local buckling, "burn-through," etc.), the back-up plates and the test specimens were preheated and continuous heating was applied in front of the arc. The welding quality was mixed (good and bad), but generally speaking acceptable.

During the experiments four types of data were collected: temperature, strain, stress and photographic. Figures 6.1 - 6.3 show typical curves for strain, stress and temperature versus time respectively (all curves are for the same specimen). Note that only the longitudinal strain ε_x was measured and hence the longitudinal stress σ_x could only be calculated.

The temperature curves looked much as expected. The traces from the thermocouples nearest the weld-line show very steep slopes as the arc approaches. Those further from the weld are not as steep or high. The temperature approaches room temperature asymptotically during cool-down.

The stress and strain curves had four distinct regions, as can be seen from Figures 6.1 and 6.2. In region 1 the welding has started but few effects are noted in the center of the plate. In region 2 the arc is approaching and there are large strains in the plate. The arc has passed in region 3. The metal is cooling and residual stresses are forming. Finally, in region 4 the plates are unclamped.

Local buckling was a major problem while welding the 1/16" plate. Whenever the plate became too hot, the surface would rear

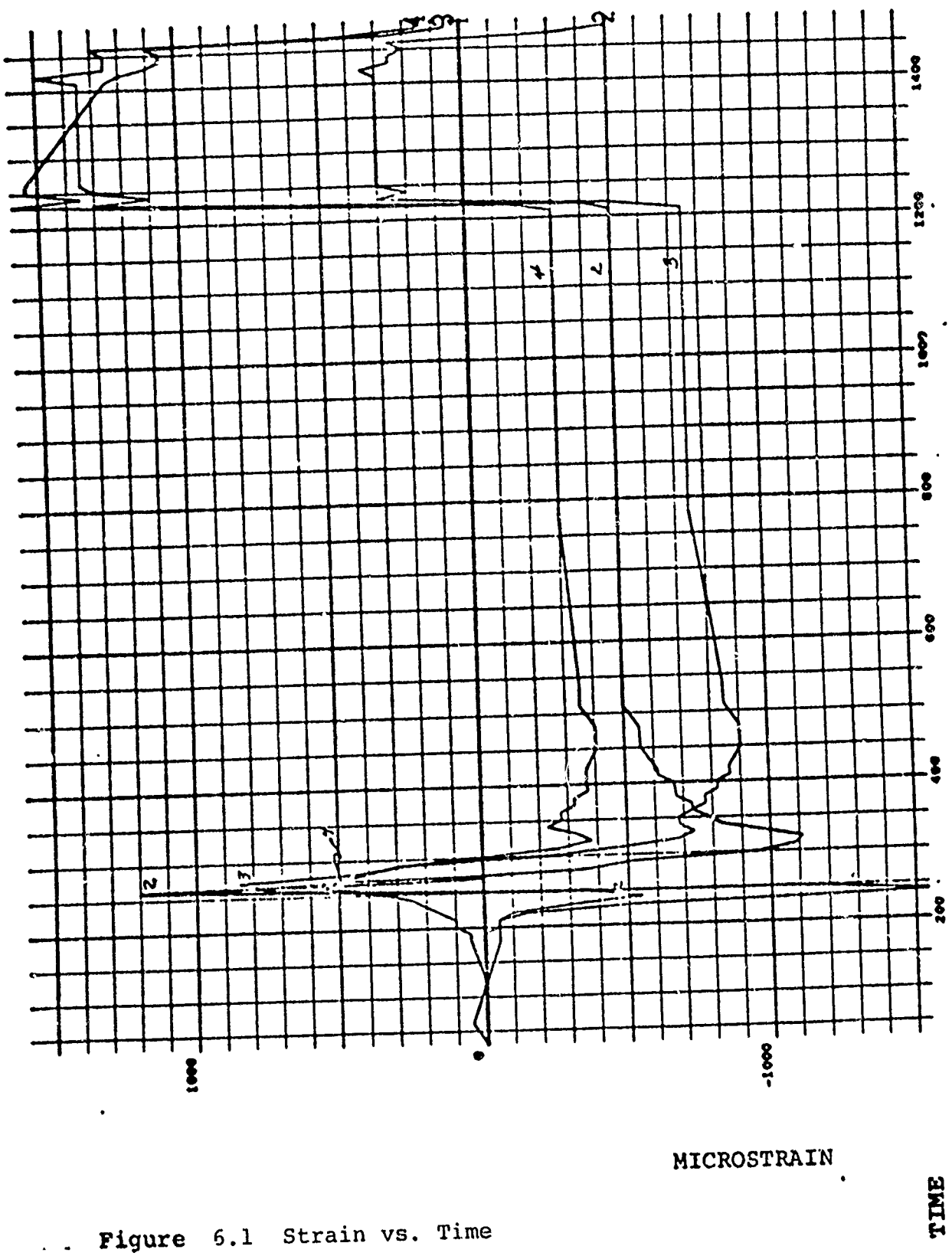

Figure 6.1 Strain vs. Time

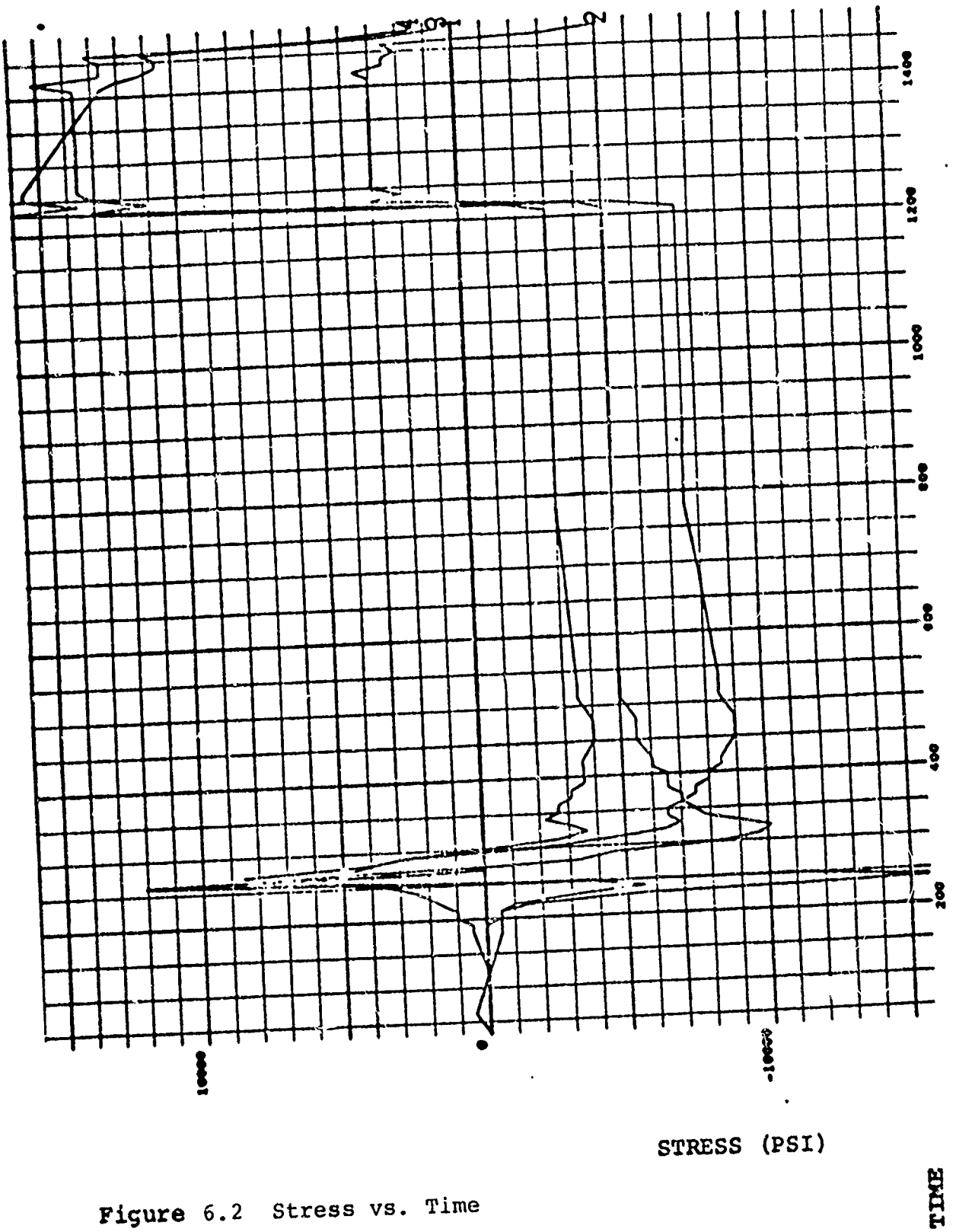

Figure 6.2 Stress vs. Time

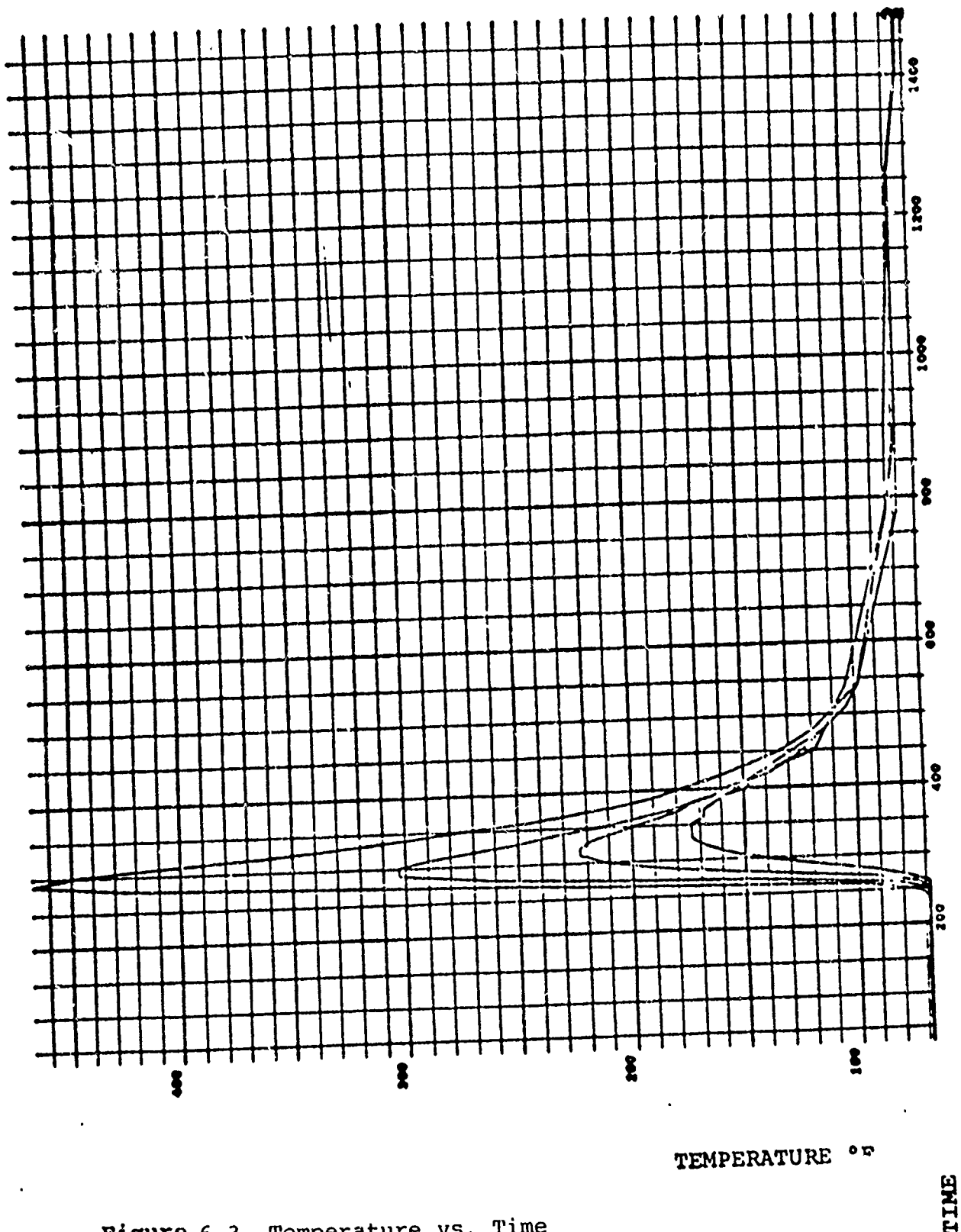

Figure 6.3 Temperature vs. Time

up and cause numerous problems. Arc instability would result. Without the presence of the back-up plate, burn-through would occur. The wave length of this buckling was about 6". The occurrance of this local buckling was not predicted by the analysis discussed in the previous paragraph, since the measured welding stresses were much smaller than the analytically predicted critical ones. It is felt that the reason for this is that the elastic analysis does not hold and so this particular problem should be examined using plasticity.

The correspondence between theory and experiments was very good in all other cases. Buckling occurred whenever the theory predicted it.

6.3 Systematic Prediction and Control of Buckling

As was pointed out in the first paragraph of this section, any plate with given dimensions has some critical buckling load. To avoid failure, the welding stresses must remain below this level. This can be achieved by welding less, using less heat or removing the heat.

The surest way to weld less is to use intermittent welding. As a rough estimate one can say that by halving the amount of welding, the critical load is doubled. Another way is to decrease the weld-bead size, which results in smaller heat requirement during welding and hence in lower stress levels. As a third way, removal of welding heat from the plate using chill bars, water-cooled backing plates, etc., also results in reduced stress levels.

Unfortunately, however, this quenching can produce brittle fractures.

One can see from the above that, within normal operating ranges, lower heat inputs are very significant in lowering the stress levels.

Finally it is worth noting that increasing the transverse moment of inertia of a structure will give as result an increase in its resistance to buckling. This can be achieved by a plate thickening or by a decrease in stiffener plating. Both ways, however, are not always the reliable alternative, since both require more welding, more material with an increase in weight and cost as a result.

Driven by these observations and based on the analytical and experimental investigations conducted so far, Pattee proposed a systematic approach to the buckling problem. A flow chart of this "system" is shown in Figure 6.4. Its components can be described as follows:

(1) Derivations that described the buckling due to welding of thin plates with commonly encountered boundary conditons (as described in section 6.1).

(2) Flexible computer programs which calculate either critical loads or critical dimensions (as those included in Pattee's thesis).

(3) A welding simulation program to predict residual stresses (as M.I.T.'s 1-D or 2-D computer programs discussed in Section 2).

(4) Claculation which determine the effect of any corrective measures (as those described in the beginning of this paragraph).

An example showing how this system works can be found in Reference 33.

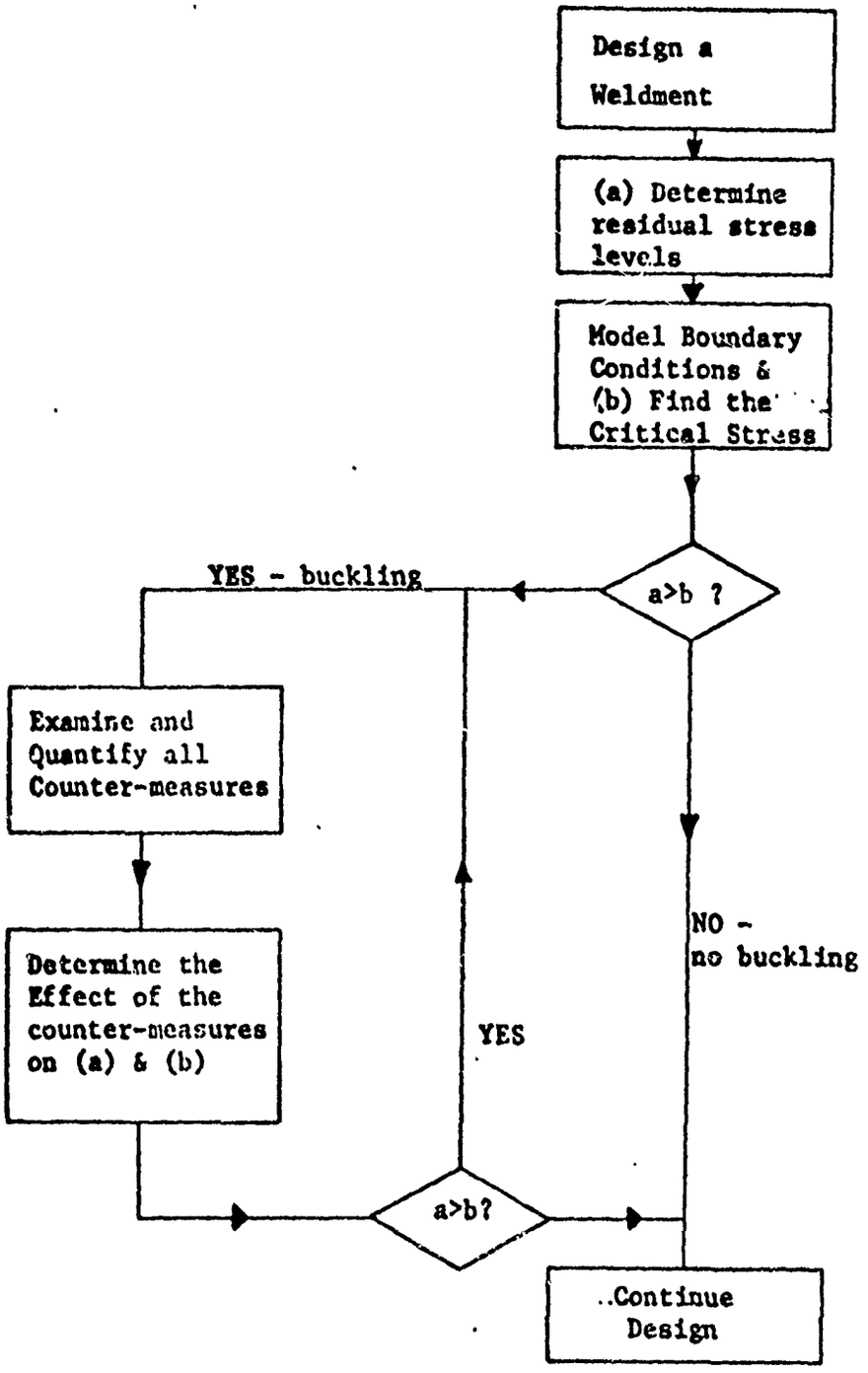

Figure 6.4 Flow chart for the "SYSTEM"

7. METHODS OF DISTORTION REDUCTION IN WELDMENTS

The reliability of a welded structure is often decreased by the presence of residual stresses and distortion. First of all, excessive shrinkage and distortion can cause joint mismatch which reduces the joint strength. High tensile residual stresses in regions near the weld may accelerate growth of a crack under cyclic loading. Compressive residual stresses in the base plate region may reduce the buckling strength of a structural member subjected to compressive loading. This effect is especially great when the member has, in addition to residual stresses, out-of-plane distortion.

All the previous sections dealt with the efforts done at M.I.T. towards an understanding of the mechanisms of the various kinds of distortion as well as with the investigations carried out for the analytical prediction of those distortions. This last section will try to analyze the methods experimented at M.I.T. for distortion reduction in aluminum weldments.

7.1 Commonly Used Methods for Distortion Reduction

Methods presently used to reduce weld distortion include proper selection of the specimen, welding process, welding sequence, forced cooling stress-relief annealing, peening, flame straightening, vibratory stress-relief, electromagnetic hammer and external constraints. Each of these methods is briefly discussed below.( )

Specimen Selection

The length and width of a plate determine the magnitudes of its residual stresses. As length or width are increased, the residual stress will increase to a point and then remain constant.

The effect of thickness on angular distortion of a free joint, as shown in Figure 5.5 and explained in section 5.1, is also an indication of the importance of the plate dimensions.

Welding Process

Since residual stress is an indirect function of welding heat input, as one uses processes that have high heat inputs, one can expect greater residual distortions, not to mention reduced ultimate strengths. The Marshall Space Flight Center investigators found that reduced heat input and narrow weld-metal areas gave higher weld strengths and smaller distortion.[35]

Electron-beam welding (EBW) gives many hopes from that aspect. Dr. Terai, in some recent lectures he gave at M.I.T., mentioned that they succeeded welding a 300 mm (11.81 in.) thick 5083 Aluminum Alloy section with one pass and without distortion for engineering purposes.[36]

Welding Sequence

Kihara[37] observed that, as far as residual stresses are concerned, the effect of welding sequence has only a minor influence on longitudinal stresses. On the other hand, transverse residual stresses were largely affected by the welding sequence.

Many investigators have also observed that differences in welding sequence cause significant difference in transverse distortion. Block welding sequences were generally found to cause less

shrinkage than the multi-layer sequence approach. Symmetrical welding sequences were also found to generate less non-uniformity than multi-pass methods.

Forced Cooling

It was previously mentioned that residual distortion is a function of heat input. Since maximum arrival temperature and time it is achieved are significant in measuring effective weld heat input, one can speculate that by controlling these two, one can, in effect, control residual distortion.

This can be achieved in one way by the absorption of heat from the base plate by forced cooling with cryogenic liquids such as CO_2 or liquid nitrogen. A follow-up auxiliary heating was found to be very effective.

Stress-Relief Annealing

Just as cold work induced stresses are relieved by annealing, residual stresses due to welding can be relieved in the same manner. By proper annealing, the microscopic grain number, size and growth rate are controlled to reduce induced stresses. In the same manner as cryogenic cooling, proper tempering of a weld's thermal cycle can be used to reduce distortion.

Flame Straightening

The use of this method for reducing distortion is universally accomplished by an oxyacetylene flame for essentially the application of heat to a localized area of metal to cause dimensional changes.

In practice, three types of flame straightening techniques

are used, often in combination with water quenching:

(1) Line heating parallel to the weld line

(2) Line heating on the back side of the weld line

(3) Spot heating

As a general observation it can be said that high temperature flame straightening has detrimental effects on the material properties of the base metal.

Vibratory Stress Relief

During cooling the plate is forced to vibrate at its resonant frequency for a time length depending on the weight of the work-piece. During this time, the low frequency vibrations induce a realingment of the lattice structure, reducing the residual stress level.

Electromagnetic Hammer

This technique relies on a magnetic field induced in the base plate to increase the plate's kinetic energy during metal forming. A rapid and predictable acceleration of the deformation is allowed, which results in distortion reduction.

External Constraints

A common practice in the fabrication of welded structures is the use of external constraints for distortion reduction. By the selection of appropriate strong-backs, jigs, clamps and rollers, investigators have found that induced distortions can be reduced.

7.2 Elastic-Plastic Prestraining

Elastic-plastic prestraining as a method of reducing out-of-plane distortion in a one pass double fillet welded T-bar of high strength aluminum was tested extensively at M.I.T. During the

past years great effort has been devoted in reducing out-of-plane distortion of steel structures using this method. However, no investigation has been made towards applying this method to aluminum structures.

Henry[34] conducted a series of experiments on this technique using 5456 aluminum-magnesium alloy plates. Using a uniform plate span and length, and relying on GMA welding process, he investigated the effects of degree of prestraining, plate thickness and number of passes.

Figure 7.1 shows schematically the method of prestraining used in the experiments. Note that the clamps only hold the bottom plate tips to the table and do not force them to be tangent. The round bar is placed under the plate along the longitudinal centerline (weld line) to induce reverse curvature counteracting the out-of-plane distortion from welding.

All test specimens were 24" by 24". Thicknesses of .250", .375" and .50" were used because they appear to have the greatest susceptibility to welding distortion. The degree of prestraining (i.e. liner height) was calculated using a surface strain model and relying on experimental data of strain measurements conducted on 5052-H32 aluminum alloy plates of same thicknesses but different dimension (18" span, 12" length). By assuming a linear approximation of liner height versus plate length, Figure 7.2 was developed. This was done in the hope that these numbers would give the liner diameter for minimum angular distortion.

Figure 7.3 shows a plot of liner height versus plate thickness

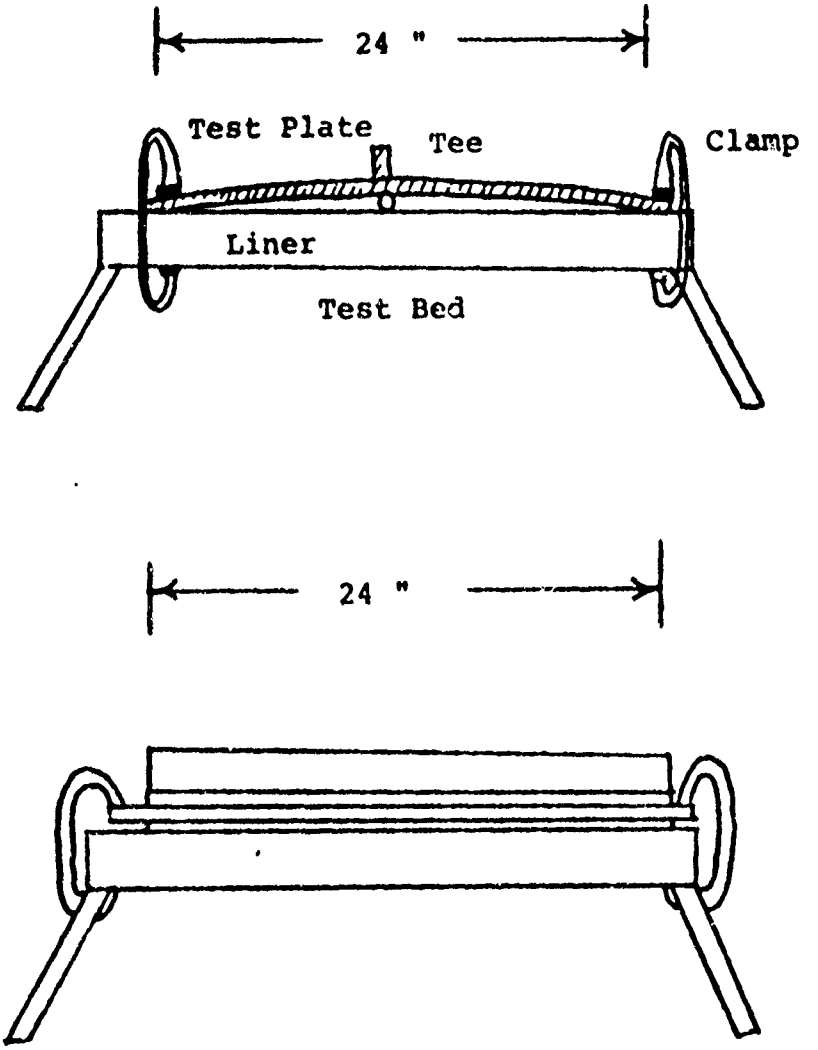

FIGURE 7.1 SCHEMATIC PICTORIAL OF TEST SETUP

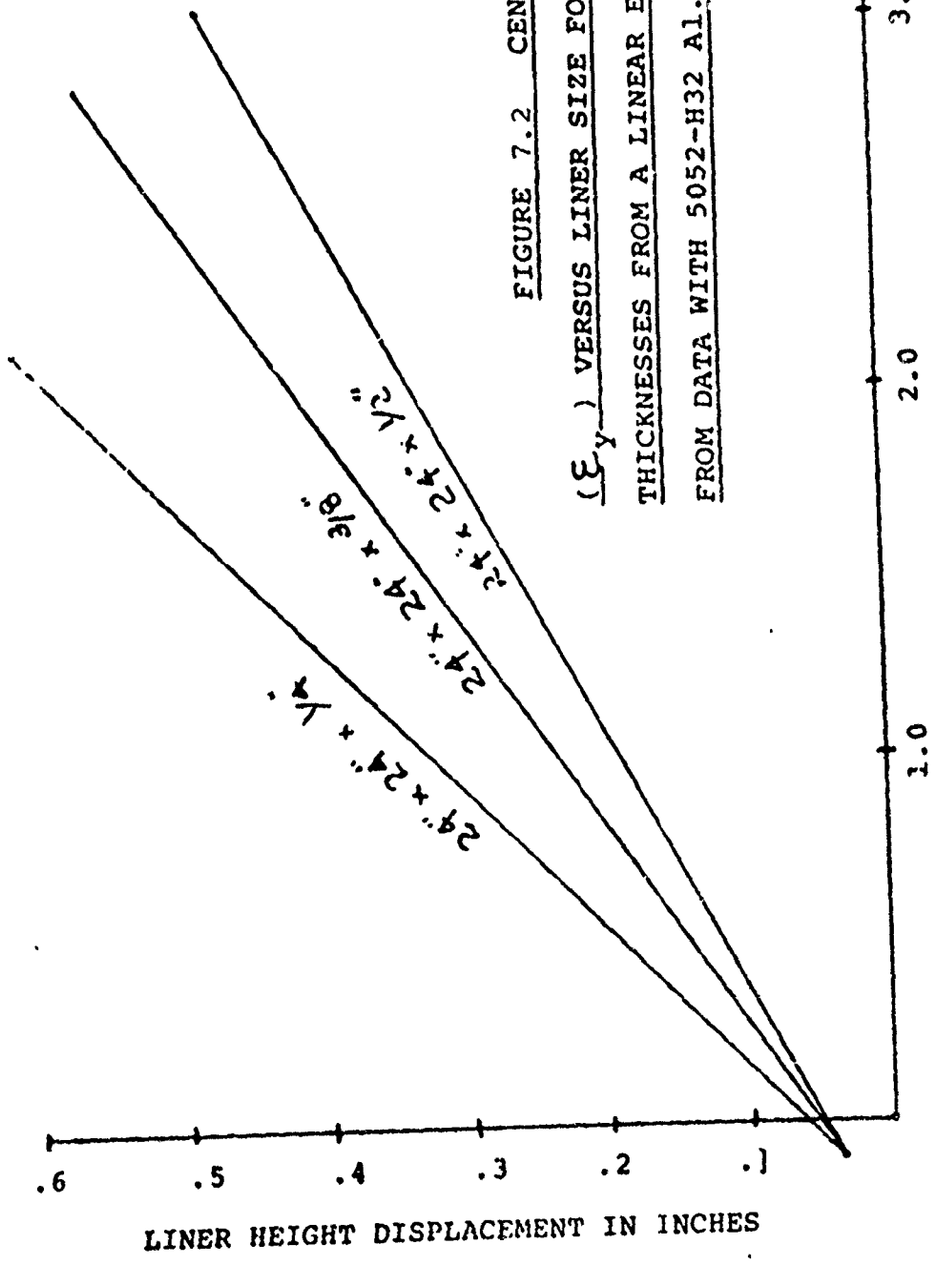

FIGURE 7.2 CENTERLINE MAX. STRAIN (ε_y) VERSUS LINER SIZE FOR SEVERAL PLATE THICKNESSES FROM A LINEAR EXTENSION DONE FROM DATA WITH 5052-H32 Al.ALLOY

FIGURE 7.3 CURVES OF IDEAL LINER HEIGHT VERSUS PLATE THICKNESS FOR A TEE HEIGHT OF 3", 5456 Al. ALLOY PLATE SIZE 24"x24"

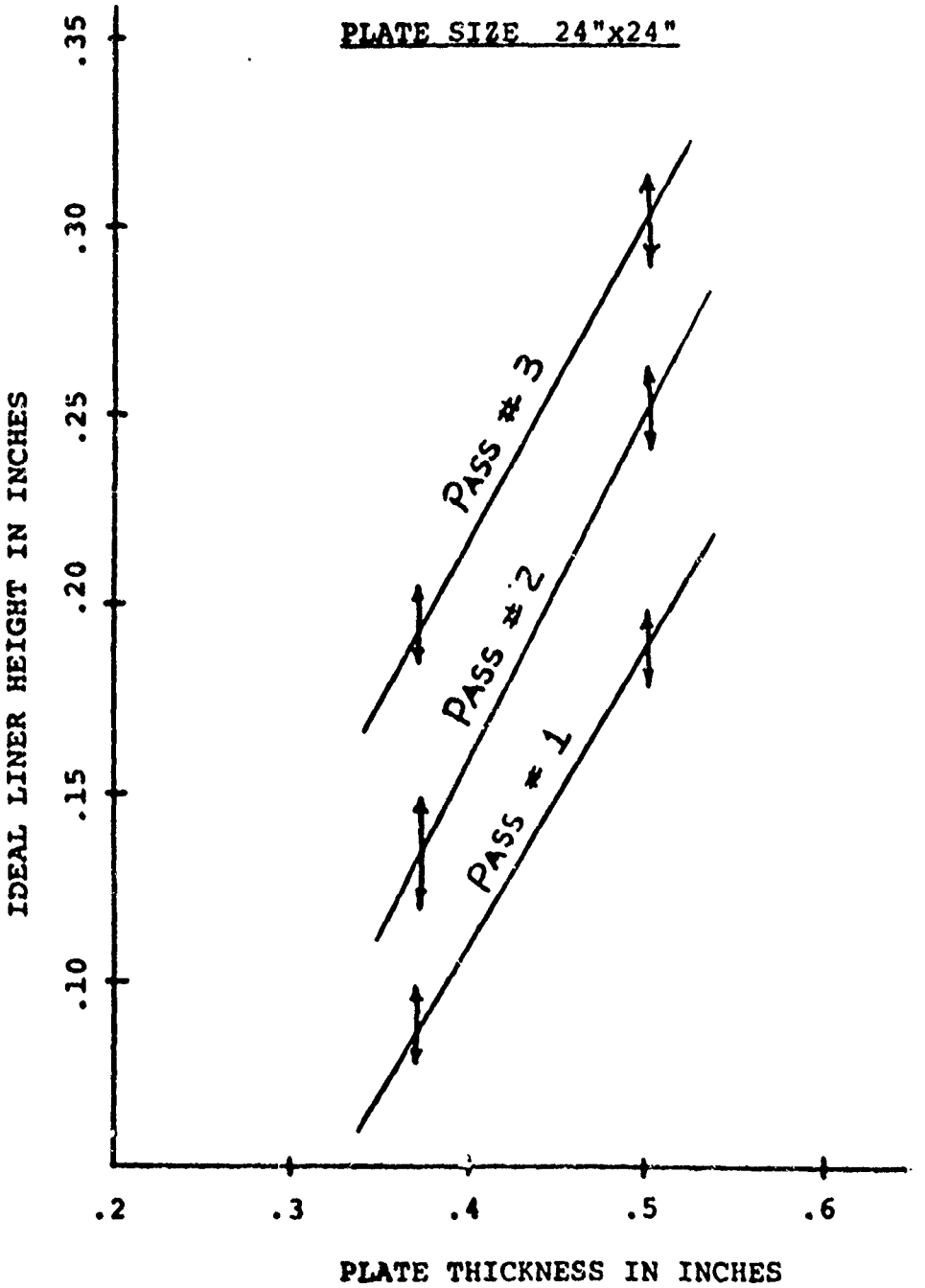

for a tee height of 3". Based on the experimental results obtained, as well as on data of out-of-plane distortion generated by Taniguchi[29] (see Section 5.1), Henry conducted an analytical study in order to find the liner height that will give the least angular distortion.

Assuming small deflections, elastic strain and using a two-dimensional model, he was able to construct Figure 7.4, which gives the liner height necessary for distortion removal. At low thicknesses there is high angular distortion and so, as thickness increases, it can be seen that the load necessary to make a change of one radian goes up cubically. At large thicknesses plate rigidity produces small distortions and the liner size decreases.

Combining Figures 7.2 and 7.3, Henry developed Figure 7.5 which gives the upper plate maximum surface strain (tensile) as a function of plate thickness. To make use of these curves, one enters with the plate thickness and required number of passes, and finds the required surface strain along the weld line.

Common industrial practice in handling the same distortion problem with steel is to clamp the plate, before welding, onto a curved platform in the form of an arc of a circle. The arc radius can be found using:

$$R = \frac{t}{2\epsilon} \qquad (7.1)$$

where t = plate thickness

ϵ = surface strain

From this formula and Figure 7.5, Henry calculated Figure 7.6 which gives the required arc versus plate thickness.

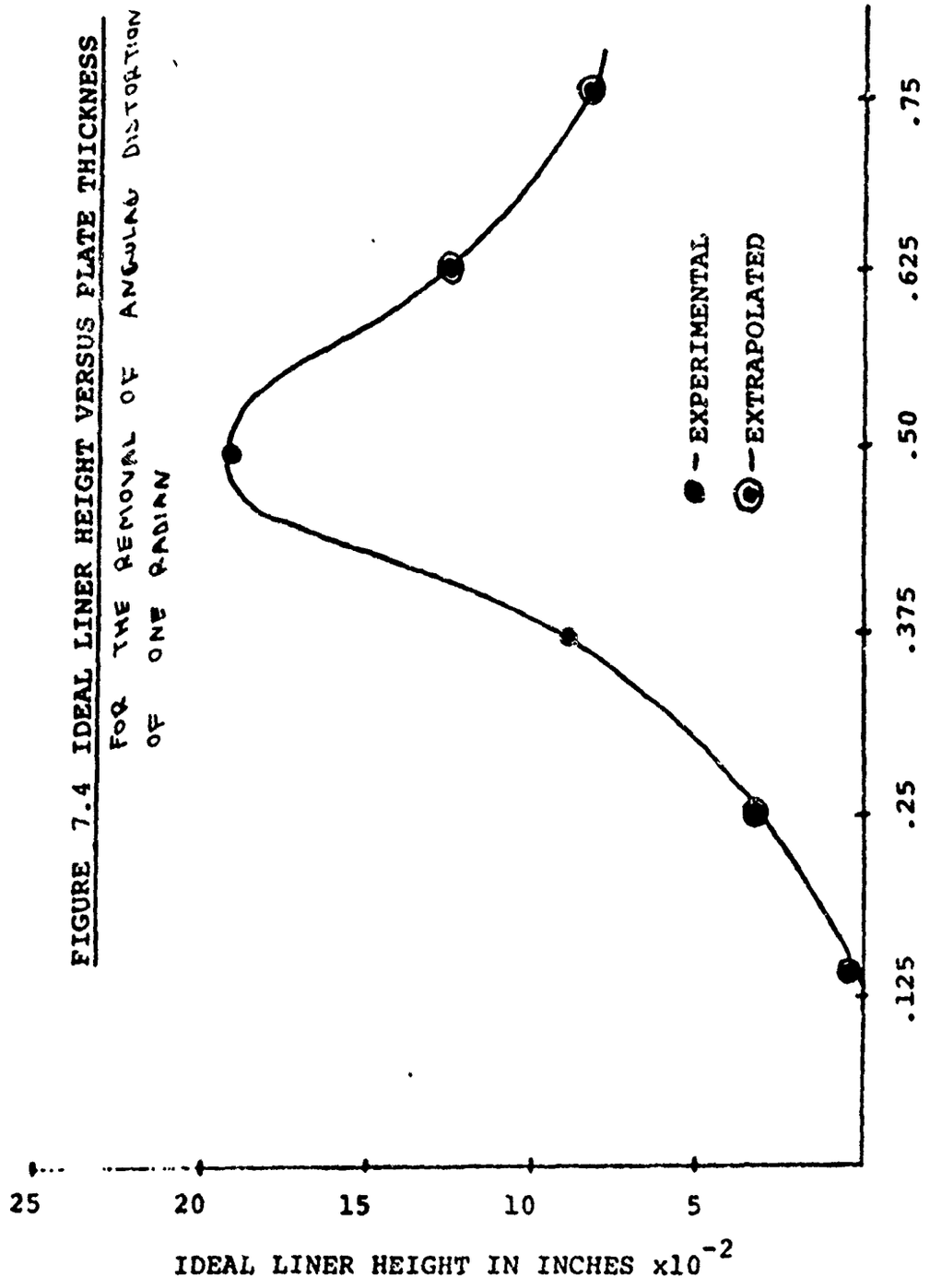

FIGURE 7.4 IDEAL LINER HEIGHT VERSUS PLATE THICKNESS FOR THE REMOVAL OF ANGULAR DISTORTION OF ONE RADIAN

FIGURE 7.5 MAX. UPPER STRAIN (TENSION) VERSUS PLATE THICKNESS FOR 3" TEES WITH 1,2, AND 3 PASSES

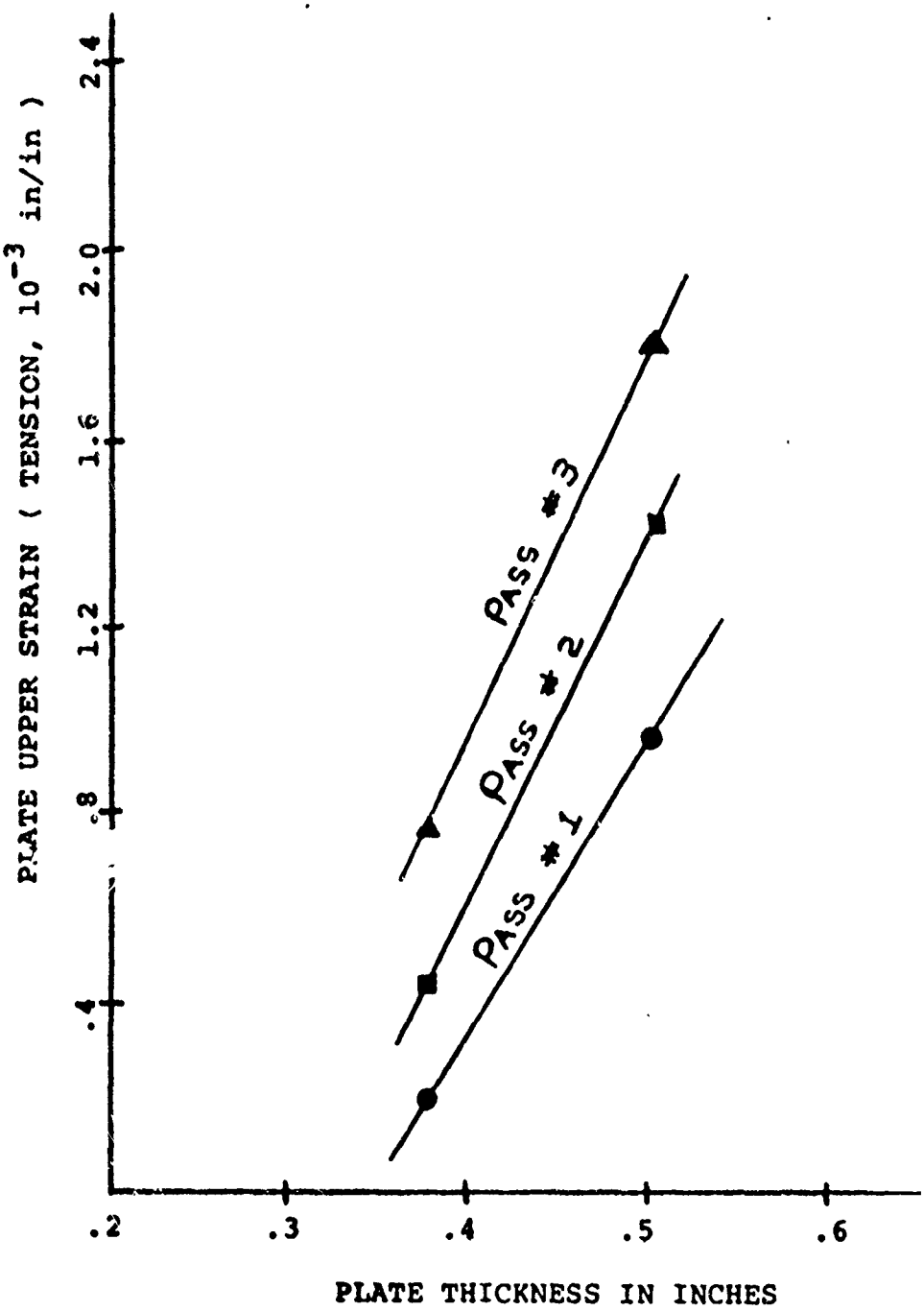

FIGURE 7.6 ARC RADIUS VERSUS PLATE THICKNESS FOR 3" TEES WITH 1,2, AND 3 PASSES

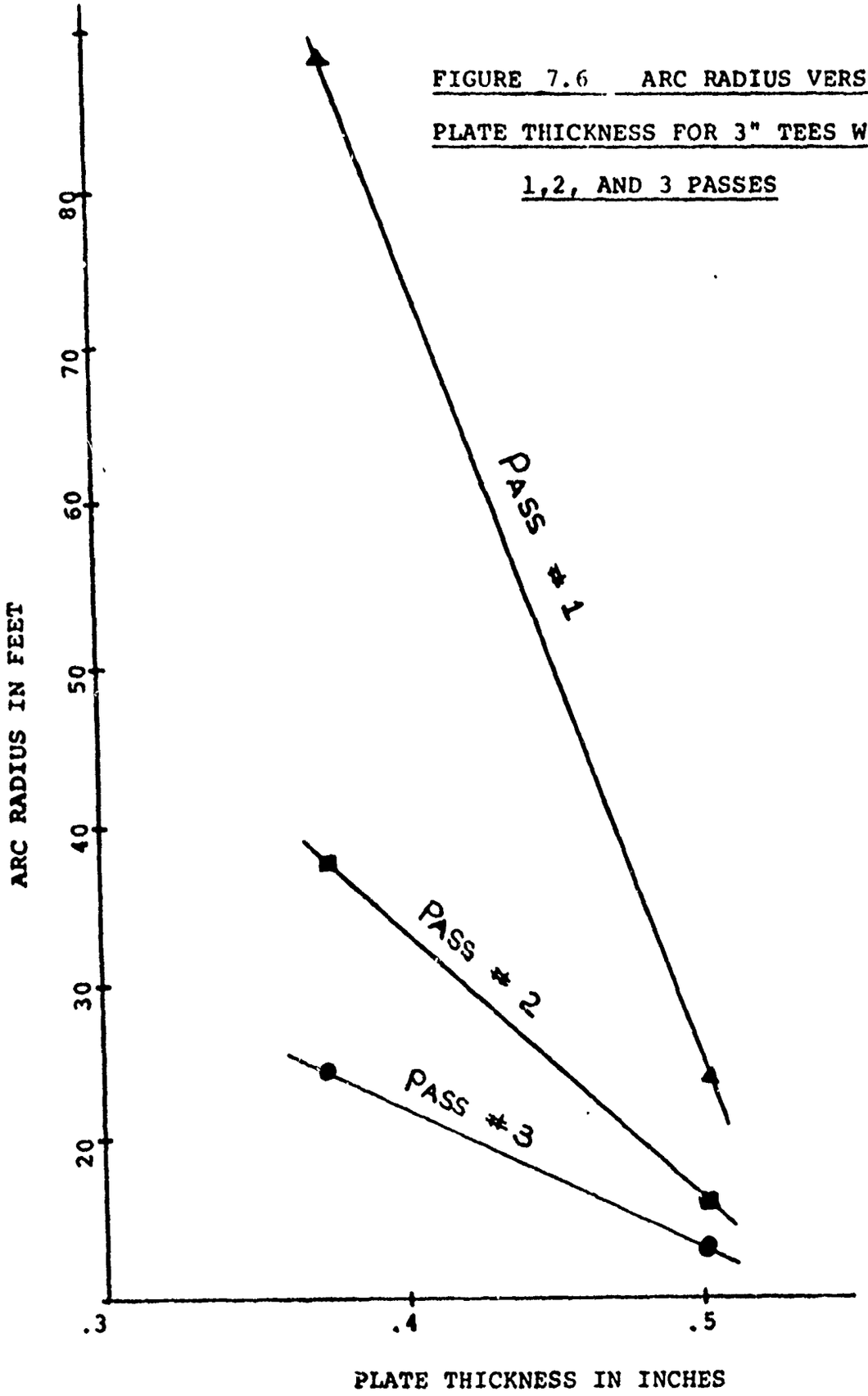

Beauchamp[38] continued and extended the work done by Henry on elastic prestraining. One of the major reasons for this was the poor results obtained by Henry in the case of 1/4" thick plates. Beauchamp thought that this was due to the clamping method used, as pictured in Figure 7.7. Instead of clamping the plate at its four corners, Beauchamp used a steel channel section to distribute the clamping force along the plate's edge. In this case the plate can be modeled as being made up of a finite number of simple beams with a uniform strain pattern.

Using the forementioned method he conducted experiments on 5052-432 Aluminum alloy plates. The geometry of the models was chosen to represent a typical stiffened panel which can be found in a vessel. The model, thus, has two stiffened panels joined by a butt weld. Figures 7.7 and 7.8 show the two model configurations used for the stiffened panels. Locations of strain gages and thermocouples are also shown on the figures. After the welding of the stiffeners, the models were joined by a butt weld to result in the configuration shown in Figure 7.9. The dimensions of the models are also shown in Figures 7.7 and 7.8. Investigations were carried out for plate thickness of 1/4, 3/16, and 1/8 in. GMA welding was used with 5556 aluminum alloy as the filler wire.

All fillet weldings were carried out using elastic prestraining. After the commmencement of each fillet weld and the cooling of it to room temperature, the plates were unclamped and residual stresses were measured. Only transverse strains and stresses were measured.

Beauchamp modeled the specimens as simply supported beams

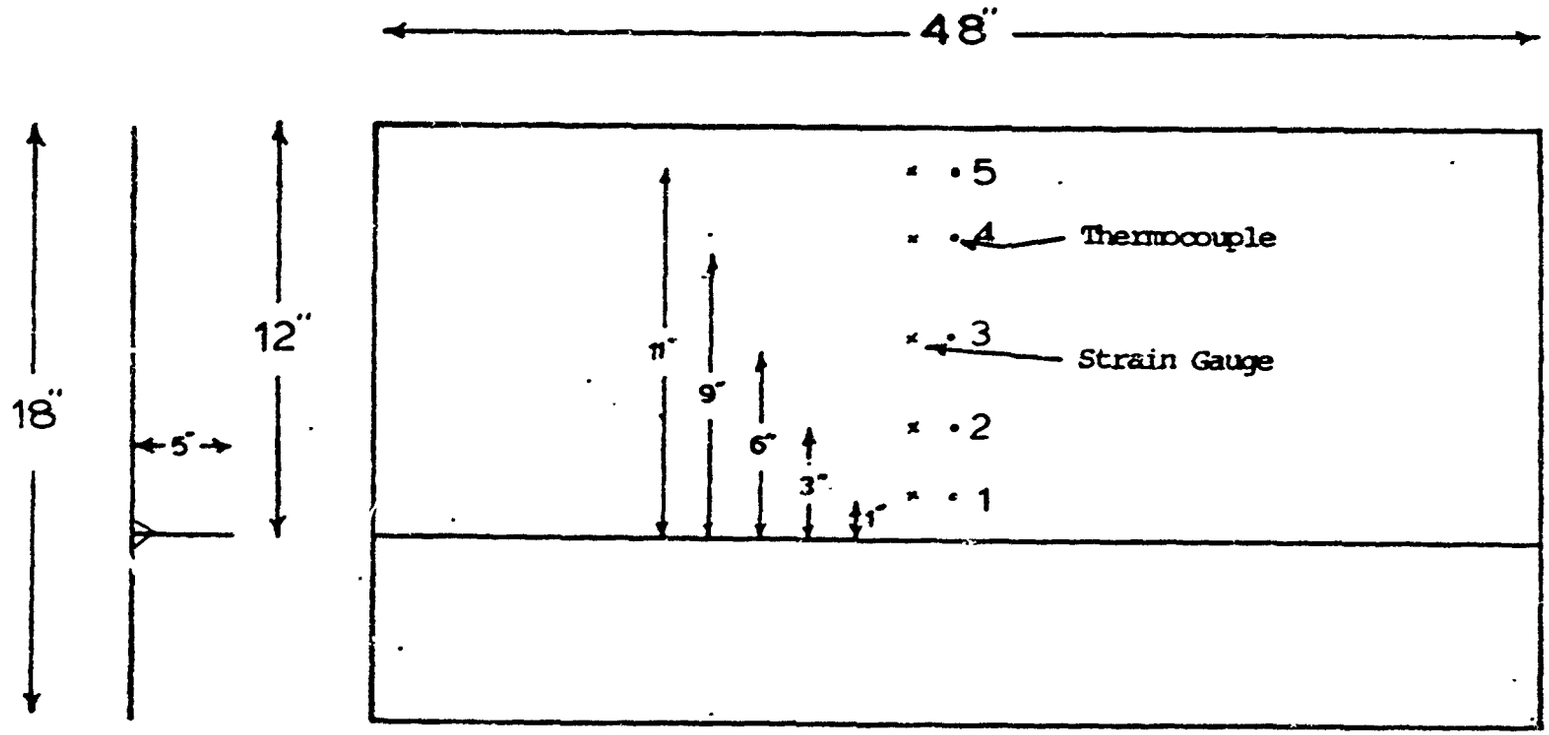

Figure 7.7 Dimensions of Models A

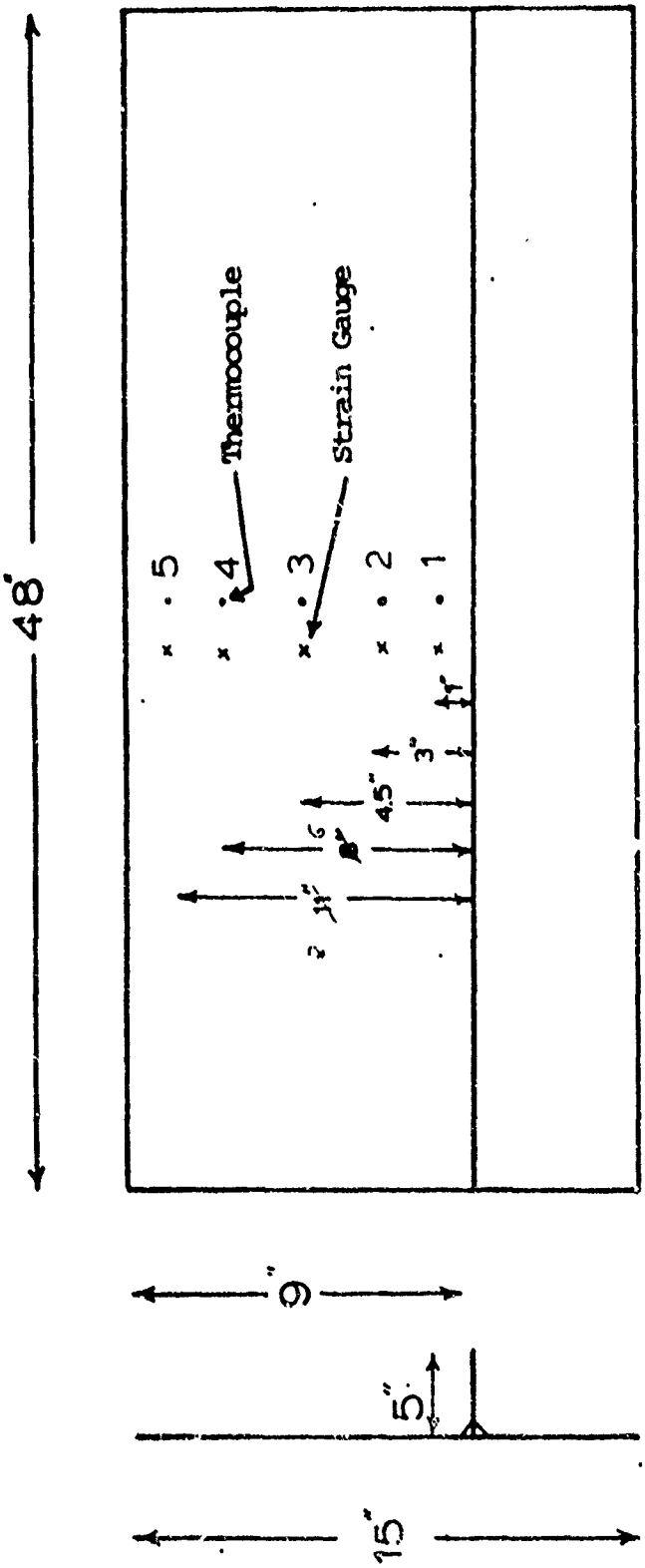

Figure 7.8 Dimensions of Models B

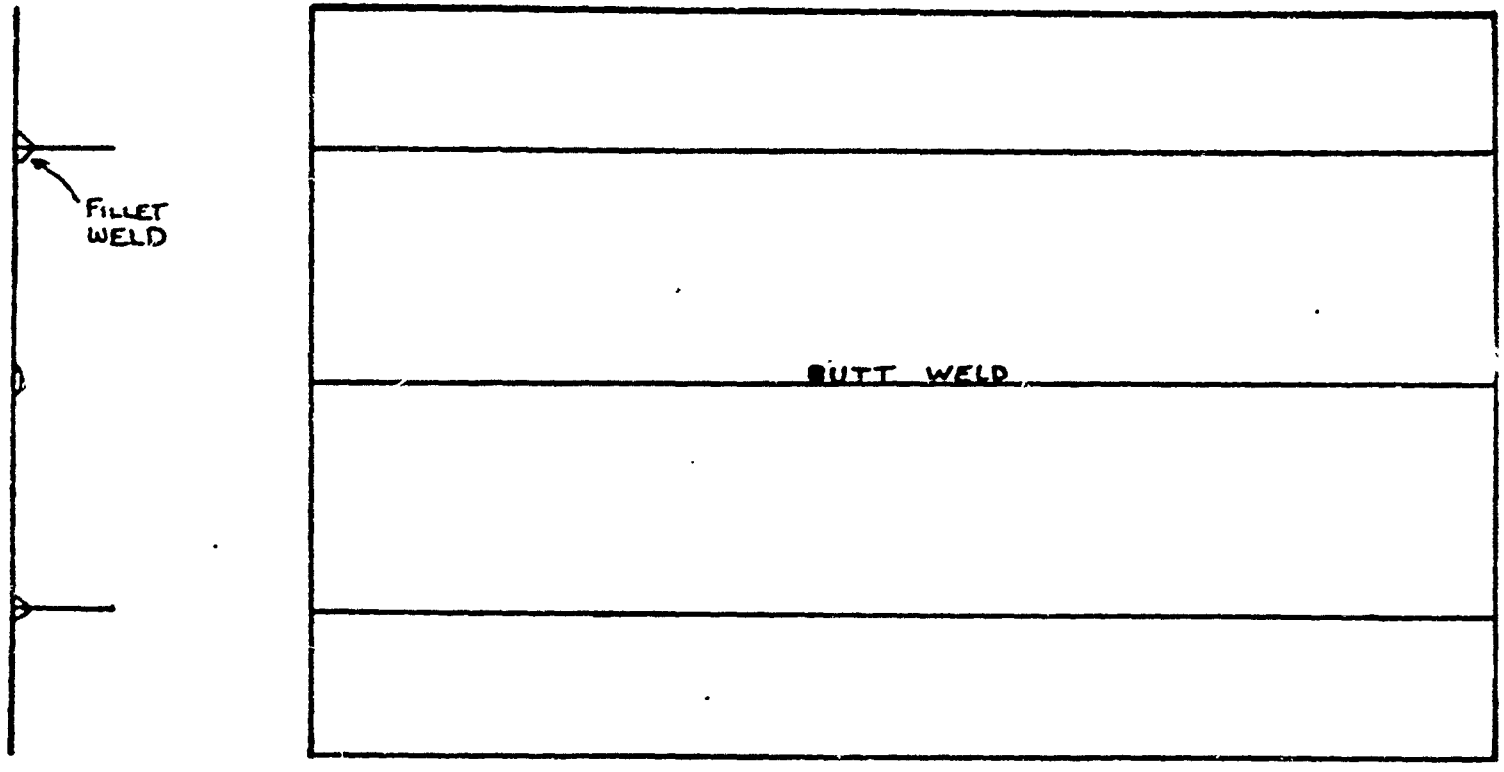

Figure 7.9 Completed Panel Configuration

experiencing a force concentrated at a point not at its midlength. Using simple beam theory, he came up with the following relation:

$$\varepsilon_y = \frac{3 \quad d \quad t \quad x}{2a \; b} \qquad (7.2)$$

where ε_y = transverse strain

d = deflection under web (due to elastic prestraining)

t = plate thickness

a = 12 or 9 in. (refer to Figs. 7.7 and 7.8)

b = 6 in.

x = 0 at plate edge

= 12 or 9 in. at web

Comparing the analytically predicted results from equation (7.2) with the measured ones after the plates were prestrained and clamped, an error of approximately 25% was found. Beauchamp thinks that this was due to the fact that the measurement of deflection was not accurate enough.

Temperature was also measured during the welding operation and until everything was cooled down to room temperature. Good agreement was found between the measured values and the predicted ones, using the two-dimensional computer program mentioned in Section 2.

Finally, strains were also measured and converted to stresses using a data-reduction computer program. Figure 7.10 shows a typical stress versus time curve (for model B, shown in Fig. 7.8 and gage 1). The two fillet welds are labelled 1 and 2 and the butt weld is labelled 3. Due to the fact that the technique of elastic prestraining was used to reduce distortion, an amount of strain

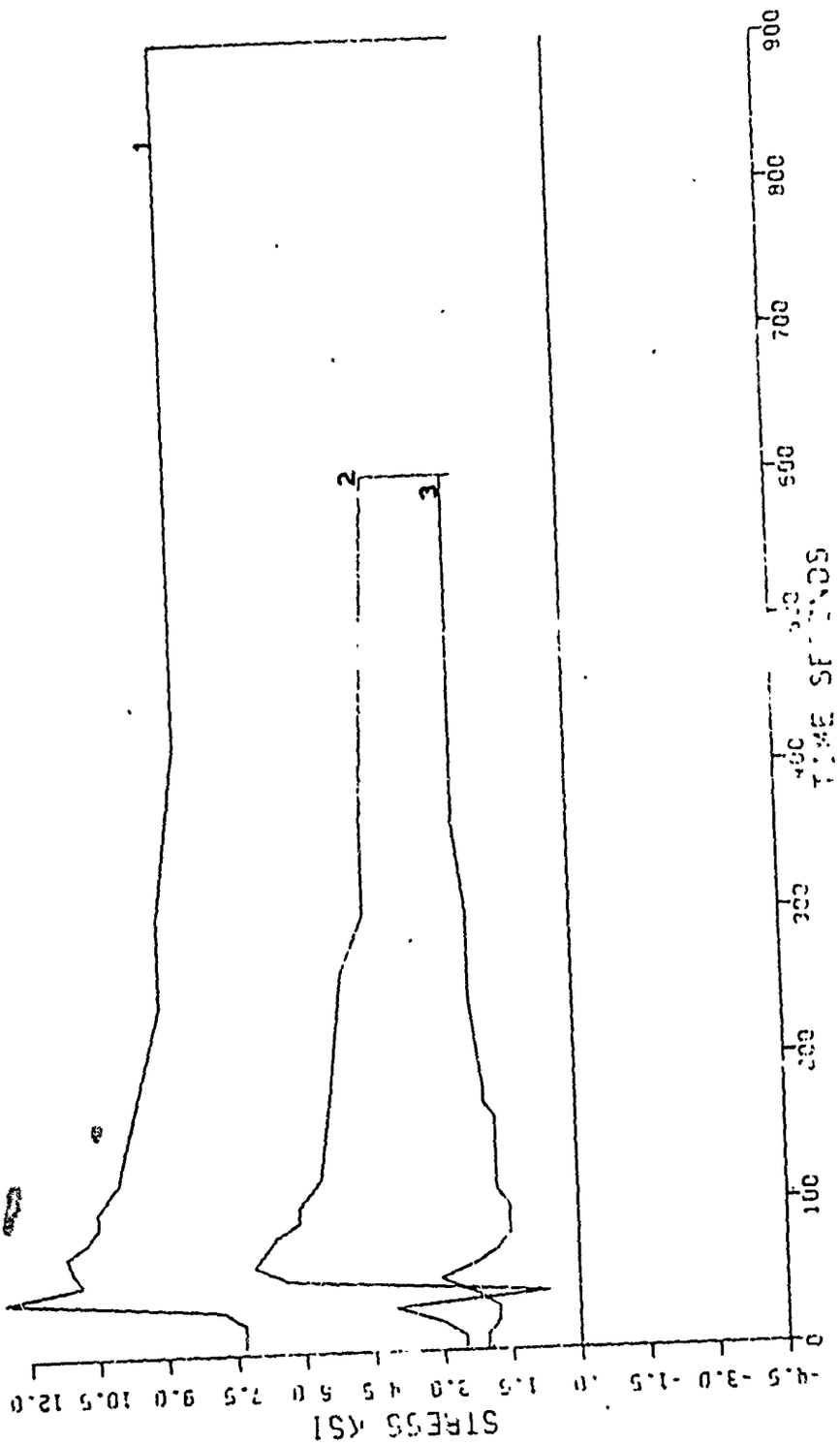

Figure 7.10 Typical Stress vs. Time Curve

was introduced into the plate before welding was started. This value of stress is indicated by the curve's intercept with the vertical axis at time zero. The vertical line for the last value of time indicates the amount of stress released when the clamps were removed.

The development of stress in the models is presented in Figures 7.11 - 7.16. The graphs show the effect of the clamping on the residual stress levels. There are six segments in each graph; the first three are for the fillet weld on one side of the web and the last three for the second fillet weld.

When the plate is free there is no stress. After clamping is completed, stress has been introduced into the plate. The amount of stress present is a function of the clamping force used and the deflection. The six graphs display this characteristic very well. The stress in the plate then undergoes a transition on the completion of welding. In every model except one the stress decreased. Model B-1 (1/4" thickness, Fig. 7.8) experienced an increase in stress. After the weld had cooled down, the clamps were removed and a new value of stress was recorded. This value is the amount of stress present in the plate due to the welding. If on the release of the clamps a zero reading for stress had arisen, this would mean that no residual stress was generated by welding. Models B-3 and B-4 (both 3/16" thick) had negative values of residual stress on the completion of both fillet welds. There seems to be no clear cut explanation for this phenomenon. One factor could be the manner in which the fabrication was carried out.

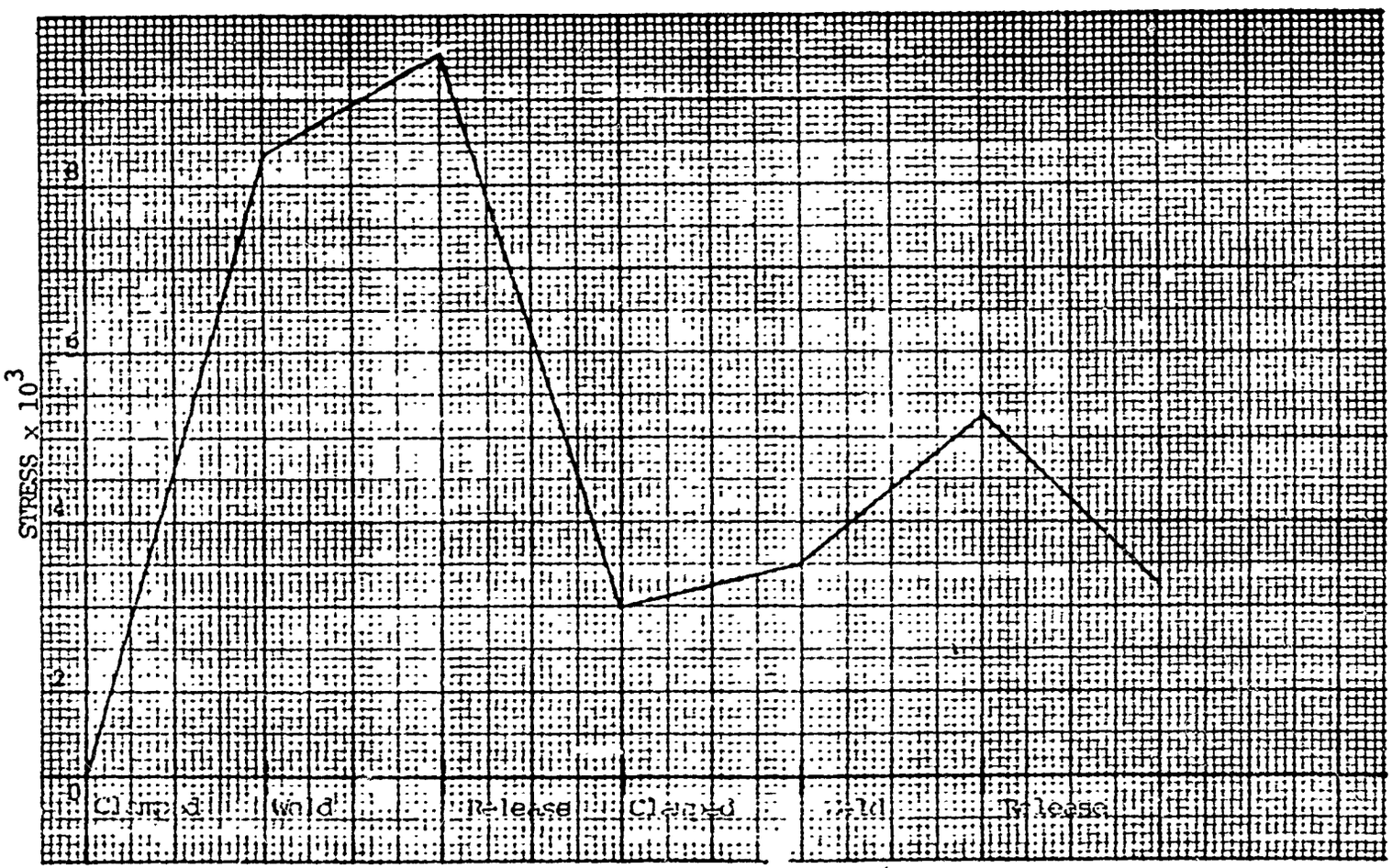

Figure 7.11 Development of Stress Model B-1

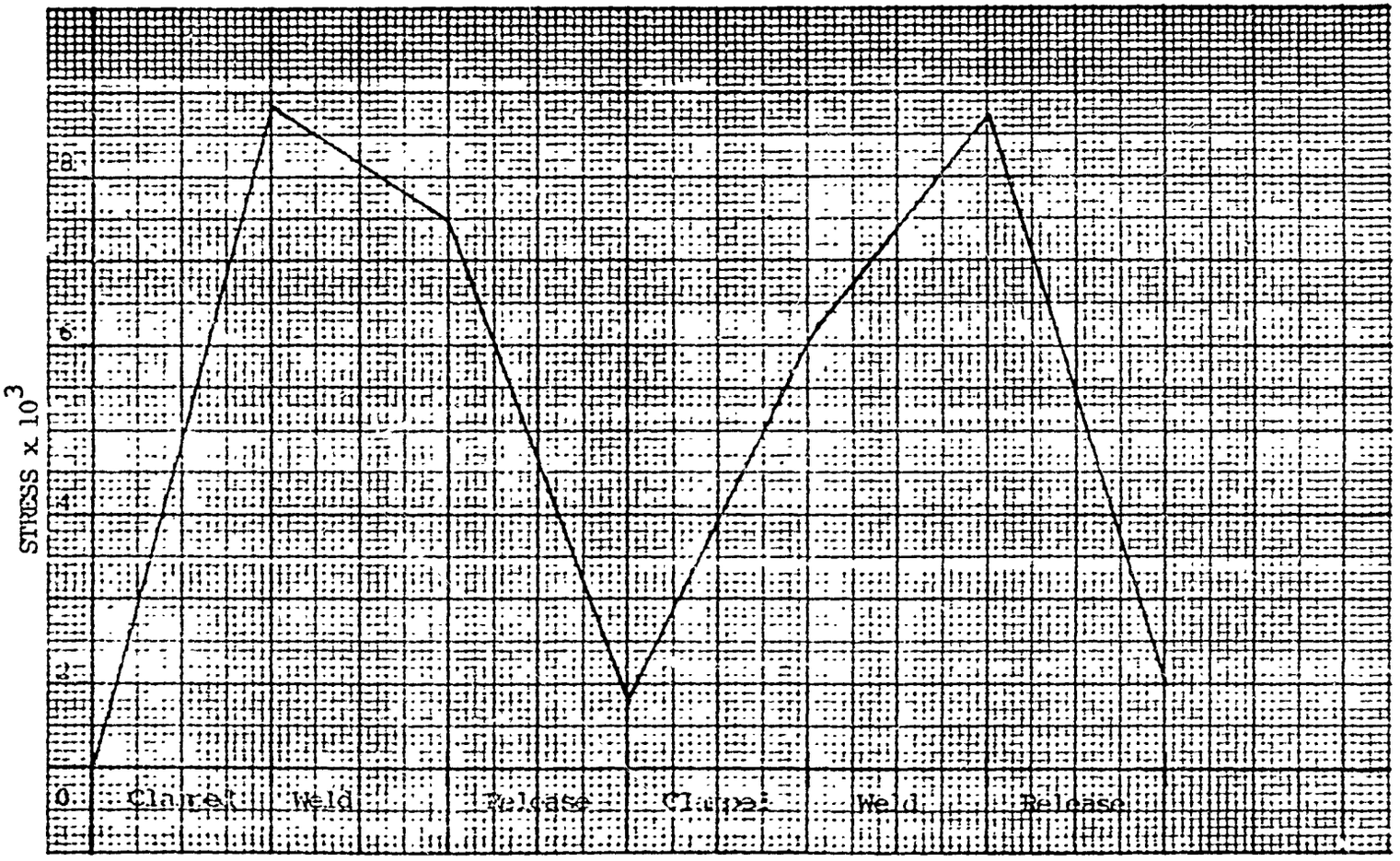

Figure 7.12 Development of Stress Model B-2

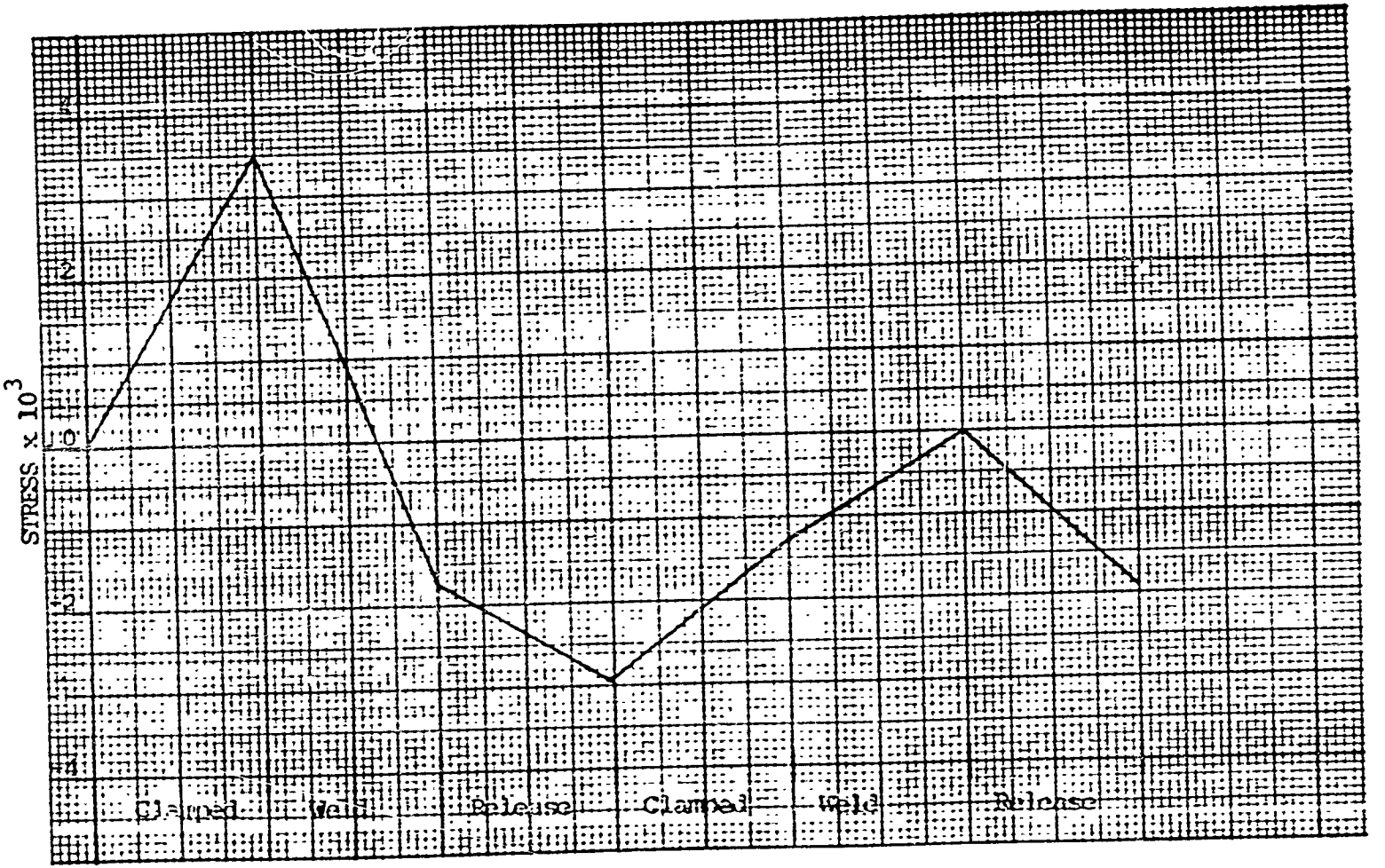

Figure 7.13 Development of Stress Model B-3

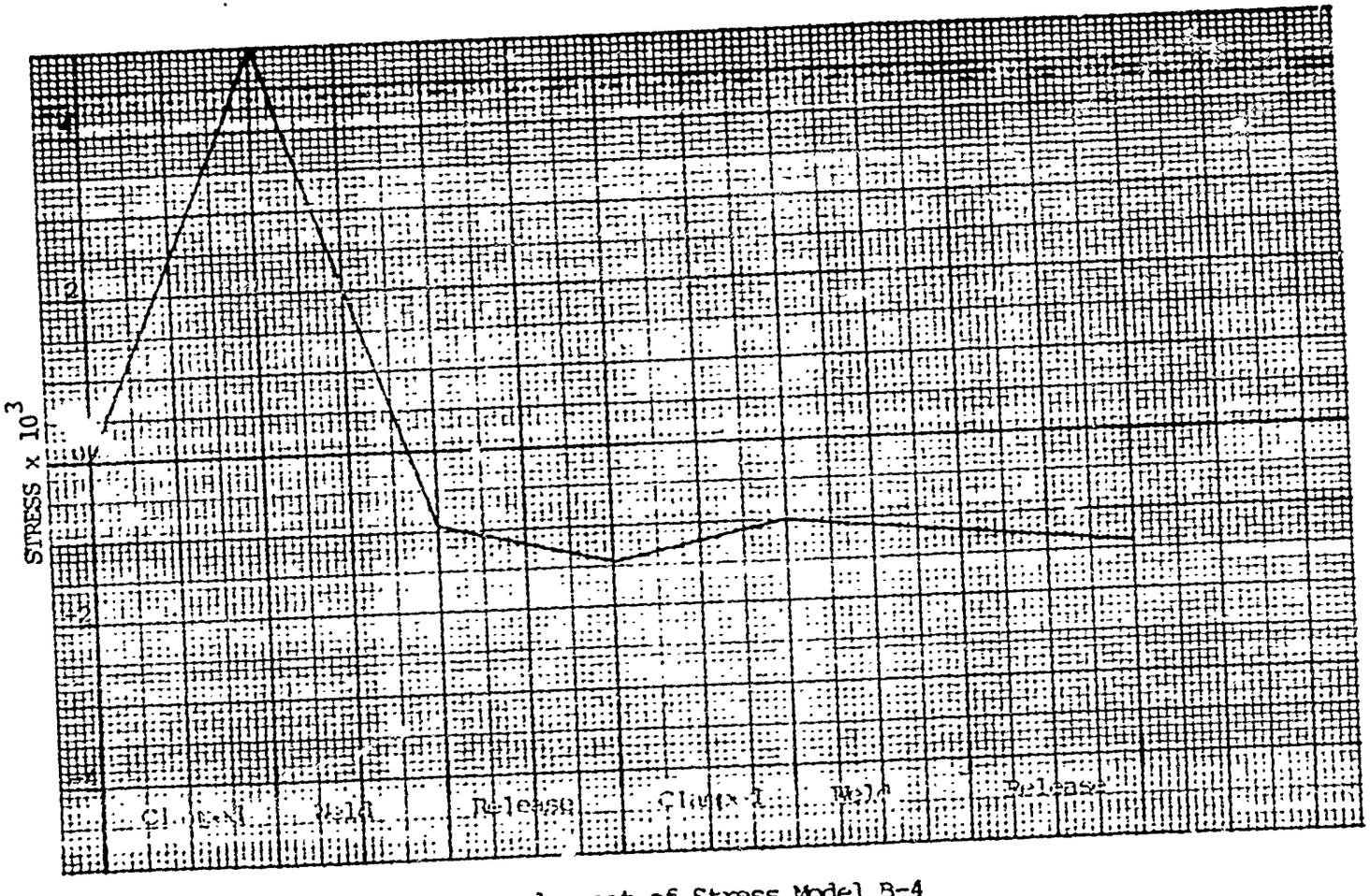

Figure 7.14 Development of Stress Model B-4

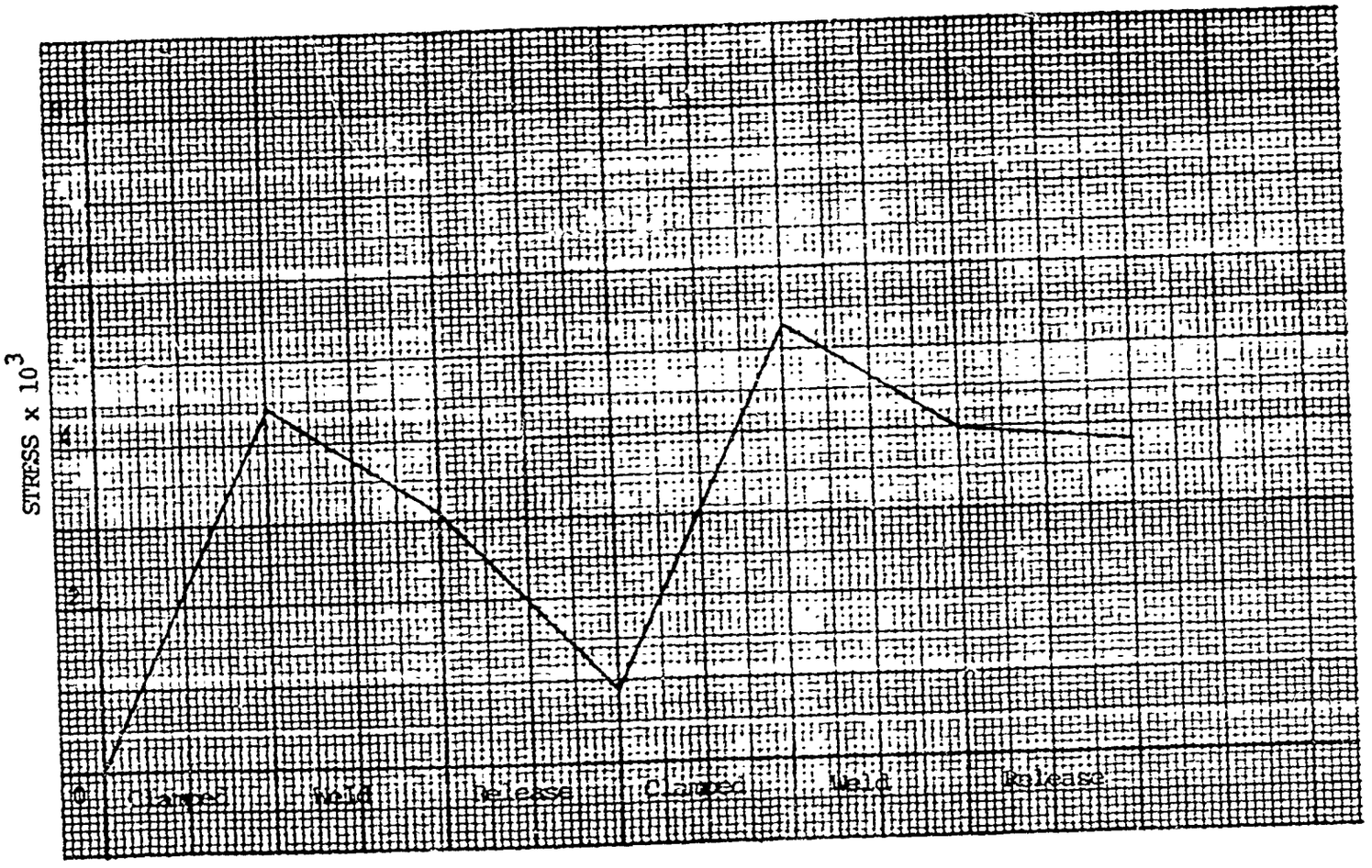

Figure 7.15 Development of Stress Model B-5

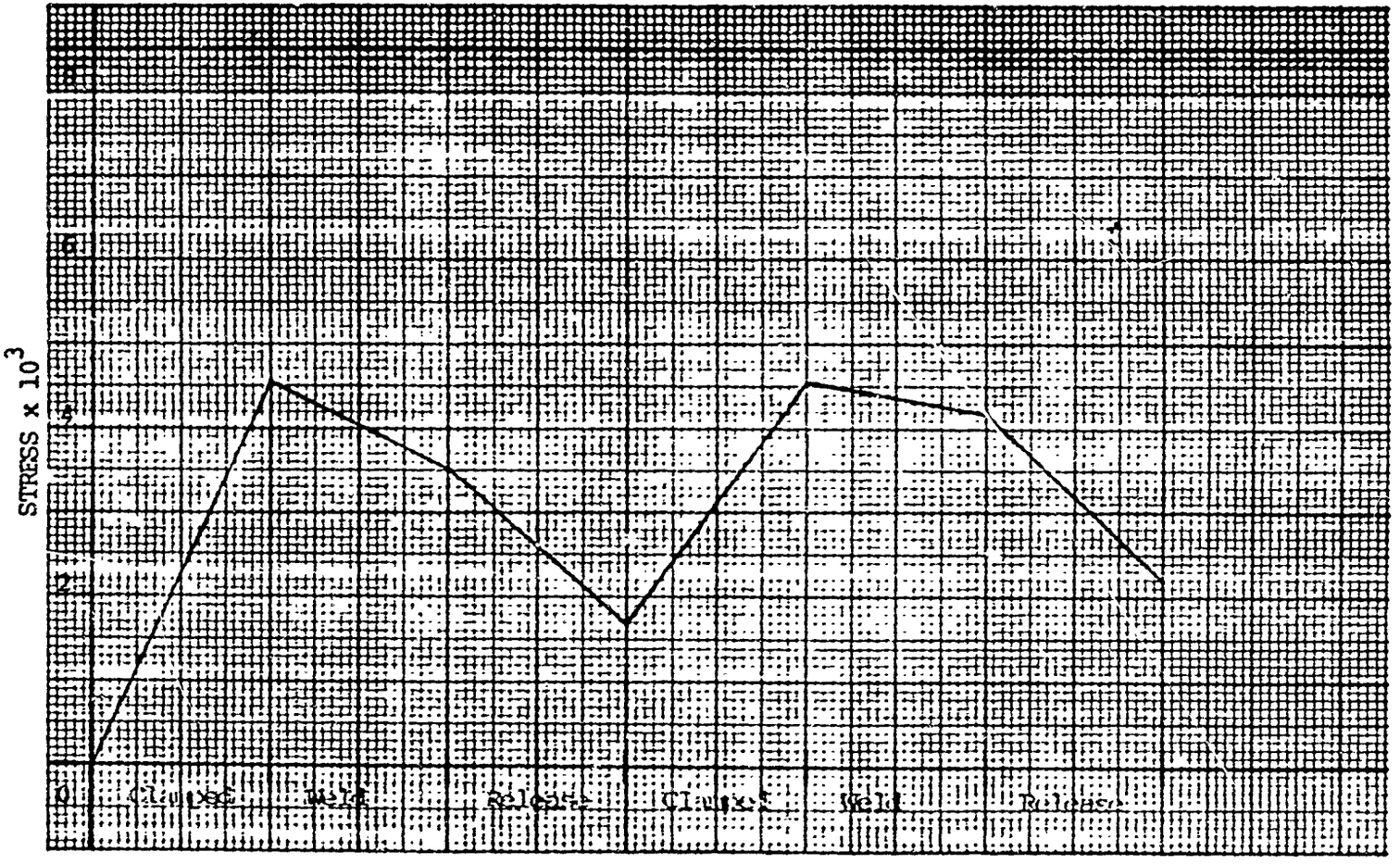

Figure 7.16 Development of Stress Model B-6

The other four models displayed the same general characteristics; a value of residual stress slightly greater than the amount of stress generated by the welding stage of the experiment. However, this stress was not excessively greater and there was no distortion present.

The above results do not agree with the rule of thumb which states that restraint reduces distortion but increases residual stress, at times to levels equal to the yield value of the material. If the simple models that have been used for the experiments are indicative of more complex structures, it would be very wise to use techniques such as prestraining to reduce distortion. However, more experiments are required to check the validity of the forementioned observations.

Concluding this paragraph one could say that the method of elastic-plastic prestraining is an effective method of reducing out-of-plane angular distortion in aluminum structures. The method can easily be incorporated into current plate welding processes with only small corrections to the numerical tape program now used in plate assembly lines.

7.3 Clamping Method

The clamping method is widely used in industry, but it is not helpful in reducing residual distortion in every situation (sometimes only transient distortion is prevented). However, it is still useful in the prevention of transient distortions from the point of view of controlling such welding conditions as root gap and arc torch distance.

As discussed in Section 4.2, Yamamoto's[27] experiments have shown that the clamping method is not effective in reducing the final deflection of T-shaped built up beams. Test specimen and clamping method used are shown in Figures 4.3 and 4.5 of Section 4.2.

Nishida[8] conducted an analytical study on the clamping method using the one-dimensional computer program discussed in Section 4.3. He simulated the clamping condition as follows:

During the welding only x-direction movement is allowed and the plastic strain built in the beam is kept. After the welding, this plastic strain is determined and a recalculation is made to make the force balance. At this time the beam is allowed to bend. Using the assumption $\frac{d^2w}{dx^2} = b$ (refer to eq. 4.11) and simple support boundary conditions at both ends, the final deflection at the

center becomes:

$$\text{deflection} = \frac{1}{8}\, l b^2 \qquad (7.3)$$

where, w = transverse deflection of beam

ℓ = length of beam

The result of this calculation is shown in Figure 7.17. This result indicates the same tendency of the final deflection to increase if clamping is used, as did the experimental data.

If predicted strains are reasonably close to measured strain - and they are - then this method of calculating distortion can be used in other experiments involving clamping. Before attempting any trial-and-error sequence, it would be useful to run this program to predict the effectiveness of the clamping method is a particular problem or situation.

7.4 Differential Heating

The term "differential heating," as coined by Masubuchi, refers to a powerful technique for distortion reduction. One of the two components to be joined is heated to some predetermined temperature. The parts are then joined and allowed to cool. The preheated part cools and contracts more than the part initially at room temeprature. The thermal stress that is generated can offset residual bending stresses that would be generated if both parts had been at the same temperature when joined. This results in a distortion reduction.

In this section we will summarize the experimental and analytical investigations carried out at M.I.T.

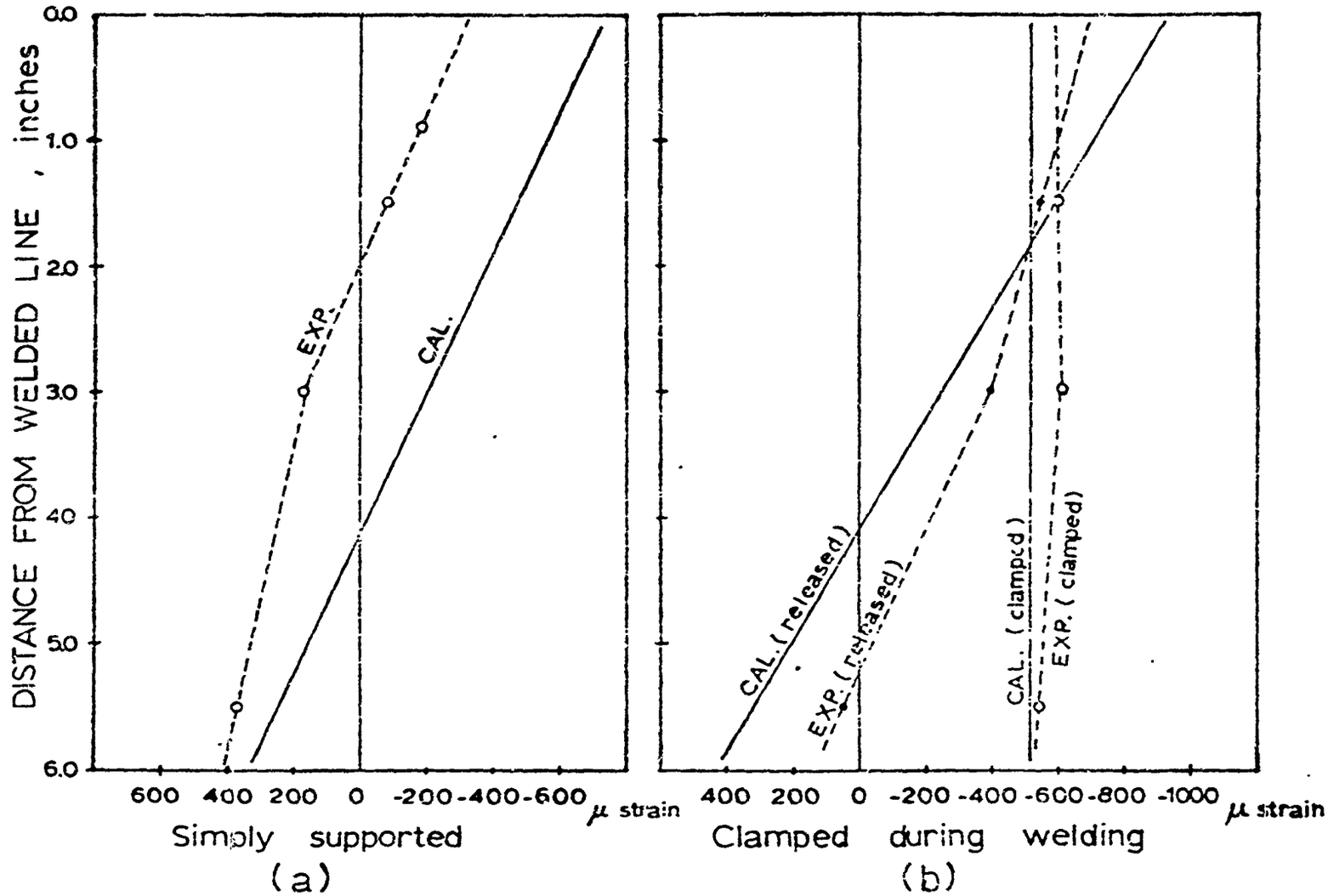

Fig. 7.17 Residual strain of clamped method

Experimental Investigation

Serotta[39] conducted a series of experiments to investigate the effect of differential heating on the reduction of longitudinal distortion of T-shaped built up beams. As a material he chose the 5052-H32 aluminum alloy, a strain-hardened and non-heat-treatable alloy, to permit ready comparison with results obtained by Yamamoto.[27] Dimensions and general arrangement of the experimental equipment were also the same as the ones used by Yamamoto[27] and are shown in Figures 4.3 and 4.4 of Section 4.2 respectively.

The aluminum plates, both the web and the flange were 0.5" thick. The experimental procedure used was the following. The base plate was positioned on the support under the welding head. The web was then heated to the desired temperature using electric resistance heaters. The dial indicator was zeroed, allingment was verified and the heated web was placed in position and manually tack-welded at the end opposite to that end from which welding was to begin. Upon commencement of welding, a read-out of the dial indicator at predetermined intervals was made, until no change was being recorded. The second pass (i.e. the pass on the opposite side of the web) was made with the specimen at room temperature. It was felt that a temperature gradient of sufficient magnitude to be effective could not be maintained once the two components had been joined. Furthermore, the additional restraint provided by the first pass would reduce the tendency of the specimen to bend.

Figure 7.18 through 7.21 present deflection versus time after

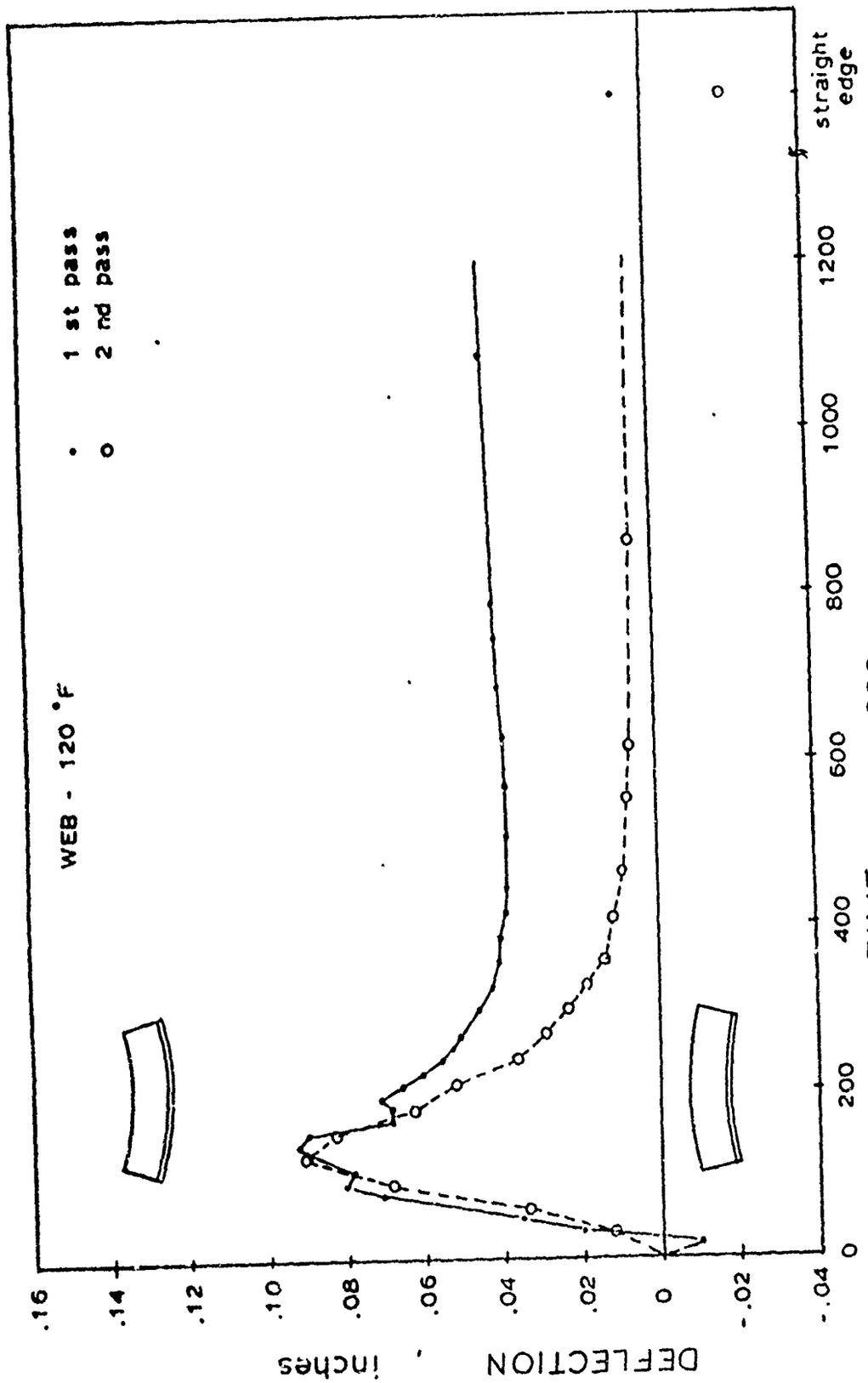

Fig. 7.18 Center deflection history (the preheated web at 120 °F)

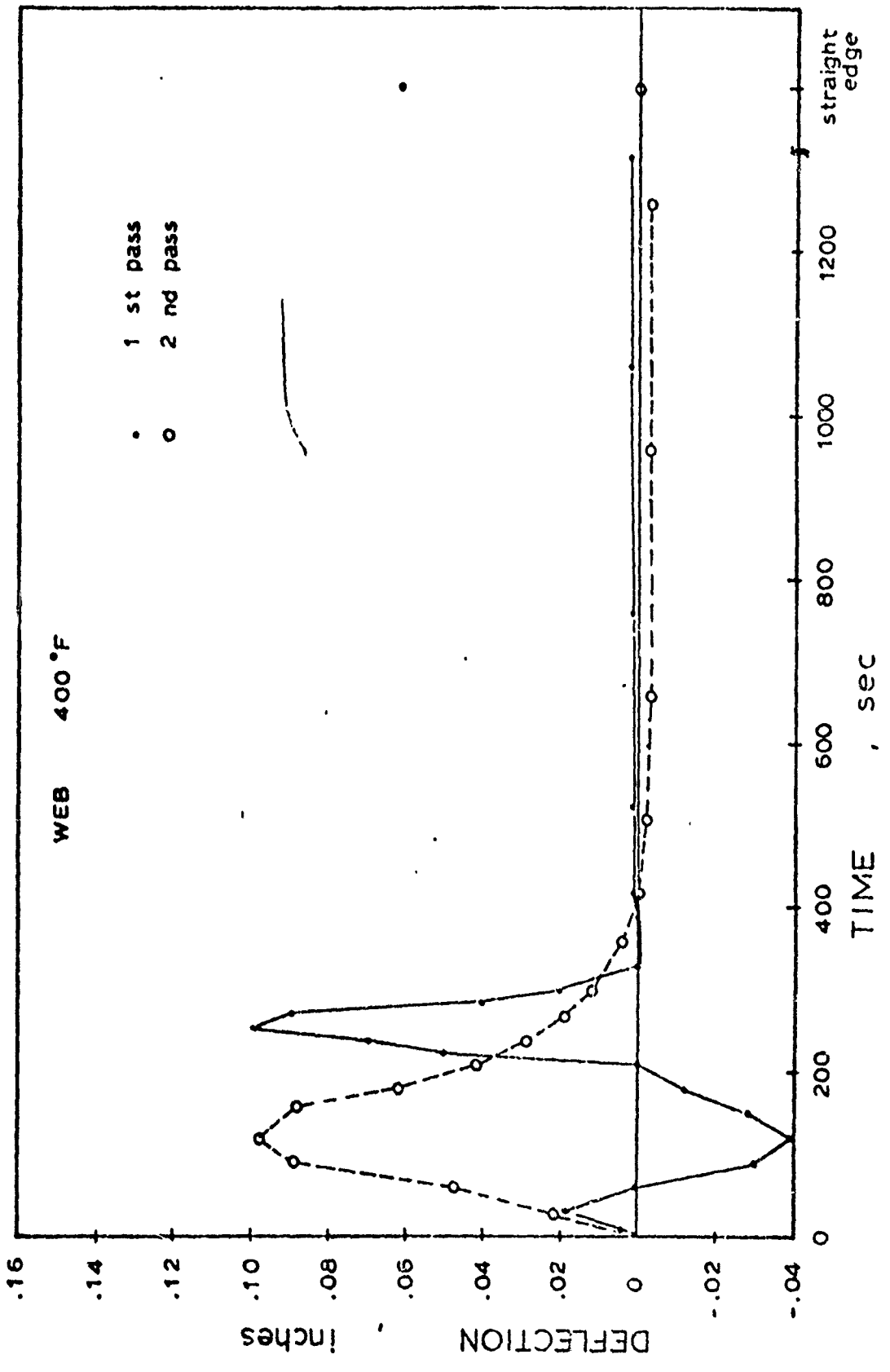

Fig. 7.19 Center deflection history (the preheated web at 400 °F)

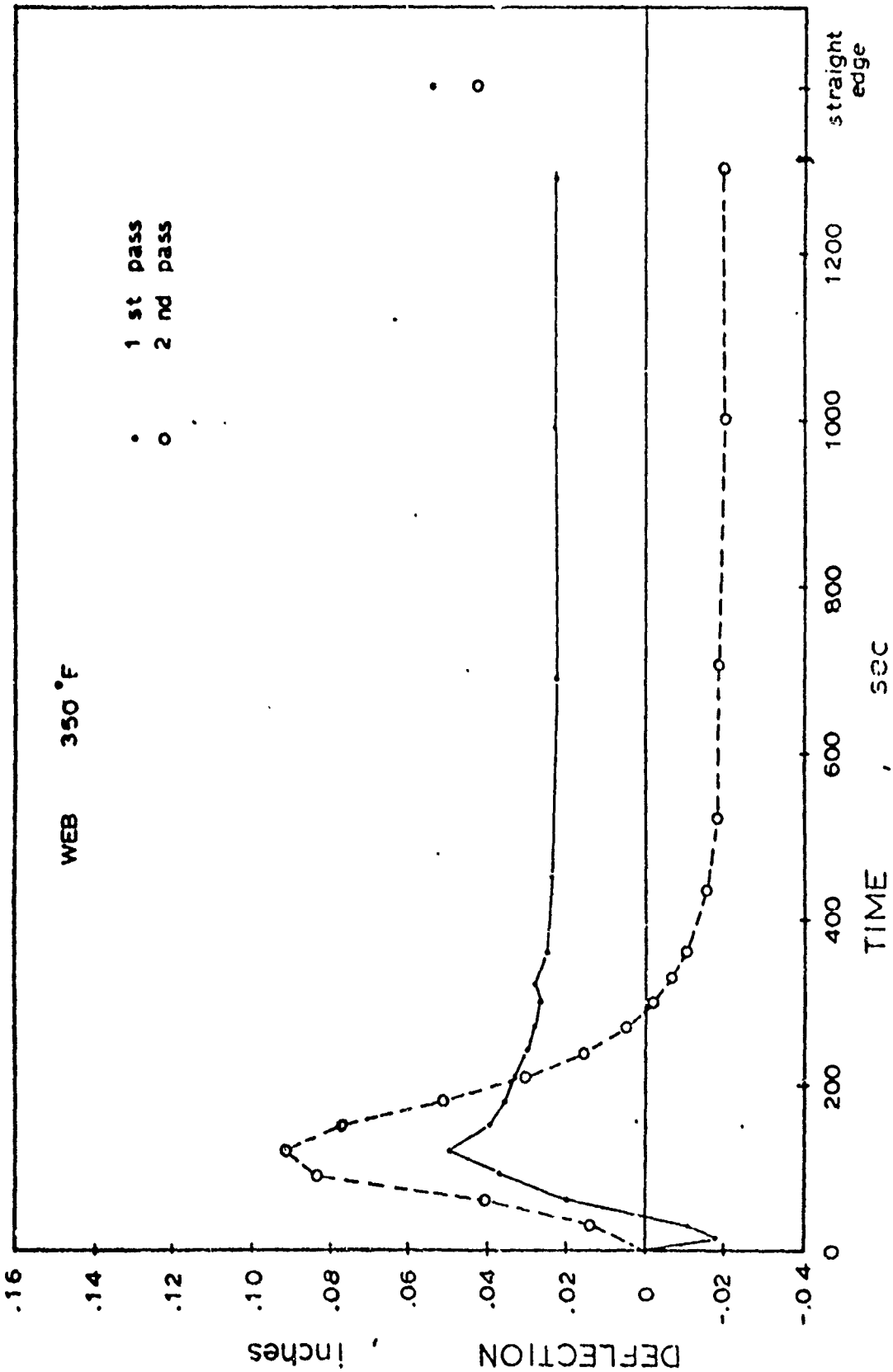

Fig. 7.20 Center deflection history (the preheated web at 350 °F)

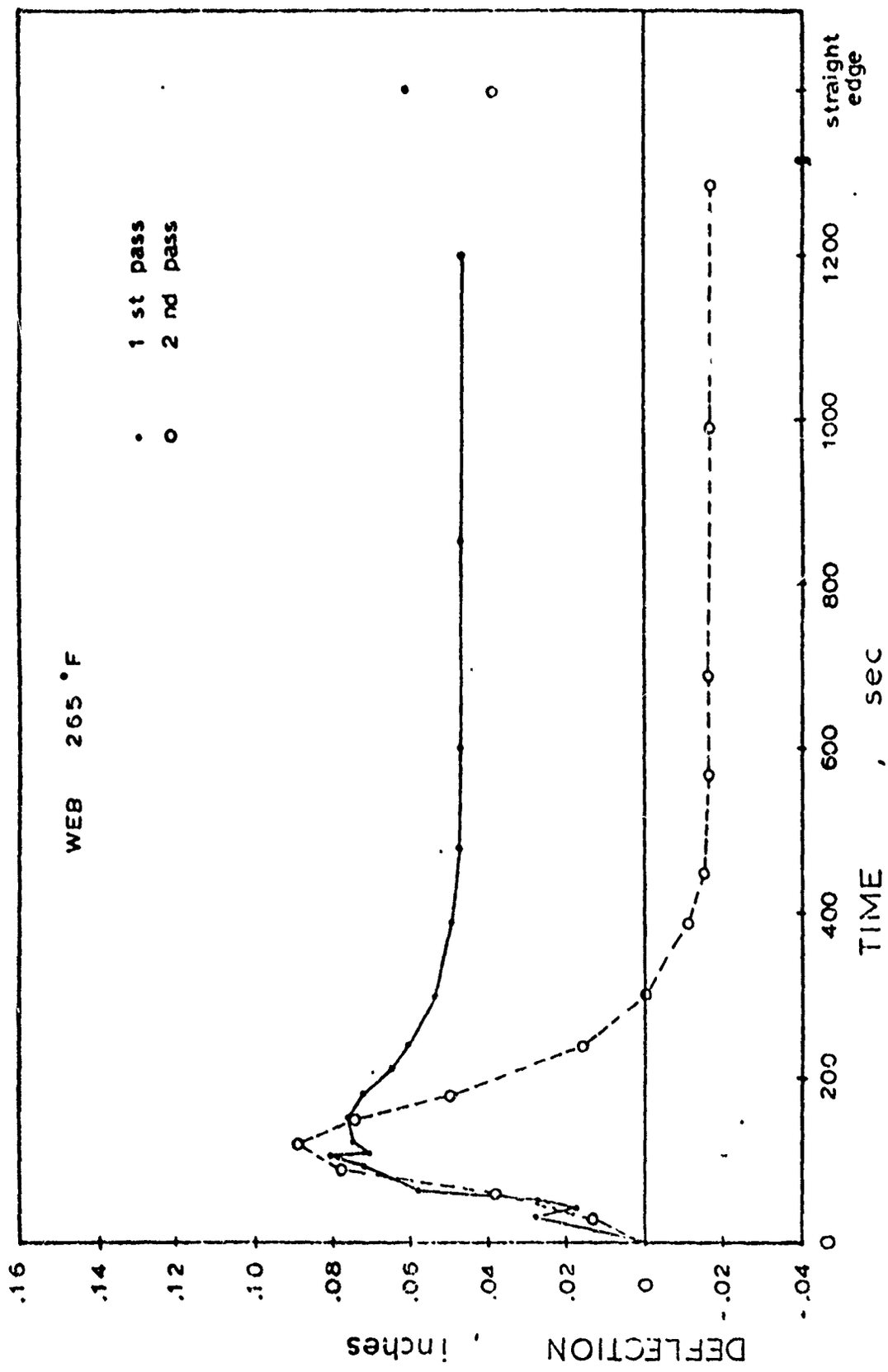

Fig. 7.21 Center deflection history (the preheated web at 265 °F)

commencement of welding, for various preheating temperatures. Figure 7.22 is a graph of final deflection versus preheating temperature.

If one assumes that the deflection resulting from welding a T-shaped member is approximately linear with length, the temperature difference which eliminates distortion for one length should eliminate distortion for all lengths. This can be easily verified by experiments on specimens of other lengths.

Estimation of the temperature difference required to eliminate distortion requires a knowledge of the force producing bending. The counteracting force associated with the temperature differential arises from the thermal contraction of the heated member. If the modulus of elasticity and the coefficient of thermal expansion are known, the required temperature differential can be estimated.

Equation (4.1), given in Section 4.1 can be used for these calculations. Given a deflected beam, the radius of curvature can be determined from geometry. The shrinkage force can then be calculated and the tempeature difference required to eliminate distortion can be estimated.

Analytical Investigation

Nishida[8] analyzed the experimental data obtained by Serotta[39] using the one-dimensional computer program discussed in Section 4.3. The quasi-stationary state was assumed for the calculation of the temperature distribution. The preheated temperature difference diminishes during welding and is a transient phenomenon.

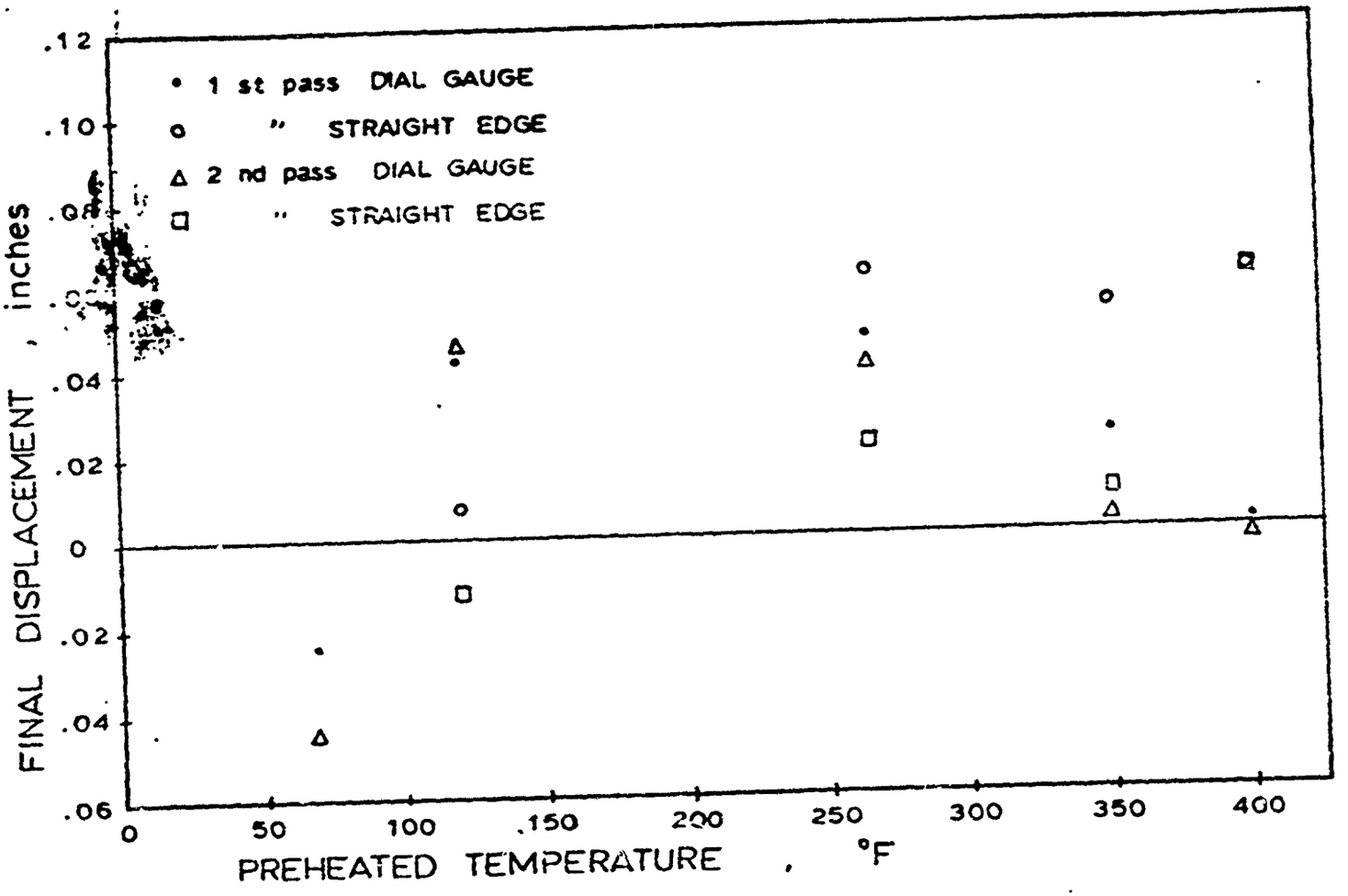

Fig. 7.22 Final center deflection vs. preheating temperature of the web

Results of the calculation are shown in Figures 7.23 and 7.24, in comparison with the experimentally obtained ones.

Figure 7.25 shows how the deflection after welding changes with the preheated temperature of the web. Discrepancies between experimental data and analytical results appear when the web is heated to a relatively high temperature. It is believed that the experimental data for high preheating temperatures are not accurate, since the temperature differential will be reduced by conduction. Figure 7.25 shows that zero deflection can be achieved by heating the web to around 120°F.

When the welding is done in two passes, the best technique is to produce a slightly positive distortion after the first welding pass by using a higher preheating temperature, 170°F for example, so that distortion after the second pass will be close to zero.

The computer program developed by Nishida can be used to determine the optimum welding and preheating conditions for joining T-beams of various sizes.

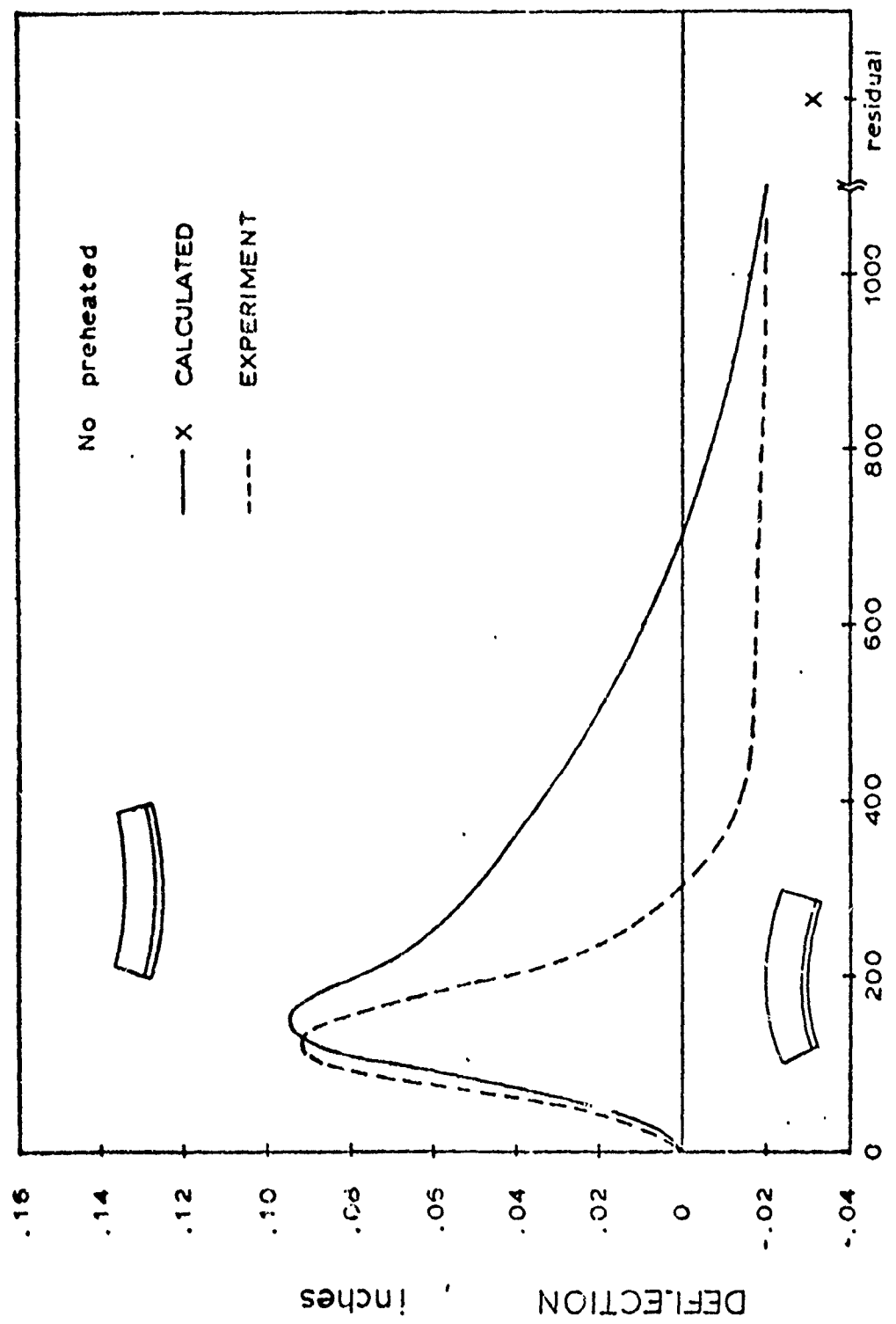

Fig. 7.23 Calculated center deflection history (NO preheat)

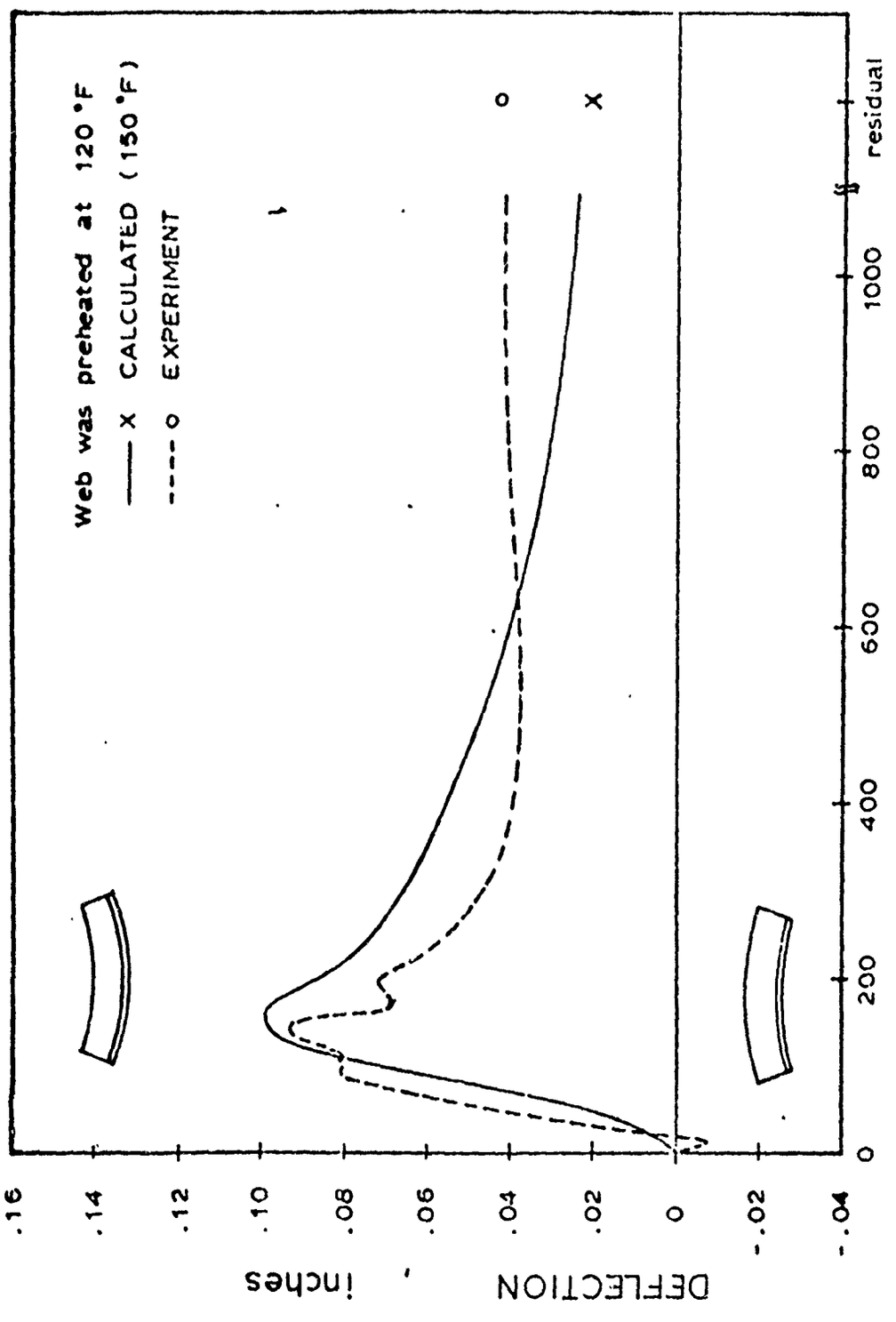

Fig. 7.24 Calculated center deflection history (preheated at 150 °F)

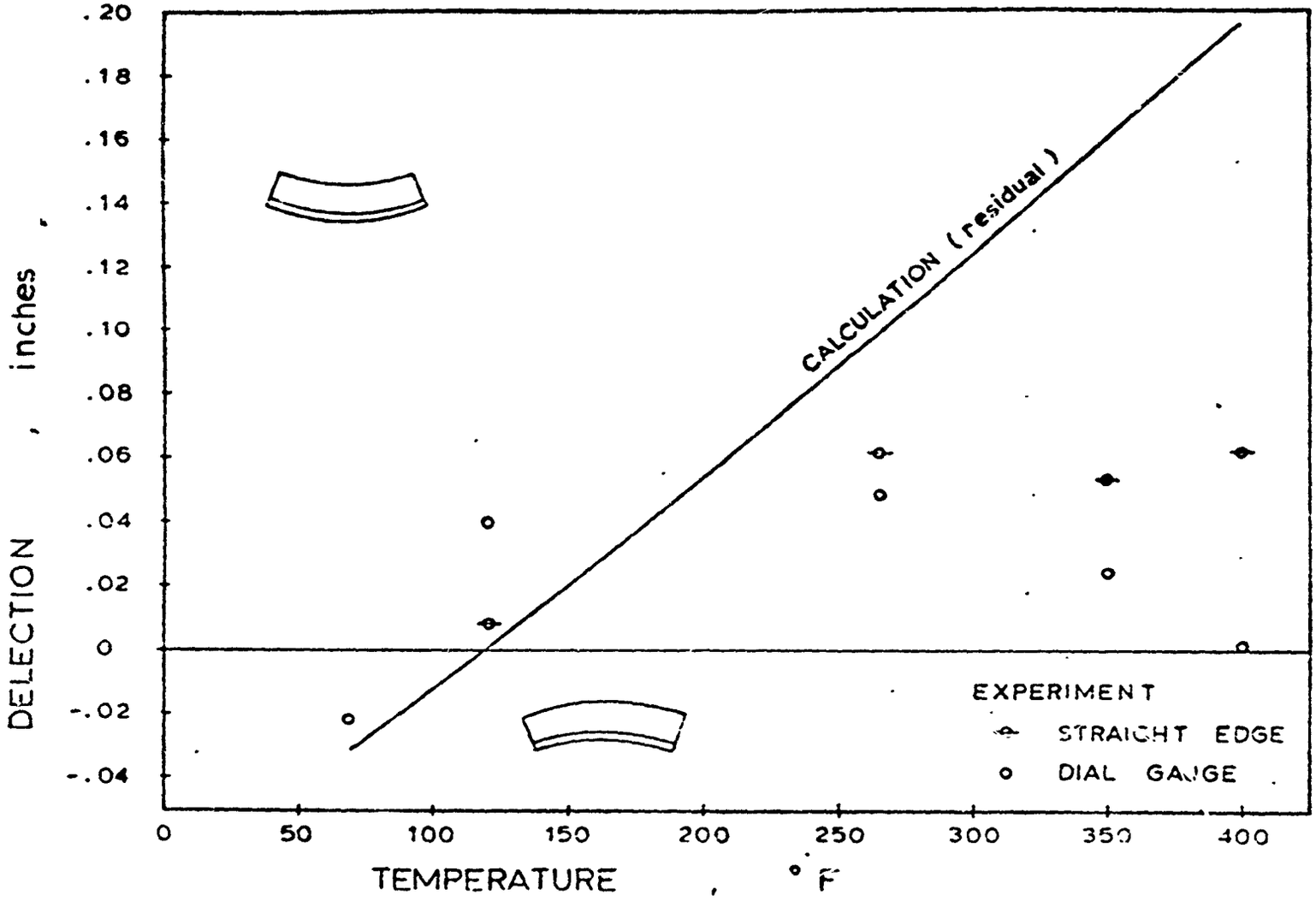

Fig. 7.25 Calculated final center deflection vs. preheating temperature of the web

8. RESIDUAL STRESSES IN LASER WELDED JOINTS

In recent years there has been an effort towards a deeper and better understanding of the laser welding process. The initial inspections from experimental studies have shown that high quality laser welds could be formed with excellent metallographic and mechanical properties. Tests carried out on CO_2 laser welded specimens from materials used in fabrication of naval ships (HY 130, HY 180, Ti-6Al-4V alloy and 5456 Al) indicated these perspectives (References 40 and 41).

Further CO_2 laser welding process's features, as those listed below (adapted from Reference 42), make this process technically and economically attractive for the aerospace and shipbuilding industry. These features could be listed as follows.

(1) Narrow Deep Welds. Experiments on representative materials have shown deep penetration, similar to that achieved by the electron-beam welding

(2) Workpiece is not Enclosed in a Vacuum. This gives to CO_2 laser welding process an inherrent advantage compared to electron beam welding process.

(3) Characteristically Long Telescope - To - Work Distances. Hence, a better view of the workpiece is achieved with obvious advantages.

(4) One Laser Can Carry Out Two or More Operations Simultaneously. This feature is achieved by beam splitting.

(5) One Laser Can Service Several Work Stations on a Time Sharing Basis.

From the above, one may conclude that the benefits of CO_2 laser welding process, if well established and parametrically investigated, should help in expanding the application of the process to the aerospace and shipbuilding industry.

8.1 Experimental Procedure

The present experimental study, carried out at the laboratories of Massachusetts Institute of Technology under the supervision of Professor Koichi Masubuchi aims to an initial evaluation of the process.

The experiments were carried out on two specimens, one from low-carbon steel and one from Ti-6Al-4V alloy, both widely used in the construction of naval ships. Table 8.1 states the properties of the materials used.

The welds were carried out at AVCO, Massachusetts, because of the lack of laser welding machine at M.I.T. laboratories. Table 8.2 lists the welding test parameters used.

Measurement of residual stresses in the butt-welded specimens was made using the complete stress - relaxation technique, as described in Reference 43. The strain gages used were of the type BLH #FAET - 18D - 12 - 56 with a resistance of 120 Ohm and gage factor 1.98. There were mounted on the surface of the specimens, using cement Eastman #910.

Figure 8.1 shows the titanium specimen with indication of the locations of the strain gages. Strain gages were installed on both faces of the specimens to account for bending stresses.

In the titanium specimen, the strain gages were located along the transverse line at midlength of the weld. However, this was not feasible for the low-carbon steel specimen because of the presence of a discontinuity in the weld at midlength. Therefore it was decided that the location of the transverse line, along which the strain gages should be installed, would be at a distance from the one edge equal to 1/4 of the whole weld length. It was understandable, of course, that at this location we would not get the maximum residual stress.

At this stage we note the following:

(1) The original width of the titanium alloy specimen was 19 in., but before the installation of the strain gages it had to be cut down from both sides to 16 in. The reason for this was the fact that the available cutting machines at M.I.T. laboratories did not have the ability of cutting plates wider than that during the application of the stress relaxation technique.

(2) During the cutting of the low carbon steel specimen, great difficulty was found in cutting the base plate near the weld as well as in cutting the weld itself. For reasons of comparison, we report that the time consumed in cutting the near-the-weld zone was almost double of this for the cutting of the rest of the plate. Similar difficulty was not encountered in cutting the titanium specimen, due to the fact that it was equally difficult to cut it throughout its whole width.

8.2 Results and Conclusions

Figure 8.2 shows the results obtained for the titanium specimen. It can be seen from the two curves that the residual stress level is much lower than the yield strength of this titanium alloy. Residual stress as low as 20,000 psi was found, compared to the yield stress of 120,000 psi. At the same time the width of the tensile zone was found to be as low as 1/4".

Results for the low-carbon steel were very strange and we would be very greateful if another specimen could be sent to us for conclusive results.

Table 8.1 Properties of Materials Used

Low Carbon Steel

Composition:

C:	0.21 max
Mn:	0.80 - 1.10
P:	0.05 max
S:	0.05 max
Tensile strength:	58,000 psi min.
Yield strength:	32,000 psi
Elongation	28%

6Al - 4V Titanium Alloy

Composition:

Al:	5,500 - 6,750
V:	3,500 - 4,500
Fe:	0.30 max
C:	0.10 max
N:	0.07 max
H:	0.015 max
O:	0.20 max
Other:	0.40 max
Tensile strength:	130,000 psi
Yield strength:	120,000 psi
Elongation:	8.0%

Table 8.2 Laser Welding Test Parameters

Material	Thickness (in.)	Weld Type	Laser Power, KW	Weld Speed (ipm)
Low Carbon Steel	1/4	Butt	8.4	100
Ti - 6Al - 4V	1/4	Butt		

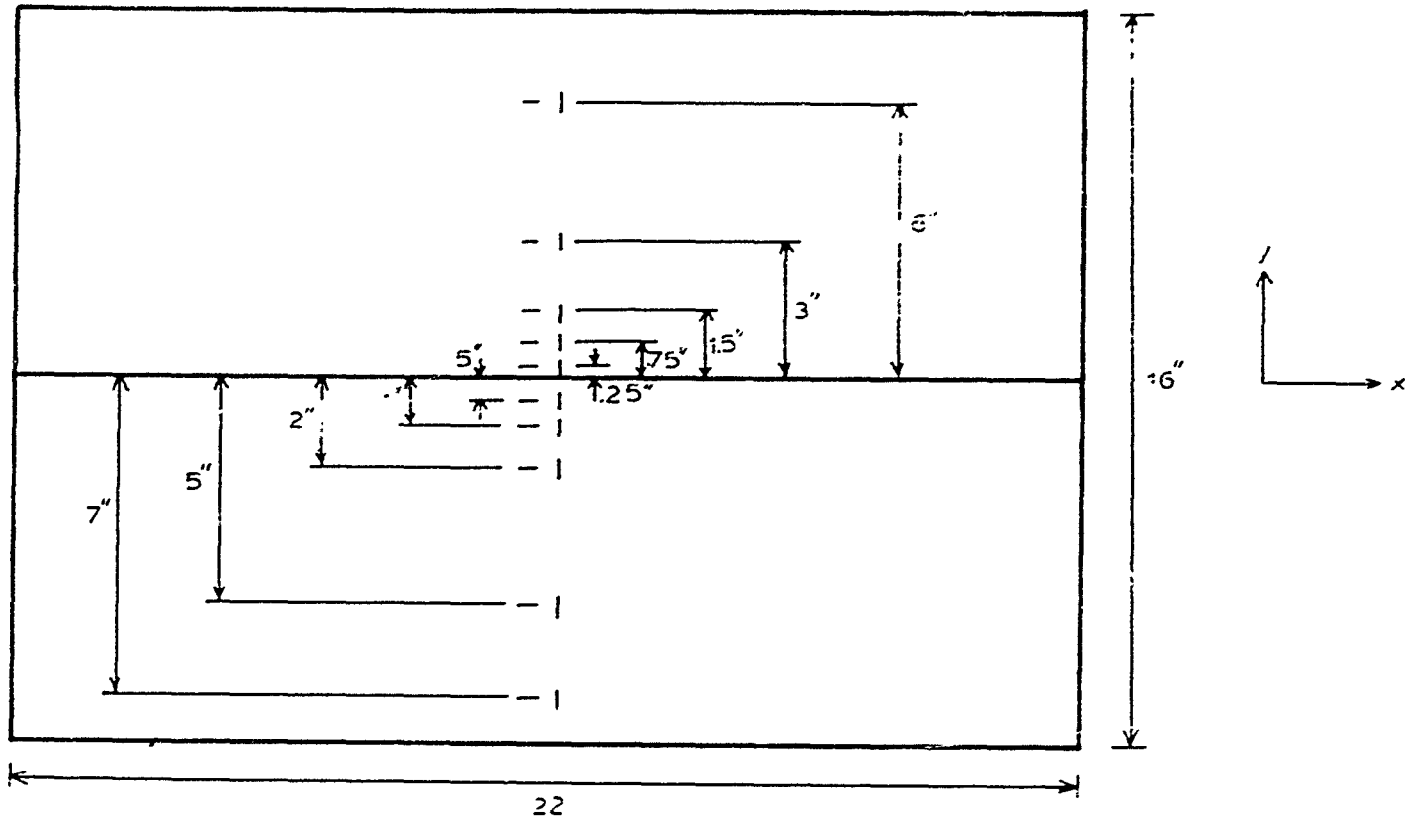

Figure 3.1 Location of Strain Gages on the Titanium Alloy Specimen

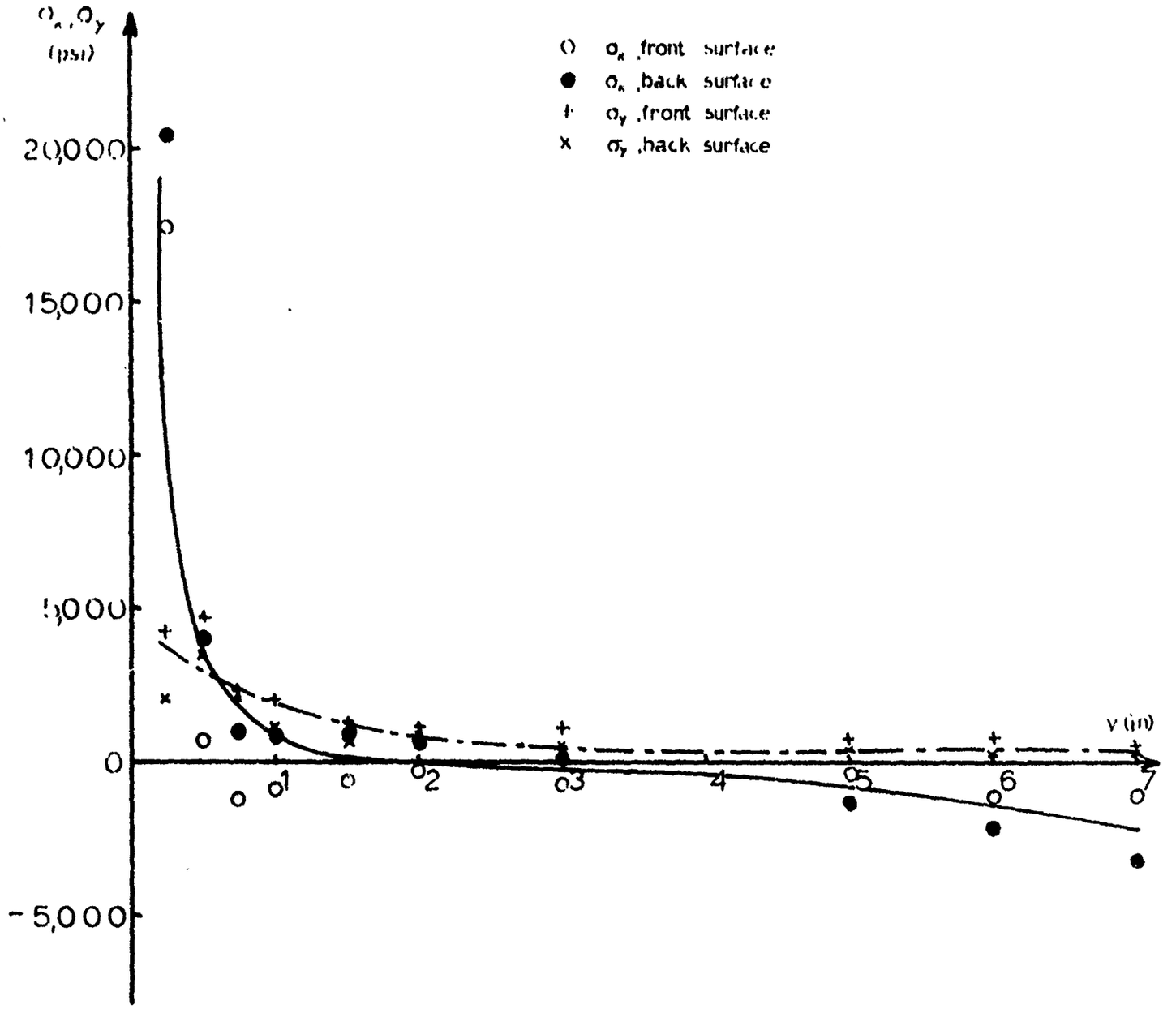

Figure 8.2 Residual Stress σ_x and σ_y the Titanium Alloy Specimen

BIBLIOGRAPHY

(1) Masubuchi, K., Progress Report under Contract No. N00014-75-C-0469, NR 031-773 (M.I.T. OSP #82558) "Development of Analytical and Practical Systems for Parametric Studies of Design and Fabrication of Welded Structures," to the Office of Naval Research from the Massachusetts Institue of Technology, June 7, 1976.

(2) Kitamura, K., and Masubuchi, K., Special Report on "Out-of-Plane Distortion of Welded Panel Structures" under Contract No. N00014-75-C-0469, NR 031-773 (M.I.T. OSP #82558) to the Office of Naval Research from the Massachusetts Institute of Technology, July 3, 1975.

(3) Masubuchi, K., "Control of Distortion and Shrinkage in Welding," Welding Research Council Bulletin 149.

(4) Masubuchi, K., "Residual Stresses and Distortion in Welded Aluminum Structures and Their Effects on Service Performance," Welding Research Council Bulletin 174.

(5) Rosenthal, D., et al., "Thermal Study of Arc Welding -- Experimental Verification of Theoretical Formulas," The Welding Journal, 17, April 1938, 2-8.

(6) Rosenthal, D., "Mathematical Theory of Heat Distribution During Welding and Cutting," The Welding Journal, 20 (5), 220s-234s, 1941.

(7) Rosenthal, D., "The Theory of Moving Sources of Heat and Its Application to Metal Treatments," Transactions ASME, November 1946, 849-866.

(8) Nishida, M., "Analytical Prediction of Distortion in Welded Structures," M.S. Thesis, M.I.T., May 1976.

(9) Muraki, T., and Masubuchi, K., "Computer Programs Useful for the Analysis of Heat Flow in Weldments," M.I.T. OSP #81499, #22016, June 1974.

(10) Andrews, J. B., Arita, M., and Masubuchi, K., "Analysis of Thermal Stress and Metal Movement During Welding," Final Report under Contract NAS8-24365 from M.I.T., December 1970.

(11) Muraki, T., and Masubuchi, K., "Manual of Finite Element Program for Two-Dimensional Analysis of Thermal Stresses and Metal Movement During Welding," M.I.T., OSP #81499, #22016, April 1975.

(12) Capel, L., "Aluminum Welding Practice," British Welding Journal, 8 (5), 245-248, 1961.

(13) Gilde, W., "Contribution to the Calculation of Transverse Shrinkage," (Beitrag zur Berechnung der Quershrumpfung), Schweisstechnik, 7 (1), 10-11, 1957 (in German).

(14) Cline, C. L., "Weld Shrinkage and Control of Distortion in Aluminum Butt Welds," Welding Journal, 44 (11), 523s-528s, 1965.

(15) Campus, F., "Transverse Shrinkage of Welds," Ibid., 26 (8), 485s-488s, 1947.

(16) Week, R., "Transverse Contractions and Residual Stresses in Butt-Welded Mild Steel Plates," Report No. R4, Admiralty Ship Welding Committee, January 1947.

(17) Guyot, F., "A Note on the Shrinkage and Distortion of Welded Joints," Welding Journal, 26 (9), 519s-529s, 1947.

(18) Sparangen, W., and Ettinger, W. G., "Shrinkage Distortion in Welding," Welding Journal, 23 (11), 545s-559s, 1944.

(19) Malisius, R., Electroschweissen, 7, 1-7, 1936, (in German).

(20) Watanabe, M., and Satoh, K., "Effect of Welding Conditions on the Shrinkage and Distortion in Welded Structures," Welding Journal, 40 (8), 377s-384s, 1961.

(21) Naka, T., "Shrinkage and Cracking in Welds," Komine Publishing Co., 1950 (in Japanese).

(22) Matsui, S., "Investigation of Shrinkage, Restraint Stresses and Cracking in Arc Welding," Ph.D. thesis at Osaka University, 1964 (in Japanese).

(23) Iwamura, Y., "Reduction of Transverse Shrinkage in Aluminum Butt Welds," M.S. Thesis, M.I.T., May 1974.

(24) Kihara, H., and Masubuchi, K., "Studies on the Shrinkage and Desidual Welding Stress of Constrained Fundamental Joint," Intl. Soc. Naval Arch., Jap. Pt. 1, 95, 181-195, 1954; Pt. 2, 96, 99-108, 1955; Pt. 3, 97, 95-104, 1955 (in Japanese).

(25) Sasayama, T., Masubuchi, K., and Moriguchi, S., "Longitudinal Deformation of a Long Beam Due to Fillet Welding," Welding Journal, 34, 581s-582s, 1955.

(26) Ujiie, A., et al., "Automatic Welding of 5083 Aluminum Alloy," The Committee of Light Metals for Shipbuilding Industry, Report 14, 1970-1972 (in Japanese).

(27) Yamamoto, G., "Study of Longitudinal Distortion of Welded Beam," M.S. Thesis, M.I.T., May 1975.

(28) Masubuchi, K., Ogura, Y., Ishihara, Y., and Hoshino, J., "Studies on the Mechanism of the Origin and the Method of Reducing the Deformation of Shell Plating in Welded Ships," Intl. Shipbuilding Progress, 3 (19), 123-133, 1956.

(29) Taniguchi, C., "Out-of-Plane Distortion Caused by Fillet Welds in Aluminum," M.S. Thesis, M.I.T., September 1972.

(30) Shin, D. B., "Finite Element Analysis of Out-of-Plane Distortion of Welded Panel Structures," O.E. Thesis, M.I.T., May 1972.

(31) Duffy, D. K., "Distortion Removal in Structural Weldments," M.S. Thesis, M.I.T., May 1970.

(32) Brito, V. M., "Reduction of Distortion in Welded Aluminum Frame Structures," O.E. Thesis, M.I.T., May 1976.

(33) Pattee, F. M., "Buckling Distortion of Thin Aluminum Plates During Welding," M.S. Thesis, M.I.T., September 1975.

(34) Henry, R. W., "Reduction of Out-of-Plane Distortion in Fillet Welded High Strength Aluminum," M.S. Thesis, M.I.T., May 1974.

(35) Masubuchi, K., "Integration of NASA Sponsored Studies on Aluminum Welding," under contract No. NAS8-24364 to George C. Marshall Space Flight Center, NASA, June 1972.

(36) Terai, K., "Recent Progress on Electron Beam Welding in Japan," Lecture given at M.I.T., March 1976.

(37) Kihara, H., Watanabe, M., Masubuchi, K., and Satoh, K., "Researches on Welding Stress and Shrinkage Distortion in Japan," Vol. 4, 60th Anniversary Series of the Society of Naval Architects of Japan, Tokyo, 1959.

(38) Beauchamp, D. G., "Distortion in Welded Aluminum Structures," M.S. Thesis, M.I.T., May 1976.

(39) Serotta, M D., "Reduction of Distortion in Weldments," O.E. Thesis, M.I.T., August 1975.

(40) Banas, C. M., "Laser Welding of Navy Ship Construction Materials," United Aircraft Research Labs, East Hartford, Conn., August 1973.

(41) Locke, E., "Laser Welding Techniques for Fabrication of Naval Vessels," Avco Everett Research Lab., Inc., Everett, Mass., July 1973.

(42) Seaman, F. D., "Establishment of a Continuous Wire Laser Welding Process," Sciaky Bros., Inc., Chicago, Ill., 9th Interim Engineering Progress Report, January 1976.

(43) Masubuchi, K., "Textbook for Course 13.17J, Welding Engineering," M.I.T.